Westinghouse Research Laboratories
Pittsburgh, Pennsylvania 15235

RESEARCH STUDY ON MATERIALS PROCESSING IN SPACE, EXPERIMENT #M512

June 15, 1972 - November 30, 1973

M. Rubenstein, R.H. Hopkins, H.B. Kim

Final Report

NAS 8-28727

January 15, 1973

Prepared for George C. Marshall Space Flight Center
Marshall Space Flight Center, Alabama

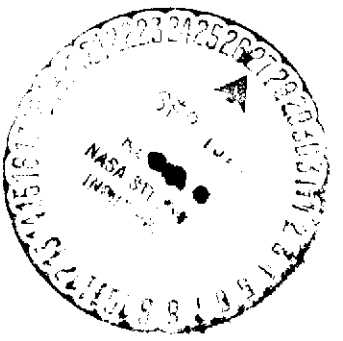

Westinghouse Research Laboratories
PITTSBURGH, PENNSYLVANIA 15235

RESEARCH STUDY ON MATERIALS PROCESSING
IN SPACE, EXPERIMENT #M512

M. Rubenstein, R.H. Hopkins, H.B. Kim

Final Report

NAS 8-28727

1. INTRODUCTION

Gallium arsenide, a commercially valuable semiconductor, has been prepared from the melt (M.P. 1237°C), by vapor growth, and by growth from metallic solutions. It has been established that growth from metallic solution can produce material with high, and perhaps with the highest possible, chemical homogeneity and crystalline perfection.

Growth of GaAs from metallic solution can be performed at relatively low temperatures (about 600°C) and is relatively insensitive to temperature fluctuations. However, this type of crystal growth is subject to the decided disadvantage that density induced convection currents may produce variations in rates of growth at a growing surface. This problem would be minimized under reduced gravity conditions.

A reduced gravity environment for extended periods of time permits the control of one parameter which has not previously been at our disposal. The most dramatic effect of free fall can be shown when one considers a liquid in which density variations are present. At normal gravity, convection currents would be formed; under free fall, the driving force for density driven convection would not be present.

During the growth of a solid crystal from a melt or from a liquid solution, appreciable density gradients may be induced by temperature differences and/or by differences in concentrations within the liquid. Such density differences in the melt could promote a non-uniform rate of atomic attachment at the surfaces of a solid growing from a liquid and thereby cause serious crystal growth rate fluctuations. Under conditions of free fall, this difficulty would be eliminated.

Using the flight ampoules designed for Skylab Experiment M555, scientists at Westinghouse Research have grown GaAs from gallium solutions under varying conditions including simulated reduced gravity experiments where convection was reduced by baffles. These techniques will provide crystals to be used as a baseline to compare and evaluate GaAs crystals grown under zero gravity and normal gravity.

The demonstrated techniques for the evaluation of GaAs crystals are standard metallographic analysis, etching, reflection x-ray topographic analysis, and electrical analysis (using the van der Pauw method as well as the Copeland probe). These will be applied to the crystals grown during the program.

Scientists at Westinghouse Research have designed an ampoule to grow GaAs from a gallium solution as described in Skylab Experiment M555. Using this ampoule with and without modifications, we have grown GaAs on substrates epitaxially as well as self-nucleated crystals in the solution cell of the ampoule.

The final report on Contract NAS 8-26122 contains calculations of the kinetics of the dissolution of the source GaAs, saturation of the gallium solvent by GaAs, and epitaxial growth of GaAs on the GaAs substrate. Many of the experiments were performed using the flight type ampoule and 99.9% gallium solvent rather than 99.9999%, since we were interested in demonstrating feasibility of growth and establishing some of the growth parameters, such as seed temperature,

temperature gradient, experiment run time, and distance between source and seed. However, several runs were performed in which the high purity gallium was used, and GaAs was epitaxially grown on a (111) A face, a ($\bar{1}\bar{1}\bar{1}$) B face, and a (100) face.

During these studies various experimental problems were encountered and solved. For example, appreciable difficulty has been encountered in the past by most workers in epitaxially growing on a (111) A face (the gallium face) of GaAs. By assuring that the growth surface was cleaned and wet with gallium to maintain a clean and active surface, we demonstrated that this technique will routinely produce epitaxial growth on the A face. Another problem was seed dissolution on the side opposite that where growth was occurring. This problem was largely solved by "passivating" the nongrowth side of the substrate with SiO_2.

Most of the crystal growing experiments were conducted in a two-zone vertical furnace in which the seed was at the lower portion of the furnace. The source GaAs was at the upper portion of the furnace. Experiments were performed to reduce convection by packing the solution cell with quartz wool or with a bundle of quartz capillaries.

Some of the GaAs crystals grown in flight ampoules have been examined by various evaluation procedures to determine the feasibility of these measuring techniques. For example, substrates with epitaxial GaAs were cleaved and the cleaved face was then stain-etched to reveal the depth of the growth and, of course, the junction. Some of the self-nucleated GaAs has been examined metallographically to observe macroinclusions of solvent. Etch pits have been observed which reveal the sites of dislocations in the crystals. GaAs crystals have routinely been measured for resistivity, Hall constant, and mobility as well as being examined with the Copeland probe.

Both epitaxial and self-nucleated GaAs crystals in flight type ampoules were grown, varying several parameters to establish baseline data for comparison with data obtained from material which will be grown in space.

Most of the decisions made during this contract were made with close cooperation between MSFC (Marshall Space Flight Center), Westinghouse, and often with UAH (University of Alabama at Huntsville).

PROGRAM

The experiments to be run in the M555 installation in the Skylab were changed to make this set of experiments more meaningful from a practical as well as from a scientific point of view. Previously, the three experiments to be run in the M555 were experiments concerning the epitaxial solution growth of high purity GaAs on different orientations of the substrate -- on the (111), on the $(\bar{1}\bar{1}\bar{1})$, and on the (100). The change was made to reflect the device orientation of the utilization of GaAs: (1) use of an undoped source and an undoped substrate, (2) use of an undoped source and a doped substrate, (3) use of a doped source and an undoped substrate.

This program comprises four parts: (A) preparation of the ground base study plan, (A-1) preparation of a crystal characterization plan, (B) laboratory test program, and (C) experiment analysis program. These parts are discussed in detail in the following sections.

PHASE A: PREPARATION OF GROUND BASE STUDY PLAN

In order to evaluate the potential advantage of solution grown crystals, the present state of the art for GaAs material must be evaluated for comparison. Therefore, the ground base studies of GaAs included the evaluation of the properties of GaAs prepared by different methods and by various modifications of these methods. GaAs samples to undergo evaluation would include:

1. Czochralski pulled high purity (undoped) single crystals with high dislocation densities.

2. Undoped single crystals with room temperature mobilities greater than 5000 cm^2/V-sec.

3. Doped single crystals (doped with silicon ca 10^{18} carriers/cc).

4. Substrates with vapor grown epitaxial GaAs.

5. Substrates with solution grown epitaxial GaAs prepared using flight type ampoules and prepared by MSFC.

The examination of the above GaAs samples gives a suitable ground base knowledge of GaAs so that the GaAs from the M555 experiment can be more readily and intelligently evaluated.

The parameters of the three ampoules with their contents and the temperatures to which they will be subjected were agreed upon The ampoules were to have the external configuration established in previous contracts; however, the source was to be a single crystal ingot about 1 cm in diameter weighing about 11 grams. The seeds on substrates were to be about 1.2 cm in diameter and 4 mm in thickness. The distance between source and seed was 5 cm. The temperature gradient was 30°C/cm with the source at 700°C and the substrate at 550°C. The three flight experiments were to be as follows:

1. An undoped GaAs seed and an undoped GaAs source.
2. A doped GaAs seed and an undoped GaAs source.
3. An undoped GaAs seed and a doped GaAs source.

The choice of the above three flight experiments was established by discussion and consensus of personnel from the Westinghouse Research Laboratories, Marshall Space Flight Center, and University of Alabama (UAH). This decision, like many others, was made during periodic visits to MSFC.

Considering the above parameters, it was decided by concensus that the following ground base experiments would be run:

1. Simulate the flight experiments (seed below source in a vertical furnace).

2. Interrupt the flight type experiment after 6 and 12 hours after temperatures had been achieved to check the dissolution of the seed. It had previously been ascertained that in the M555 experiment GaAs would begin to grow epitaxially on the substrate about 11 hours after the experiment had begun.

3. Same as 1 above except the seed was placed above the source in a vertical furnace to increase convection currents.

4. Increase the temperature gradient by a factor of two.

5. Decrease distance between seed and source to 2.5 cm.

PHASE A-1: PREPARATION OF CRYSTAL CHARACTERIZATION PLAN

The properties of GaAs crystals are expected to depend strongly on the method used to grow them. One would try to correlate these properties -- dislocations (types, arrays, and concentrations), macro-inclusions, micro-inclusions, native defects, resistivities, net carrier concentrations and mobilities -- with methods of preparation.

To study these properties one can use a variety of techniques:

- Aqueous solution techniques
- Minor constituent analysis
- X-ray diffraction single crystal examination
- Standard metallographic analysis
- Scanning reflection x-ray topography
- Optical microscopy
- Surface profiling (Surf Analyzer)
- Etching and stain-etching
- Copeland probe.

The above techniques do not necessarily give one value for one aspect of crystal quality. Each of these techniques provides an item of information which one can then integrate into an over-all picture of the crystal characteristics.

A plan for handling the evaluation from receipt of the furnace from the M555 run experiment through complete evaluation of GaAs source, GaAs self-nucleated, and GaAs substrates with epitaxial growth by Westinghouse, MSFC, and UAH is presented later in this report.

PHASE B: LABORATORY TEST PROGRAM

During this phase, the ground base study program defined in Phase A will be conducted and the evaluation and characterization of various types of GaAs crystals will be conducted as described in Phase A-1. One of the primary purposes of this phase is to become thoroughly acquainted with the various evaluating techniques so that the flight crystals can relatively routinely be examined and evaluated. The evaluating techniques have been discussed on several occasions among the representatives of MSFC, Westinghouse, and UAH.

Initially, the three experiments to be used as flight experiments were to consist of ampoules containing two single crystal seeds with the $(\bar{1}\bar{1}\bar{1})$ face as the growth surface and one single crystal seed oriented so that the (100) face was the growth surface. The seeds and sources were all undoped GaAs.

During this contract, three flight ampoules and three back-up ampoules were fabricated so that the flight ampoules could reflect an improved set of Skylab experiments. These experiments are briefly outlined at the beginning of this report. Experiment 1 was to demonstrate the growth of GaAs on GaAs when both source and substrate

(seed) were relatively pure and undoped. This may be considered the control experiment. Experiment 2 was to determine how the growth would take place if the source were doped and the substrate were undoped. It was calculated that we should have a growth layer of about 5×10^{16} net donors on a substrate of 2×10^{16} net donors. The third experiment was to determine how growth would take place if the source were undoped and the substrate were doped.

In these three experiments it was decided that all the single crystal substrates have (100) orientation faces for growth. The reverse side would be coated with amorphous SiO_2 (vapor phase deposition) to prevent solution attack from this reverse side. The seeds were to be 4 mm thick before lapping and polishing. The growth side of the seed would be cleaned (of oxide layer) by treatment with hydrogen (600°C) and then covering the cleaned side with liquid gallium metal before placing the seeds in the flight-type ampoules. The source material was to be a single crystal in the form of a cylinder, whose flat surfaces were (100) in orientation. The GaAs material was all obtained from Texas Materials Laboratories, Inc. Undoped GaAs was to have $1\text{-}2 \times 10^{16}$ net donors per cc, having a room temperature mobility of greater than 5,000 cm^2/V-sec and a resistivity $0.10 \pm .05$ Ω-cm. The doped GaAs was to be $1\text{-}2 \times 10^{18}$ silicon atoms per cc, having a resistivity of 0.002 Ω-cm. Enough GaAs was to be purchased so that some of the ground base experiments could be performed with the same type of material used in the flight experiments. The fabrication of these three flight ampoules and the three back-up ampoules was under Phase D of this contract, but it was felt that the above discussion should be in Phase B because it was necessary to understand the formulation of Phase D in order to understand the ground base experiment and crystal characterization of Phase B.

There was some fear that the source material in the form of a cylinder might on vibration break the quartz disk (cut out disk)

which restrained the source GaAs from the solution cell. A dummy ampoule was prepared and successfully withstood the vibration test at MSFC. The dimples used to hold the quartz cut-out disk extend deep enough into the source cell to protect the quartz disk from the GaAs source cylinder.

In recapitulation it was decided that the zero gravity solution growth experiments have certain parameters:

1. Source temperature of 700°C.
2. Seed temperature of 550°C. These two conditions lead to a temperature gradient of 30°C/cm when the
3. Distance between seed and source is 5 cm.
4. The seed diameter is 11 mm.
5. The seed thickness for flight runs is 4 mm and 2 mm for flight simulated seeds.
6. The seed orientation is (100).
7. The flight source is a single crystal with the 100 direction parallel to the axis of the source ingot. The ingot weighs about 11 grams and is about 11 mm in diameter. Flight simulated experiments use 11 grams of GaAs with no other specifications.
8. The runs usually lasted 100 hours.

Experiments which were run varying some of these parameters to observe the effects bythe variations include reducing the distance between seed and source, increasing the temperature gradient and reducing the temperature gradient, reducing the time from 100 hours. Since these ground base experiments were performed to note effect of variations from the above parameters, one experiment was performed to induce convection -- placing the seed above the source in the vertical two-zone furnace. All other experiments were performed with the seed below the source. Other experiments utilized an n+ seed and an n+ source.

In this program samples of epitaxial growth and self-nucleated growth were generated exhibiting solution growth under a variety of conditions.

PHASE C: EXPERIMENT ANALYSIS PROGRAM

During this phase the flight crystals shall be measured by many techniques so that a proper evaluation and characterization can be expected. It is anticipated that the effects of zero-G processing should be delineated. Unfortunately, the M-555 experiment has not yet been run so there are no self-nucleated or epitaxial growths to evaluate.

LABORATORY TEST PROGRAM -- PHASE B

Phase B is split into two parts: Ground Base Experiments which deals with Phase A and Crystal Characterization Program which deals with Phase A-1.

Ground Base Experiments

The program of ground base studies was initiated to clarify the effects of gravity on the growth of GaAs crystals from a liquid gallium solution. A number of experiments were designed and run in flight-type ampoules under controlled conditions. Some of these conditions were to approximate the three experiments to be run as the M-555 in the Skylab. Some conditions were to intensify and reduce certain differences between one-G and zero-G.

One of the problems which concerned us from the beginning was the dissolution of the seed. In order to prevent the attack of the seed from the reverse side to the coldest portion of the growth cell (approximately one centimeter away), this side of the seed was vapor coated with an amorphous or glassy layer of SiO_2 (approximately 400 Å thick). All the ground base runs and the flight and back-up ampoules have seeds which are protected using this SiO_2 layer. This protective layer has been quite successful.

It was important to ascertain the amount of dissolution and type of dissolution on the seed in a flight-type ampoule during the initial heating portion of the run. Before the flight runs begin, the temperature of the ampoules is high enough to prevent the gallium from freezing (gallium melting point is 29.75°C). The power of 23 volts is applied to the three ampoules in the M-555 flight package, so that a temperature distribution of 700°C at the source and 550°C at the seed

may be established. During this heat-up time, the distribution of arsenic in the gallium solution has not been stabilized. The arsenic in the gallium solution comes primarily from the source GaAs since the temperature in this portion of the ampoule is much higher than the temperature around the only other possible arsenic source -- the seed. From the time the power is applied to the flight ampoule until the arsenic distribution is stabilized in the ampoule, the time is approximately 11 hours. The temperature distribution of 700°C at the source and 550°C at the seed is reached within 3 hours after power is applied. At the time of 11 hours after power is applied, GaAs begins to grow on the GaAs seed. There was some apprehension that during this time period GaAs might dissolve from the seed. The solubility of GaAs in gallium at 550°C is approximately 3×10^{-4} mole fraction of arsenic. The time the seed is at 550°C before the saturation arsenic concentration is reached is 8 hours; however, the arsenic concentration does not change near the seed from zero to saturation instantaneously. During this 11 hour period before GaAs begins to grow on the seed, the arsenic concentration in the solution around the seed is increasing. Because of the above discussion, one can see that the tendency for arsenic from the GaAs seed to saturate the gallium solution near the seed is less than the solubility of arsenic in a gallium solution would indicate.

Two runs were made to investigate what happens to the seed during this 11 hour period.

82-8 Flight-type run, seed vertically below source, $\Delta T = 30°C/cm$, $\Delta x = 5$ cm, time = 6 hours

82-1 Flight-type run, seed vertically below source, $\Delta T = 30°C/cm$, $\Delta x = 5$ cm, time = 12 hours

These 2 experiments were run in flight-type ampoules (except the quartz wall thickness was 1 millimeter thick rather than 3 millimeters thick); the heating was by a resistance furnace; the ΔT was the temperature difference per centimeter between the seed and the source;

the x was the distance between the seed and the source. Photographs and profile scans of these seeds will be shown and discussed in the section dealing with the Crystal Characterization Program.

28 Flight type run, ΔT = 30°C/cm, Δx = 5 cm, time = 100 hours

This experiment was to simulate the flight experiment as much as possible. By placing the seed vertically below the source, it was hoped that one could minimize convective flow and more closely approach growth at zero-G.

24 Flight type run, ΔT = 30°C/cm, Δx = 5 cm, time = 100 hours seed vertically above the source

This experiment was designed to see what would happen when convective flow was "encouraged". By placing the seed vertically above the source and, of course, the 700°C source below the 550°C seed, convection due to thermal effects as well as density effect due to differences of arsenic in the solution would abound. In addition, any crystallites which would free themselves would float up to the seed surface where they would rest and start growing.

25 Flight type run, ΔT = 20°C/cm (seed at 550°C), Δx = 5 cm, time = 100 hours

82-4 Flight type run, ΔT = 60°C/cm (seed at 400°C), Δx = 5 cm, time = 100 hours

The purpose of these two experiments was to increase the growth rate on the seed by increasing the temperature gradient from 30°C/cm to 60°C/cm. This might also tend to increase the convection currents.

82-8 Flight type experiment, ΔT = 40°C/cm, Δx = 2.5 cm, time = 100 hours

82-9 Flight type experiment, ΔT = 20°C/cm, Δx = 2.5 cm, time = 100 hours

These two experiments were run with the distance between the seed and source reduced from 5 to 2.5 cm to try to reduce convection currents. The seeds were maintained at 550°C. In 82-8 the source was 650°C which gave a $\Delta T = 40°C$. In 82-9 the source was 620°C which gave a $\Delta T = 20°C$.

82-7 Flight type experiment, $\Delta T = 30°C/cm$, $\Delta x = 5$ cm, time = 100 hours, seed n+(Si) doped

This run was to simulate the experiment to be run in the Skylab in which the source was undoped and the seed was doped.

82-3 Flight type experiment, $\Delta T = 30°C/cm$, $\Delta x = 5$ cm, time = 100 hours, n+(Si) doped source

82-6 Same as 82-3

These two runs were to simulate the experiment to be run in the Skylab in which the source was doped n+(Si) and the seed was undoped.

Compilation of Ground Based Experiments

82-2	6 hour run
82-1	12 hour run
28	Flight type, $\Delta x = 5$ cm, $\Delta T = 30°C/cm$, time = 100 hours
24	Flight type, seed above source
25	Flight type, $\Delta T = 60°C/cm$, seed 550°C
82-4	Flight type, $\Delta T = 60°C/cm$, seed 400°C
82-8	Flight type, $\Delta x = 2.5$ cm, $\Delta T = 40°C/cm$
82-9	Flight type, $\Delta x = 2.5$ cm, $\Delta T = 20°C/cm$
82-7	Flight type, seed n+(Si) doped
82-3	Flight type, source n+(Si) doped
82-6	Flight type, source n+(Si) doped

Crystal Characterization Program

In order for the crystal characterization to proceed smoothly once the experiments were run at low gravity such as in the Skylab, it

is necessary that the individual laboratories know what measurements they have to perform and in what order they perform these experiments. The timing for each of these measurements is also important so that the various laboratories will be prepared to perform the experiments when the crystals arrive at that laboratory.

By performing these measurements on ground base samples of GaAs, each laboratory will be more prepared to handle their respective measurements on the experiments run at low gravity. The following operations also include the time period necessary to complete the operations and the laboratory which will perform the operation.

Characterization Program

1. Furnace with ampoules arrive at MSFC and are quickly transferred to the Westinghosue R&D Center. Ampoules kept warm at all times until they are opened.
2. Ampoules opened; GaAs separated into source cell, solution cell, and substrates; GaAs separated from gallium by aqueous techniques. GaAs is weighed from each area of the ampoule. Seven days. Westinghouse.
3. Preliminary optical examination. Note surface uniformity and crystalline growth behavior. Two days. Westinghouse.
4. Laue x-ray diffraction to determine crystal orientation and single crystallinity. One day. Westinghouse.
5. Scanning back reflection x-ray topography (SBRT) to observe details within the surface layer. Three days. Westinghouse.
6. Some samples of self-nucleated crystals given for emission spectrochemical analysis for minor constituents. Three weeks. Westinghouse.
7. Complete optical mapping. MSFC, SSL.
8. Complete x-ray analysis by Lang technique to study crystal perfection and surface irregularities. MSFC, SSL.
9. Room temperature AC resistivity measurements, UAH
10. Photoluminescence and bulk photo-voltaic measurements to obtain impurity levels. MSFC, SSL.

11. Low temperature AC resistivity. UAH.
12. Surf Analyzer measurement to scan surface. If surface is too rough, the surface will have to be lapped and polished. Three days. Westinghouse.
13. Copeland Probe to measure carrier concentration profiles. Eight days. Westinghouse.
14. Substrates with epitaxial growth cleaved in half. Two days. Westinghouse. Half to MSFC, SSL.
15. Junction analysis. Two days. Westinghouse.
16. DC resistivity and Hall. Possibly by Westinghouse or UAH. Eight days.
17. Etch pit analysis.
18. Emission spectrochemical analysis. Three weeks. Westinghouse.

The portion of the crystal characterization program which Westinghouse is responsible for in catalog fashion starting with the receipt of a quartz ampoule after an experiment is run is as follows:

open ampoule, separate GaAs from gallium
preliminary optical examination
x-ray topographic analysis (Laue) - SBRT
surface profile
Copeland probe
junction analysis
D.C. resistivity and Hall
emission analysis

The ampoules are opened by being deeply scored using a silicon carbide (rubber bonded) cut-off wheel. The ampoule is cut on the cold side of the seed and on the hot side of the cut-out quartz disk restraining the source material. This divides the ampoule into source cell and solution cell. If possible, the seed is removed. Most of the gallium metal is removed by vacuum filtration. Residual amounts of gallium are removed by vacuum probe suction and finally by concentrated hydrochloric acid solution.

The seed is photographed to note obvious features. Then a few sections may be microphotographed.

Scanning back reflection x-ray topography (SBRT) may be used to study crystal surfaces. If the surfaces are too rough, one may merely obtain a type of shadow-graph of the sample surface, as if visible light were being shone on the sample at a low angle of incidence. For more precise information, a polished sample is mounted, flat face vertical, in the goniometer of a specially designed x-ray diffractometer. The x-ray beam (ribbon-shaped in cross-section after collimation through two slits 42 cm from the x-ray tube) impinges on the sample. If the sample is precisely oriented diffraction occurs according to Bragg's Law $\lambda = 2d \sin \theta$ (λ = x-ray wavelength, d = interplanar spacing and θ = the diffraction angle). The sample and recording film held in fixed relative position are traversed in the x-ray beam so that all of the sample surface is in turn irradiated and a photographic image of the diffracted intensity from the surface is built up. There is a point for point correspondence between the sample and its photographic image. Since the sample must be precisely oriented for diffraction to occur, defects in the crystal which produce deviations in sample orientation, e.g. subgrains, will decrease the diffracted intensity from the portion of the sample containing the defect. Similarly, defects such as dislocations which locally alter the value of the interplanar spacing, d, will produce enhanced diffraction by locally altering the Bragg condition.

In the case of GaAs for which the line's absorption coefficient for x-rays is fairly large ($\mu \approx 343$ cm^{-1} for Cuk$_\alpha$ radiation), only a thin layer near the crystal surface will be sampled by the x-ray beam. In fact for the reflections and x-ray wavelength used in these experiments, more than 90% of the diffracted x-rays will come from the first 10-20 μm of the sample surface. Hence, the SBRT technique is a sensitive tool for evaluating the perfection of a polished flat single crystal surface.

The surface profile and roughness curves are made by a unit called a Surf Analyzer. The primary advantage of this instrument over many other similar ones is that this instrument is capable of tracing not only a flat polished sample, but also a sample which is quite rough. The scales are indicated in the data box for each profile. The roughness profile is normalized about the abscissa and is run without a filter so that this curve contains the high frequency vertical change not noted in the surface profile.

The Copeland probe is a technique for quickly measuring the impurity profile particularly around a junction in a material. A metallic deposit is placed on the semiconductor surface forming a Schottky barrier. The Copeland method is used to determine the carrier concentration vs. depth into a sample from measurements of non-linear capacitance of a Schottky barrier on the surface of a sample. This technique involves driving a Schottky barrier diode with a small constant RF (at 5 MHz). The depth of the depletion layer is varied by the dc bias, and monitored by the voltage across the diode at the fundamental frequency (5 MHz), which is proportional to the depth x. The second harmonic voltage (10 MHz) is monitered to plot the carrier concentration. This plotter has the advantage of analog interpretation of the ordinary differential C-V method without going through point by point calculations involving a digital computation method of the C-V data. The resolution is limited only by the Debye length in most cases. The immediate results of concentration profile at each Schottky barrier diode make the economical mapping of the surface of the wafer possible.

The mapping scheme provides the profile and the apparent thickness of the epitaxial layer, and yields a measure of the uniformity of the profile and thickness across the wafer surface. This measurement does place a metallic film on the surface (by room temperature aqueous electro-deposition).

DC resistivity and Hall measurements can be obtained by using the Van der Pauw technique. The Van der Pauw method is used to determine the electrical resistivity, carrier concentration and mobility using Hall effect and resistivity measurements. This measurement can be made on irregularly shaped samples of epitaxial layers grown on insulating substrates or of bulk material, but cannot be used for epitaxial layers grown on substrates having a low electrical resistivity, unless the substrate has been removed.

Measurements of the Hall coefficient vs. temperature enable us to determine the ionization energy of unknown defects, as well as the donor and acceptor concentrations. This method is partially destructive since it requires placing four ohmic contacts on the grown layer.

Junction Analysis is a set of techniques to observe the boundary between substrate and growth on a substrate. After a sample of GaAs on which GaAs has been epitaxially grown has been cleaved perpendicular to the flat face of the seed, one often can visibly with a microscope see that junction or interface between the substrate and the grown layer. At times it is necessary to use an etch to more clearly show the junction. A preferential etch composed of CrO_3, HF, and H_2O may be used to delineate a junction. One can also angle lap a sample to "spread out" a junction. This can be followed by an etch or one can even "look" at this "spread out" junction with SBRT.

Emission arc analysis can be utilized on small samples of materials to determine various impurities in a material as well as doping impurities. This technique can be used with self-nucleated crystals as well as epitaxial growth.

CRYSTAL CHARACTERIZATION

The preliminary optical examination of a number of substrates with and without epitaxial growth have been examined. The optical

examination includes macrophotography as well as microphotography of a few selected portions of the surfaces. Scanning back reflection x-ray topographic analyses have been performed on many of these crystals. Surface profiles have also been made of several of these crystals.

Most of this data is presented in several groupings: (1) flight seeds and flight type seeds, (2) samples used in the crystal characterization program, and (3) crystals used in the ground base experiments. The first set is not complete because time requirements from the time the flight seeds were purchased and were received until it was necessary for them to be processed and delivered in sealed ampoules for flight and flight back-ups was not sufficient. The second set of samples have not, as yet, been returned from MSFC and UAH where measurements are being made. When this set is received by Westinghouse, electrical measurements will be made. The third set of crystals have had preliminary optical measurements made but until some of these crystals are lapped flat and polished, no other measurements can be made.

FIRST SET

Figure 1 shows a photograph of a polished substrate which is 12.0 mm in diameter. These seeds were 4 mm thick for flight and flight back-up substrate, 2 mm thick for ground base experiment. These dimensions were before lapping, polishing, and SiO_2 coating on non-growth surface. The sample 13-8 shown in Fig. 1 was not used as a flight-type seed since it had a chipped region on an edge.

Figure 2 shows the profile and roughness traces of a polished seed -- seed 9A. This seed was rejected because of an imperfection in the surface which can be noted in traces on this face labeled III and IV.

The upper curve of Fig. 2 (labeled I, we shall call the profile), which is almost flat, has a vertical scale in which the smallest subdivision is 500 microinches and a horizontal scale in which

the smallest horizontal subdivision is 10,000 microinches. From M to N the distance is almost the entire diameter of the sample (44 subdivision x 10,000 x 10^6 inches x 25.4 mm/inch = 11.17 mm compared to a sample diameter of 12.0 mm). The second curve (labeled II) we shall call the roughness. This curve is normalized about the abscissa and is run without a filter so that it contains the high frequency vertical changes. The profile curve is run with a filter and does not have the high frequency vertical changes. This second curve (II) has a vertical scale of 500 microinches.

Profile III is the same sample as Profile I and the only difference is the vertical scale in which the smallest subdivision is 20 microinches rather than 500 microinches. The roughness curve IV differs from II in the vertical scale which has the smallest subdivision as 20 microinches rather than 500 microinches. Curves V and VI are the profile and roughness curves for a surface measurement taken approximately 90° from III and IV in the plane of the polished surface.

Figure 3 shows the profile (curve III) and roughness (curve IV) traces, less reduced than in Fig. 2. The profile from one side of the seed to the other side of the seed (in this case, a diameter) is indicated as A to B. B to A is merely a repeat of A to B and the curve shows that A to B is a mirror image of B to A. The rounding (non-planarity) is shown in curve V-A' to B' (Fig. 1) is 180 microinches = 4.6 x 10^{-3} mm = 4.6 microns. This same rounding is shown in curve III A to B (Fig. 2 or 3) is 13 x 20 microinches = 6.6 x 10^{-3} mm = 6.6 microns. The letters A, B, A' and B' show the direction on the surface of the polished sample as indicated in the small drawing above III or Figs. 2 and 3 and below VI on Fig. 2. In this case, the line A-B is approximately perpendicular to A'-B'. The scales for III, IV, V, and Vi are identical. Curves III and V (profiles) use a filter to remove the high frequency motions and curves IV and VI (roughness) do not use the filter.

Toward the center of curve III (see Fig. 3) one can see a spike or projection (opposite of a hole) in the profile traverse A to B. This spike is about 1/4 micron in height. This same spike appears in the roughness profile A to B and is about 1/2 micron in height. The sharp line associated with this spike is artifact due to pen overshoot. This spike is not an artifact. The variation of maximum rounding between 6.6 microns and 4.5 microns is probably due to the closeness to the edge of the seed the instrument went, since there is much more rounding as one gets closer to the edge of the sample.

Figure 4 shows the SBRT (scanning back reflection topographic analysis) photographs. In all these runs, unfiltered Cuk_{α} radiation was used; the sample serves as its own monochrometer. Images were obtained from the variants of the (440), (622), (620), and (531) reflections. In all photographs the lighter regions are areas corresponding to increased x-ray intensity, the darker to reduced or zero diffracted energy from the sample.

The substrates shown in Fig. 4 are the flight seeds used in Package 3, Phase D (Modification of M555 Ampoules). These x-ray reflections were taken from the non-growth surface of the flight seed, after the substrates were polished and before they were coated with SiO_2.

The sample shown in 4(a) is an undoped substrate. This specimen contains one prominent subgrain whose misorientation from the average is estimated at about 0.2°. One other low angle boundary crosses the crystal but the misorientation there is apparently slight. The amount of linear background features such as dislocations seems to be relatively low.

The substrate shown in Fig. 4(b) is also an undoped substrate. The (440) topograph of this specimen reveals that the sample is quite homogeneous except for a small subgrain in the lower left hand corner

of the image. The misorientation, evidently a tilt, could not be measured by a standard Laue photograph. It is estimated < 0.3°.

Figure 4(c) shows substrate ID -- an n+(Si) doped seed (10^{18} silicon atoms/cc). The cellular substructure present in this highly doped crystal is plainly visible, as is a small subgrain in the upper right hand corner of the (620) topograph. The size of the cell structure appears to vary by a factor of 2-3 over the specimen cross-section. There is also some indication of a linear dislocation structure near the subgrain position.

Figure 5 shows two rejected seeds (a and b), and a third seed (c) obtained from a company other than Texas Materials Laboratory.

Substrate 3c shown in Fig. 5a is composed of at least three large subgrains each of which contains regions of smaller misorientations and a fine array of linear features illustrated in Fig. 5a, a (422) reflection. The misorientation between subgrains is only a fraction of a degree yet the substructure is clearly discernible. The linear features appear to be dislocations since their contrast varies from reflection to reflection.

Seed 3B is shown in Fig. 5b. The slice contained a pit and striations visible to the naked eye. The (422) topograph from this slice, Fig. 5b, confirms the visual examination in a striking manner. The pit shows up as a non-diffracting spot at the lower left hand area of the photograph. Much of the rest of the photograph is also black indicating misorientations so great that no diffraction occurs from those areas of the sample. Laue photographs of the sample indicated that the subgrain misorientations responsible for the lack of diffraction were in the range 2-4°. Comparing this to the fractional degree misorientations in sample 3C (Fig. 5a) illustrates the sensitivity of the topographic method to both fine scale and gross defects.

Specimen 13-8 was obtained from another company. The (531) topograph from this sample, Fig. 5c, illustrates two other features readily distinguished by x-ray analysis: cellular substructure and mechanical damage. The upper and lower portions of the x-ray image contain fine networks of enhanced contrast which form a network or cell structure generally characteristic of a doped material grown with a nonplanar solid-liquid interface. The cell boundaries are usually made up of dislocations and solute accumulations thus producing local variations in d-spacing and x-ray contrast. The scratches appearing as broad white streaks at various positions on the sample show enhanced contrast because of the strain associated with the scratchdamage.

When a replacement was needed for a damaged seed in the flight ampoule 93-5 (seed 4C had been cracked when the flight package was bumped and the ampoule had been broken), two seeds (1C and 95-1) were polished and coated with passivating SiO_2 for flight status. A "scratch" was noted on the surface of seed 1C. On SBRT measurement one saw that half of this seed was misoriented with respect to the other half of the seed. Other irregularities can also be noted. See Fig. 6.

The other seed designated 95-1 was used in ampoule 93-7 in the flight package. The SBRT is shown in Fig. 7.

SECOND SET

The set of data presented above concerns the first group of samples -- flight substrates and flight type seeds. The second grouping of samples were those which were in the crystal characterization program. These samples were set into a program simulating the flight crystals after being returned from being run in the Skylab. Operations were to be done at Westinghouse, then back to MSFC where NASA and UAH would perform their operations, then back to Westinghouse for measurements, then back to MSFC for measurements. This set of 6 samples were measured at Westinghouse, returned to MSFC, and should return soon to Westinghouse.

E-2 a flight type seed, edges were chipped for an analysis (spectrographic arc); an example of melt grown GaAs

W-1 Vapor grown, tin doped GaAs grown on Cr high resistivity substrate

W-2 Vapor grown GaAs grown on n+(Si) doped substrate

W-3 Vapor grown tin doped GaAs grown on n+(Si) doped substrate

NASA-2 Solution grown GaAs on undoped GaAs seed.

NASA-3 Solution grown GaAs on undoped GaAs seed.

These six samples of GaAs were given the preliminary optical examination, scanning back reflection x-ray topographical (SBRT) examination, and in some cases a surface profile. This data is shown in the next twelve figures. Macrophotography and microphotography at a few selected locations on the surface are shown, arrows are indicated on the macrophotographs indicating where the traces A and B for profiles and roughness were taken.

Fig. 8, E-2, (b) probably scratches.

Fig. 9, W-1, (b) and (c) probably indicate a certain amount of irregular deposit. This surface basically seems to show a good deposit of GaAs on GaAs.

Fig. 10, W-2, (b) indicates lowered circles over the surface. This may also be noted in the SBRT for this sample (Fig. 14(c)). (c) and (d) show a certain roughness over a small portion of the right side of the surface. This may have been due to poor surface preparation before vapor deposition.

Fig. 11, W-3. This surface was fairly smooth considering the large size of the slice. (b) shows some striations. (c) shows a fairly large growth imperfection. This imperfection could be seen with the naked eye.

Fig. 12, NASA-2 demonstrates in (a) solution growth of GaAs on GaAs. (b) shows some growth on the non-growth side. (c) position A is a small area of original surface without growth. (d), (e), and (f) seem to indicate a small amount of (100) growth which has not quite filled in the whole surface. The rectangular geometry in the center of (d) is indicative of (100) growth.

Fig, 13, NASA-3. (a) shows the growth surface which may be divided into two primary portions with a vertical line to the right of center dividing the two portions. (b) this back surface (non-growth side) clearly indicates there are two crystals. (c) and (d) indicate a small amount of growth that hadn't yet covered the entire surface. (e) is demonstrating (100) growth at the grain boundary at position C. (f) and (g) are from positions D and E and both these photographs show (100) growth. (h) from position F shows that transition from the rounded geometry to the rectangular geometry. (g) also shows a small amount of the rounded geometry with a predominant rectangular geometry.

Fig. 14. (a) The SBRT of E-2 shows some type of strain or tilt on the left side (the dark shaded area). (b) some tilt or strain is seen on the lower right side of W-1. (c) one feature that shows up in the SBRT of W-2 are the circular up-raised small areas (also noted in Fig. 10). (d) the dark areas of W-3 could show the strain caused by the breaking off of some portions of this crystal (at top of photograph).

Fig. 15. (a) The SBRT of NASA-2 shows 3 areas -- one area of non-growth (left side of photograph), the other areas of growth and the third areas of spiked growth. The spiked growth probably grew on cool-down. The x-rays were absorbed by the spikes and give a shadow effect. (b) the SBRT of NASA-3 show 3 areas of growth. All of the growth seems to be (100).

Fig. 16. Trace A and B show a rather smooth surface with some rounding at the edges. The vertical scales are 20 microinches per division and the horizontal scales are 2,000 microinches per division.

Fig. 17. Profile and roughness traces of W-1 show a smooth surface with more rounding in trace B than trace A. The vertical scales of 20 microinches per division and the horizontal scales are 2,000 microinches per division.

Fig. 18. The profile and roughness traces of W-2 show a quite smooth surface except for the imperfections. These imperfections are probably the circles mentioned previously. The scales are indicated in the figure captions.

Fig. 19. Profiles and roughness traces of W-3 show a smooth surface with more rounding in trace A than in trace B. No irregularities are noted.

Copeland Probe and Junction Analysis

One of the techniques to be used in this program for the electrical characterization of samples in the Crystal Characterization Program is the use of the Copeland Probe. The Copeland method was used to determine the carrier concentration profiles of the samples which were in the crystal characterization program (Ref. Phase B Report, NAS 8-28727, May 30, 1973). This set includes:

E-2	a flight type seed.
W-1	vapor grown, tin doped epitaxial GaAs grown on Cr doped high resistivity substrate.
W-2	vapor grown undoped epitaxial GaAs grown on Si(n+) doped substrate.
W-3	vapor grown, tin doped epitaxial GaAs grown on Si(n+) doped substrate.
NASA-2	solution grown GaAs on undoped GaAs seed.
NASA-3	solution grown GaAs on undoped GaAs seed.

Schottky barrier diodes were made by electroplating Au on the GaAs surface and delineating the Au-metals into circular dots of .010", .005", .003", and .002" in diameter by photo-lithography. The Copeland profile plot is made on each Schottky barrier dot. This provides the carrier concentration profile at each Schottky barrier dot location, and in addition the mapping of the surface of the wafer is achieved.

The cross-section of the epitaxial-substrate interface and the epitaxial layer was examined by cleave-delineating method on the above set of the samples, excluding the seed, E-2. This method reveals the gross crystallographic defects and the surface and the interface planarity.

Sample E-2

The chemical-mechanically polished surface of this sample was smooth and flat, and was suitable for electroplating Au Schottky barrier dots. Figure 20 shows the results of the Copeland profile measurements. The carrier concentration deviation across the surface of the wafer ranged from 3×10^{17} to 4.3×10^{17} cm^{-3} at room temperature (300°K)(Fig. 21). The maximum penetration of the profile was 900 Å from the surface and the profile was flat. Figure 21A and B show the carrier concentration mapping on the sample E-2. Rows and columns of the Au Schottky barrier dots were designated alpha-numerically as shown in Fig. 21A, and the carrier concentration measured at each dot location achieve the mapping of the wafer surface.

A correlation of the concentration mapping and the x-ray topography of the sample E-2 by the scanning back reflection method was observed in Fig. 21B and C. The shaded area of scanning back reflection x-ray topograph (SBRT) corresponds to the area with the higher carrier concentration in the concentration map. SBRT technique provides point to point mapping of the sample crystalline perfection

below the surface (down to about 15 to 20 micrometers). Defects in the crystal, i.e., subgrains, dislocations, and striations, produce the contrasting shades in the photographic image of SBRT. The correlation of the shaded area in SBRT to the higher carrier concentration region suggests the defects in the sample W-2 incorporated high impurity concentration during the melt growth process. Further trace analysis and DIMA type of methods are necessary to uncover the type of impurities in the defects.

Sample W-1

The vapor epitaxially grown surface of this sample was planar and smooth, and was suitable for electroplating Au Schottky barrier dots for the Copeland measurements. The carrier concentration deviation across the surface of the wafer ranged from 1.0×10^{17} to 1.3×10^{17} cm^{-3} as shown in Fig. 22. The concentration profiles were flat and had 2500 Å of maximum penetration from the surface before the leakage currents became excessive. Since the epitaxial layer thickness of the wafer is approximately 3 micrometers, step removal of the epitaxial layer is necessary to profile the depth beyond 2500 Å. This involves etch removal of the epitaxial layer which is a destructive test, and hence it was deferred as an appropriate later test. Figure 23 shows the concentration mapping of the sample W-1 and SBRT. Again, the correlation between the concentration mapping and SBRT was observed although the deviation in the concentration was less pronounced as was the case of E-2. Since the shaded area in SBRT photographic images are merely sensitive to crystalline imperfections rather than to the concentration deviations, its correlation to concentration deviation is only pronounced when the defects encompass impurities.

Figure 24A shows the cross-section photomicrograph of the epitaxial layer W-1. The sample was cleaved to reveal {110} surface and etched to delineate the epitaxial-substrate interface. The interface was planar as were the surface of the epitaxial layer. Thickness of epitaxial layer was 2.8 micrometers.

Sample W-2

The surface of this sample was planar and smooth, and was suitable for electroplating Au Schottky barrier dots. The carrier concentration deviation across the wafer ranged from 3×10^{15} to 4.2×10^{15} cm^{-3}. The concentration profile had a slight decline near the surface from 6×10^{15} to 4×10^{15} cm^{-3} as shown in Fig. 25. The thickness of the epitaxial layer ranged from 1.4 to 1.9 micrometers measured by Copeland profiles in Fig. 25. Figure 24B shows the photomicrograph of the cleaved {110} surface having the interface delineated by etching. The thickness of the epitaxial layer was 1.9 micrometers, well in agreement with the results obtained by the Copeland profiles. The interface appeared planar and sharp.

There was no obvious defect centers detected by SBRT to correlate with the concentration mapping of this sample W-2, as shown in Fig. 26.

Sample W-3

The vapor epitaxially grown surface of this sample was smooth and planar and was suitable for electroplating Au Schottky barrier dots. Figure 27 shows photomicrograph of the {110} cleaved and etch-delineated surface. The interface was sharp and planar, and the thickness of the epitaxial layer was 1.2 micrometers.

The carrier concentration at zero bias condition (approximately at 6000 Å) was 4×10^{15} cm^{-3}. The concentration profile was not flat and had a steep slope of about a decade increase per 4000 Å of penetration as shown in Fig. 28. It reached to 4×10^{16} cm^{-3} at the epitaxial-substrate interface. The thickness of the epitaxial layer obtained from the profile ranged form about 0.9 to 1.2 micrometers. No meaningful surface concentration mapping was achieved due to the steep increasing concentration profile, and the deep zero bias depletion.

Samples NASA-2 and NASA-3

The surface morphology of these solution grown samples appeared as nearly polycrystalline or extremely small grained having non-growth areas interspersed. The electroplating of Au Schottky barrier was accomplished on NASA-3, but was unable to delineate Schottky barrier dots by photolithographic process. Any impurity distribution in these samples can best be measured by other evaluation methods, such as DIMA and trace analysis. Figure 29 shows the cleaved 110 cross-section of the NASA-2. The etch delineated interface appeared relatively flat compared to the surface of the epitaxial layer. Grown-in voids were often observed in the epitaxial layer as shown in Fig. 29B and C. The thickness of the epitaxial layer was about 31 to 38 micrometers. Figures 30 and 31 show the cleaved 110 cross-section of the NASA-3. The etch delineated interface appeared relatively flat as was the case of NASA-2, compared to the epitaxial layer surface. Again, the grown-in voids were often observed throughout the epitaxial layer as shown in Figs. 30 and 31. The average thickness of the epitaxial layer was about 148 micrometers for NASA-3.

THIRD SET

The third set of crystals for which data is being presented is the set of crystals from the ground base experiments.

		Figures
82-2	Dissolution experiment - 6 hours	32,33
82-1	Dissolution experiment - 12 hours	34,35
28	Simulation of flight experiment	36
24	Seed above source	37
25	Twice temperature gradient - seed 550°C	38
82-4	Twice temperature gradient - seed 400°C	39
82-8	Δx = 2.5 cm ΔT = 40°C/cm	40
82-9	Δx = 2.5 cm ΔT = 20°C/cm	40

		Figures
82-7	n+(Si) seed	41
82-6	n+(Si) source	42
82-3	n+(Si) source	42

Fig. 32. The two areas of experiment 82-2 A and B of Fig. 32 (a) are probably portions of the original surface of the seed. This surface is shown in the microphotographs (c) and right hand side of (d). These two surfaces are probably coated with small droplets of gallium which were not completely cleaned from the surface. There is definite attack on this seed in the area indicated at position E shown in the microphotograph (g). Microphotograph (e) and (f) from positions C and D show (100) etching by gallium.

Fig. 33 shows the profiles and roughness traces of 82-2. In the vertical direction of these traces the scale is 500 microinches/division and in horizontal direction the scale is 5,000 microinches per division. One portion of the original surface is shown in these profile traces.

Fig. 34 shows the macrophotographs and microphotographs of experiment 82-1. There is no obvious attack at any one area at noted in 82-2. The back of this seed does show some attack at the lower center of this seed. (d) at position B shows the typical attack on a (100) surface.

Fig. 35 shows the profiles and roughness traces of experiment 82-1. The scales are the same as indicated in Fig. 33.

Fig. 36 contains the macrophotographs of experiment 28. There is attack on the seed around position 1 and there is also shown in (c) (the stricted lines) (b) shows some attack on the back surface of this seed. (d), (e), and (f) show (100) growth.

Fig. 37 has the macrophotographs of experiment 24. This deposit shown in (a) is polycrystalline and not epitaxial. There is some attack on the back surface.

Fig. 38 shows some of the secondary growth (on cool down) in (a). (b) shows the seed with secondary growth removed. This seed shows gross attack. The microphotograph shows growth on a (100) surface.

Fig. 39 shows the very polycrystalline growth of experiment 82-4. The growth temperature of 400°C was too low for single crystal growth. (c) and (d) show the side views of this growth.

Fig. 40 shows the growth of experiment 82-8 where the ΔT was twice that for 82-9. More arsenic was approaching the growth surface in 82-8 than in 82-9. Possibly that is why 82-9 suffered such attack. There is definitely growth on what is left of the seed in photograph (c).

Fig. 41 shows growth and attack on the seed for experiment 82-7.

Fig. 42 shows growth and attack on seeds from experiments 82-6 and 82-3.

Each of the above experiments in this third set, except 82-2, 82-1, 24, and 82-4, exhibits growth which certainly appears to be epitaxial growth. Although this growth is not smooth, these surfaces will be lapped and polished, and will undergo measurements (electrical, junction, etc.).

It was decided that a group of substrates with epitaxial deposits from the ground base experiments would become part of the Crystal Evaluation Program. Substrates 28, 82-6, 82-7, 82-8 were selected.

28	Simulation of flight experiment
82-6	Undoped seed, n+(Si) doped source
82-7	n+(Si) doped seed, undoped source
82-8	Distance between seed and source 2.5 cm rather than 5 cm, ΔT = 40°C/cm.

These four samples all show (100) growth which seems to be epitaxial with an overgrowth of gallium arsenide. One might well expect such substrates with epitaxial growth grown in such experimental conditions to exhibit a non-smooth surface because the GaAs in solution at the temperature of growth conditions will rather quickly precipitate as the temperature rather quickly falls to end the run. This fast precipitation should yield a certain amount of dendritic growth or a resultant uneven growth.

The surfaces of the above four samples were too rough for the Surf Analyzer to measure the profiles (Fig. 36, Fig. 42, Fig. 41, Fig. 40). As an experiment in obtaining a relatively smooth surface, two other substrates (run 25, Fig. 38 and run 82-3, Fig. 42) on which epitaxial GaAs has been grown were treated to make them smooth enough for electrical measurements. These two samples were mounted on lapping-polishing jigs, lapped with 400 mesh wet and dry paper, then lapped with 600 mesh wet and dry paper. There were finally lapped with 5 micron Al_2O_3 abrasive. A chemical polish was then used composed of concentrated sulfuric acid, 30% hydrogen peroxide, and water (5:1:1). These substrates are relatively smooth but do contain holes. Electrical measurements will be performed on these seeds and several more samples will be treated in the same manner if electrical measurements can be made on the two seeds whose surfaces were prepared as described above.

Since it was decided that such samples as treated above to produce relatively flat surfaces could be measured by the Copeland Probe, the four samples (28, 82-6, 82-7, and 82-8) would similarly be treated.

82-8	$\Delta T = 40°C/cm$, $\Delta S = 2.5$ cm (distance between seed and substrate is normally 5 cm)
82-7	n+ seed

82-6 n+ source

28 Flight type run, $\Delta T = 30°C/cm$, $\Delta X = 5$ cm, $T_{seed} = 550°C$, $T_{source} = 700°C$, source and seed undoped.

	82-8	82-7	82-6	28
Original substrate thickness	1.212 mm	1.224 mm	1.330 mm	1.652 mm
After chemical polish etch	1.430 mm	1.275 mm	1.460 mm	1.360 mm

All of these samples have more than 75 percent of the surface as relatively smooth surface which can be measured electrically. Scanning x-ray back reflection topography (SBRT) was used to study these surfaces of these four samples.

Photographs of the substrate with growth from experiment 28 are shown in Fig. 43. Figure 43a shows the lapped sample and Fig. 43b shows the sample treated by a chemical polish etch. Figure 43c is the SBRT scan showing the depressions (attack on the seed) as well as holes in growth (non-growth areas). However, the relatively smooth area of epitaxial growth is shown over 75% of the surface.

Figures 44a,b,c show this same sequence of photographs for run 82-6. Figure 44a is the lapped surface; 44b is the polish etched surface, and 44c is the SBRT scan. This surface is less uniform than the surface shown in Fig. 43c.

Figures 45a,b,c show this sequence of photographs for run 82-7. The three dimensional aspect of the surface in Fig. 45c is quite striking.

Figures 46a,b,c show this same sequence of photographs for run 82-8.

Copeland Probe Measurements. A preliminary result of the impurity profile analysis by Copeland method on the three simulated flight-growth conditions is presented in this report. This set includes the growth conditions of

1) an undoped GaAs source and an undoped GaAs seed, designated as undoped/undoped; Sample 28-Flight T,

2) an undoped GaAs source and a doped GaAs seed, designated as undoped/n+, Sample 82-7,

3) a doped GaAs source and an undoped GaAs source, designated as n+/undoped; Sample 82-6.

In addition to the above three samples, a variation of the growth condition 1) is included to see the effects of the growth rate; Sample 82-8 represents undoped/undoped structure with the faster growth rate.

Because of the extremely non-planar and cratered surface morphology that these samples had in the grown layer as shown in Figs. 36, 40, 41, and 42, the grown layer was lapped and polished down to yield a reasonably flat region (see Fig. 43a and b, 44a and b, 45a and b, 46a and b) on which Schottky barrier diodes could be made for the Copeland measurements.

(1) Undoped/undoped

Schottky barrier diodes were made by electroplating Au on the polished surface and by delineating the Au metals into circular dots as shown in Fig. 47. Even after the lap-polishing of the surface, flat surface area retained many craters as evidenced in the Fig. 47. Copeland profiles were obtained on those Schottky barrier dots without the craters. Figure 48 shows the carrier concentration profile of the sample 28, Flight T. The concentration ranged from 3×10^{15} to 5×10^{15} cm^{-3} near the surface. The concentration increased to $5\text{-}7 \times 10^{15}$ cm^{-3} at 2.5 micrometers depth. A concentration profile obtained in the shallow crater verified the higher concentrations observed at the depth. The maximum penetration was at 3 micrometers depth. The breakdown of the Schottky barrier diodes prevented any further penetration by depletion. No attempt was made to map the

surface at this time due to numerous craters. The monotonically increasing carrier concentration with depth should continue to the substrate concentration level of about 2×10^{16} cm^{-3}, and this aspect and the concentration profile near the interface region will be ascertained later, since this requires removal of the entire grown layer and is a destructive experiment. This sample 28 is of the Flight type experiment, where $\nabla T = 30°C/cm$, $\Delta X = 5$ cm, and time = 100 hours.

(1) Undoped/undoped; Faster growth condition

Figure 49 shows the Schottky Au metal barrier diodes delineated on the polished surface of the sample 82-8. Again, the sample surface was marked with numerous craters in the grown layer. The carrier concentration profiles measured on this sample 82-8 are shown in Fig. 50. The concentration ranges from 1.5×10^{15} at the center of the wafer to 4.5×10^{15} cm^{-3} at the edge of the wafer. The carrier concentration in the shallow crater shows a monotonically increasing value from 1.5×10^{15} at the surface to 8×10^{15} cm^{-3} at 3 micrometers depth. This concentration gradient of about 2×10^{15} cm^{-3}/micrometer for the sample 82-8 is greater than the concentration gradient of $2/3 \times 10^{15}$ cm^{-3}/micrometer of the sample 28, flight type. The maximum penetration of the profile was about 3 micrometers, the maximum depletion depth before the breakdown. Again, more information should be obtained later. The faster growth conditions were $\Delta T = 40°C/cm$, $\Delta X = 2.5$ cm, time = 100 hours, and hence of reduced convection currents.

(2) Undoped/n+

Figure 51 shows the Schottky barrier diodes mapping the polished surface of the sample 82-7. Part of the sample was dissolved away leaving deep erosion on the surface and many craters in the grown layer. The carrier concentration profiles are shown in Fig. 52. The concentration ranged from $1.8\text{-}3 \times 10^{15}$ cm^{-3} near the surface

increasing monotonically to 3-3.5 x 10^{15} cm^{-3} at about 2 micrometers depth. The carrier concentration of 2 x 10^{17} cm^{-3} was observed in the shallow craters, and of 9 x 10^{17} cm^{-3} in the region of the deep erosion. The concentration gradient is small, 2/5 x 10^{15} cm^{-3}/micrometer. Again, the concentration profile near the interface should be most informative and will be measured later. The low concentration level of about 2 x 10^{15} cm^{-3} and the small concentration gradient of 2/5 x 10^{15} cm^{-3}/micrometer shown in the grown layer near the surface (depth to 2 micrometers) indicate that the Ga solution was not totally doped by the dissolution of the n+ seed during the growth process, although the seed was severely dissolved as shown in Fig. 5. The growth conditions were ∇T = 30°C/cm, ΔX = 5 cm, and time = 100 hours.

(3) n+/undoped

Figure 53 shows the photomacrograph of the Au metal Schottky barrier diodes delineated on the polished surface of the sample 82-6. Severe erosion of the seed wafer was evidenced as shown in the Fig. 7. The carrier concentration profiles taken on the sample 82-6 are shown in Fig. 54. The concentration profiles were very flat throughout the depletion depth of 0.6 micrometers at which the breakdown occurred. The concentration level remained constant at 1.8-2.0 x 10^{16} cm^{-3}, and the concentration gradient was nearly zero. The concentration level of 5 x 10^{16} cm^{-3} was calculated for the grown layer using the doped source (Ref. p. 3, 73-9F8-GAAST-M5) and the undoped seed of 2 x 10^{16} cm^{-3}. The emission spectrographic data shown in Table I of the report indicated Si atom concentration of 2.3 x 10^{17} cm^{-3} for the recrystallized sample 82-6C (on source) and of 4.6 x 10^{17} cm^{-3} for the recrystallized sample 82-6A (on seed). The electrically active net carrier measurements obtained by Copeland method resulted Si atom concentration level by an order of a magnitude below in this case. The growth conditions were ΔT = 30°C/cm, ΔX = 5 cm, and time = 100 hours.

The preliminary results on the impurity profile analysis of the three simulated flight-growth conditions show the growth system retained a relatively pure condition having the net carrier concentration of 2-5 x 10^{15} cm^{-3} for the undoped source and of 2 x 10^{16} cm^{-3} for the doped source. The latter was predicted to be about 5 x 10^{16} cm^{-3}. The effects of the faster growth condition and the reduced convection in the solute were observed in the concentration profiles of the sample 82-8. The faster growth condition resulted in the steeper gradient in the concentration profile, and the reduced convection in the greater deviation of the carrier concentrations at the center and the edge of the wafer. Another set of the impurity profile measurements should be performed on these samples when these samples could be expendable for the destructive experiments.

Emission Spectrochemical Analysis. Analyses were performed on a group of GaAs samples.

4G	an undoped flight seed
90-2	undoped GaAs, scrap from ingot from which 4G was cut
90-4	undoped GaAs, scrap from ingot from which undoped seeds were cut
90-5	undoped GaAs, residual pot material after pulling undoped crystal
90-3	doped GaAs, scrap from ingot from which n+(Si) seeds were cut
82-3 C	ground base experiment, doped source, sample-recrystallized source
82-3 B	ground base experiment, doped source, sample-walls of solution cell
82-6 C	ground base experiment, doped source, sample-recrystallized source
82-6 A	ground base experiment, doped source, sample-crystallites around seed
28 B	ground base experiment, simulation no doping, sample-walls of solution cell.

Table I gives the analyses, for several samples of GaAs, of elements in parts per million by weight, except for the last column which gives the silicon concentration in atoms of silicon per cc GaAs. These results show that the silicon in the seeds is low (4.56×10^{16}), the silicon in the outer portions of the original ingots are somewhat higher (2×10^{17}), the silicon in the pot after the ingot has been pulled is even higher (3.42×10^{17}) and the silicon in the doped (nominally 1×10^{18}) GaAs is 9.12×10^{17}. The n+(Si) doped source will probably add some donor character to the grown crystals but this donor contribution will not be very high. One of the problems in this analysis is the danger of having even a tiny sliver of quartz mixed with the GaAs to be evaluated (quartz from the opening of the ampoules). These measurements will help in making later measurements on experiments in which either seed or source were doped.

In the process of evaluating samples of GaAs by emission spectrochemical analysis a rather interesting problem arose. Several samples were reported as having silicon concentrations greater than 100 ppm. Since the maximum concentration of silicon in solid solution with GaAs is about 10 ppm (10^{18} carriers/cc), it was realized that one was dealing with some type of contamination. By heating these same samples of GaAs before the emission spectrochemical analysis with aqueous HF, these extraordinarily high silicon concentrations fell to more reasonable levels. Apparently, some small slivers of quartz was contaminating the GaAs. When one breaks open an ampoule, there are bound to be some particles of quartz sucked into the ampoule. This technique of heating the GaAs samples with aqueous HF will be incorporated into the procedures for emission spectrochemical analysis.

TABLE I

SPECTROGRAPHIC ANALYSIS
(ppm by weight)

	Elements												
Sample	Si	Al	Ag	Bi	Cr	Cu	Fe	Mg	Mn	Ni	Pb	Ti	Si atoms Si/cc GaAs
4G	.4	ND<.5	ND<.1	ND<.2	ND<.4	<1	<.4	<.1	ND<.1	ND<1	ND<.4	ND<1	4.56×10^{16}
90-2	1.0	<.5	ND<.1	ND<.2	ND<.4	<<1	<.4	<.1	ND<.1	ND<1	ND<.4	ND<1	1.14×10^{17}
90-4	2.0	<.5	ND<.1	ND<.2	ND<.4	<<1	<.4	<.1	ND<.1	ND<1	ND<.4	ND<1	2.28×10^{17}
90-5	3.0	<.5	ND<.1	ND<.2	ND<.4	<1	<.4	<.1	ND<.1	ND<1	ND<.4	ND<1	3.42×10^{17}
90-3	8.0	ND<.5	ND<.1	ND<.2	ND<.4	<<1	<.4	<.1	ND<.1	ND<1	ND<.4	ND<1	9.12×10^{17}
82-3 C	2												2.3×10^{17}
82-3 B	2												2.3×10^{17}
82-6 C	2												2.3×10^{17}
82-6 B	4												4.6×10^{17}
28 B	2												4.6×10^{17}

SUMMARY AND CONCLUSIONS

There is some attack on the growth surface of many of these substrates in the ground base experiments. Even the experiment which was interrupted after six hours showed visible attack on the growth surface; however, the experiment which was interrupted after twelve hours does not show attack on this surface. Other similar runs which showed greater or lesser attack on this growth surface do not demonstrate any consistent factors for clarifying reasons for this attack, i.e., lower seed temperature.

We feel that this attack on the growth surface probably is caused by some type of preferential flow over a portion of the crystal surface, induced, for example, by the non-vertical alignment of the ampoule in the axis of the furnace (perhaps a few degrees misalignment). If this flow is a result of density-induced convection, at zero-G this effect would not be present.

Seed attack from the non-growth face is probably caused by a scratch or an imperfection in the SiO_2 coating. This attack is relatively minor and in no case did this attack cause a hole through the substrate.

The experiment in which the seed was vertically above the sources showed no epitaxial growth. Convection currents caused much nucleation and growth from the walls of the solution cell. This experiment was specifically designed to assure substantial convection. The substrate, however, did not show a surface attack. In this experiment, solute saturation is achieved long before eleven hours calculated for the reduced convection growth type of experiment. In a relatively

short period of time a layer of polycrystalline growth forms on the substrate surface. This indicated saturation of GaAs in the solvent preventing dissolution of the seed. As a result, growth is initiated quickly and substrate attack does not occur.

In the experiment in which the temperature gradient was doubled and the seed was maintained at 400°C, much polycrystalline (non-epitaxial growth) was observed on the substrate. This seed temperature is so low that the rate of nucleation is very high for the low solubility. Therefore, much polycrystalline growth was found on the seed.

In conclusion, it seems that the conditions of $\Delta T = 30°C/cm$, seed temperature = 550°C, distance between seed and source = 5 cm, diameter of ampoule = 12.7 mm, seed vertically below source -- the conditions for the ground base experiments simulating the zero-G experiments for measurable epitaxial growth on a substrate is very close to optimized conditions for thick epitaxial growth on a seed for a 100 hour run.

As a result of this program, alternative configurations for a successful experiment were derived. For example, increasing $\Delta T > 30°C/cm$ will increase the rate at which GaAs arrives at the seed; decreasing the distance between seed and source from 5 cm to 2.5 cm decreases the time for saturation and subsequent epitaxial growth and increases the amount of GaAs deposited on the seed per unit time. The seed temperature of 550°C seems to be an optimum temperature, and alternate configurations should be designed to maintain this seed temperature. Low seed temperature results in polycrystalline non-epitaxial growth, and higher seed temperatures cause too rapid seed dissolution before saturation is reached.

If one reduces the distance between the seed and source from 5 cm to, perhaps, 2.5 cm, more GaAs will epitaxially grow on the seed per unit time. Therefore, one could still grow a relatively thick

(in the magnitude of 1 mm) epitaxial layer in a total of 50 hours rather than 100 hours of run time. One must remember that instead of taking 11 hours for the "arsenic front" to reach the seed (at which time GaAs begins to grow on the seed), this "front" will reach the substrate in about 6 hours if the distance between seed and source is reduced to 2.5 cm. Furthermore, if one can only run such experiments with the reduced distance for 30 or even 24 hours, a thinner layer of GaAs would epitaxially grow on the substrate (thick enough to evaluate). In all cases, self-nucleated GaAs would also grow and such crystals will be evaluated with respect to morphology, size, perfection, and electrical characteristics. In addition, if one could program the cooling of the ampoules by "slowly" reducing the power into the heat source so that the source temperature lowered to 575°C over a period of perhaps 6 hours, there would be less dendritic growth and increased growth on self-nucleated crystals, resulting in larger sizes.

In every ground base experiment (excepting the run which increased the temperature gradient with the seed at 400°C, the two dissolution experiments, and the run with the seed vertically above the source) epitaxial growth was observed. This ground base growth is not smooth because of such factors as density-induced convection, attack on the growth surface (particularly before solute saturation is achieved), and dendritic grown on the fast cooldown. As a result, one would expect growth at low gravity to be much smoother than growth at one G.

We conclude that this experiment can yield valuable results in a shorter timeline than that originally projected. If space is available in the Multipurpose Electric Furnace, an effective experiment could be run in approximately 30 hours. The thickness of the epitaxially-grown GaAs would be reduced relative to initial expections in the 100 hour experiment. However, substantially the same evaluation

developed in this program can be accomplished on films 10-20 μm thick and the goals will not be compromised. In addition, one can expect substantially more data to be derived from the self-nucleated crystals. The usually self-nucleated GaAs crystals obtained from supersaturated solution during diffusion will be substantially enlarged during programmed cooldown. As a result, important data can be derived from analysis of diffusion controlled self-nucleated crystals as well as the epitaxial material.

By all means the M555 experiments should be carried out in the next available low-gravity mission -- the ASTP.

APPENDIX

M-555 FLIGHT PACKAGE

During the June 1973 report period we were informed by MSFC that the M-555 Flight Package had been damaged. The furnace cannister was opened at MSFC and free gallium was observed.

Although this indicated that at least one ampoule was, at least, cracked, there was no indication what had caused the quartz ampoule or ampoules to be cracked. Toward the end of June 1973 the Flight Package was brought to the Westinghouse Research Laboratories and opened.

It was found that ampoule 93-5 at position 2 was the only one which had leaked gallium. There was a crack in the quartz in the plug and fingers, where this component forms a wall of the ampoule containing the gallium (this is where the nickel heat seal withdraws heat from the ampoule). At position 1 it was noted that the quartz cup which is positioned around the opposite end of the ampoule (farthest from the GaAs seed) had a star crack in the center of the flat portion of this cup. It was apparent that all three ampoules had suffered one or more longitudinal shocks. It was decided that all three ampoules had to be opened, examined, and reassembled.

Ampoule 93-5 (the cracked ampoule) was opened and the seed (an undoped one) was chipped so that it had suffered a loss of about 6.3 weight percent. Another undoped seed, 4 mm thick by 12 mm in diameter had to be polished, coated with SiO_2, and subjected to scanning back reflection x-ray topography (SBRT). The doped source did not appear to have been damaged.

Ampoule 93-4 (with the cracked quartz cup) was opened and appeared to suffer no ill effects to seed or source. Ampoule 93-6 was opened and the seed and source also did not seem to have suffered.

Both of these seeds were examined to ascertain if there were any damage particularly to the SiO_2 protective films. The films under microscopic examination (100X) showed no damage.

It was our recommendation that Flight Package Serial Number 4 should remain the back-up unit for SL-3. Furthermore, we recommended that Flight Package Serial Number 2 which was refurbished and reidentified as Flight Package Serial Number 2B be assigned to flight status for SL-3. There is more information known on the three seeds (primarily through scanning back reflection x-ray topography, SBRT) which will be incorporated into Flight Package Serial Number 2B. Flying this Flight Package Serial Number 2B will result in a set of experiments with greater scientific significance.

Ampoule 93-7 is a replacement for ampoule 93-5 in Flight Package 2B (designated 95-1, see page 16 of this report). A new seed had to be supplied for the fabrication of this ampoule (93-7) since the seed in 93-5 was badly chipped. X-ray back reflection scanning topographs were made on this replacement seed (95-1). The seeds and source materials used to prepare 93-4B, 93-6B, and 93-7 (except for the replacement seed) were the same which were used in 93-4 and 93-6.

These three ampoules were loaded into Experiment Package Number Two and this Package is now reidentified as Experiment Package Two B.

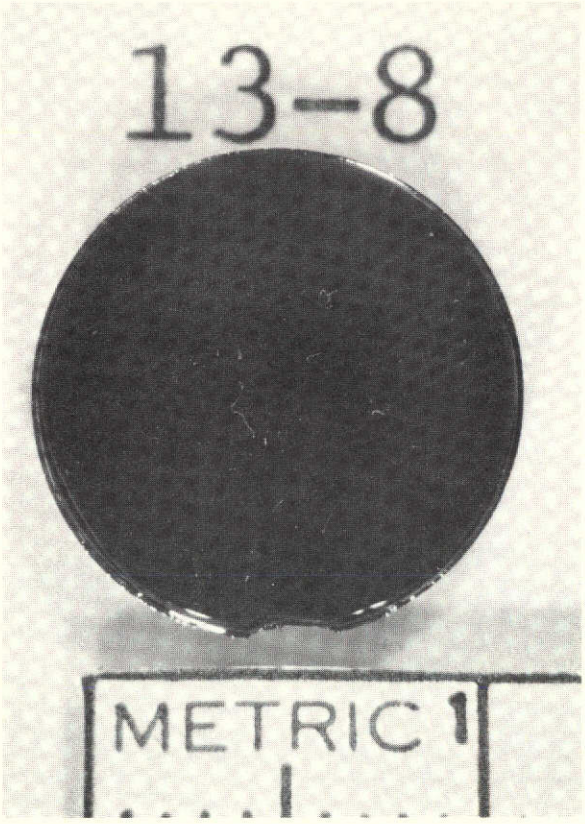

Fig. 1 -- This is a photograph of a representative polished seed -- 12.5 mm diameter x 4 mm thick for flight and back-up substrates (2 mm thick for ground base experiments).

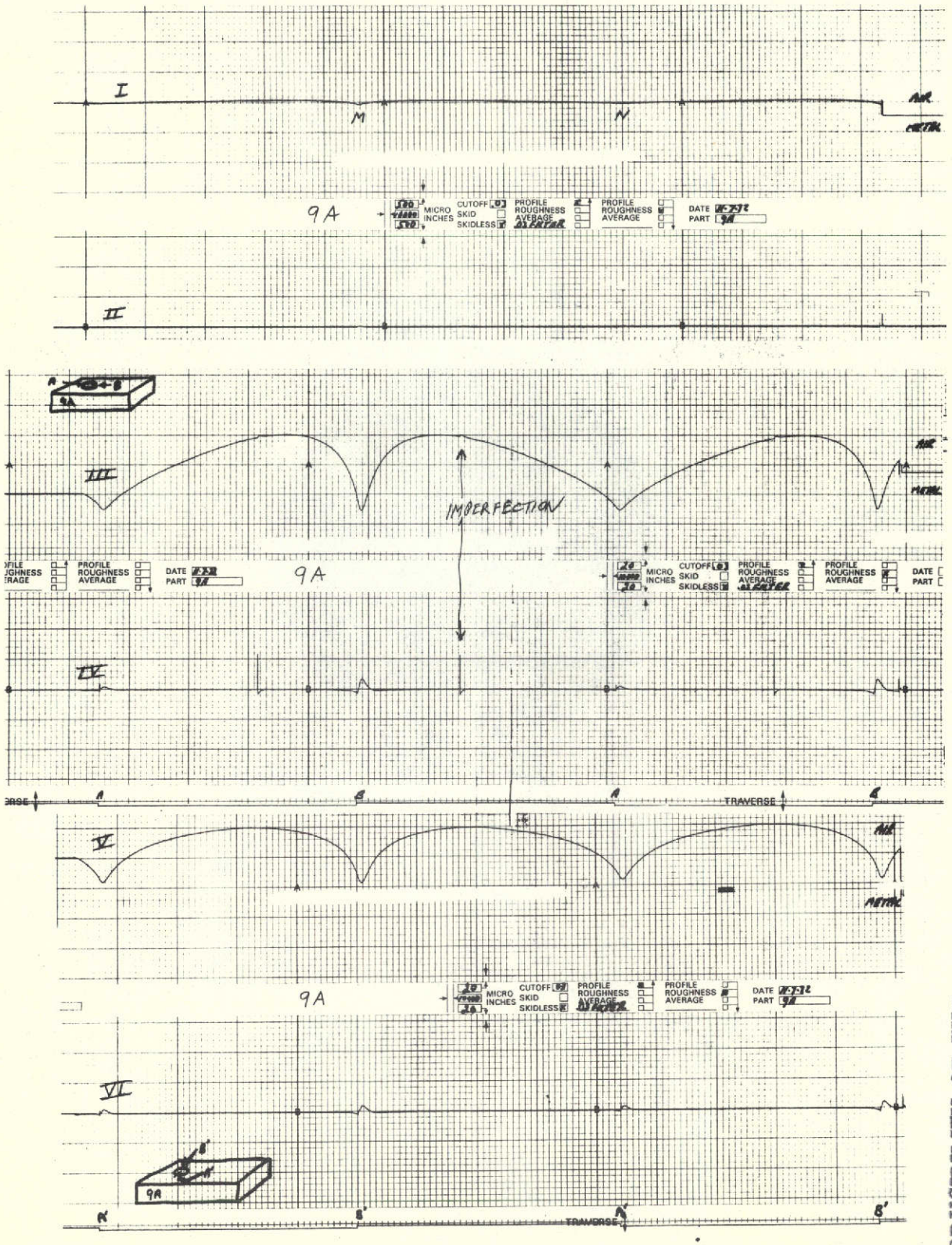

Fig. 2 -- Profile and roughness traces of seed 9-A.

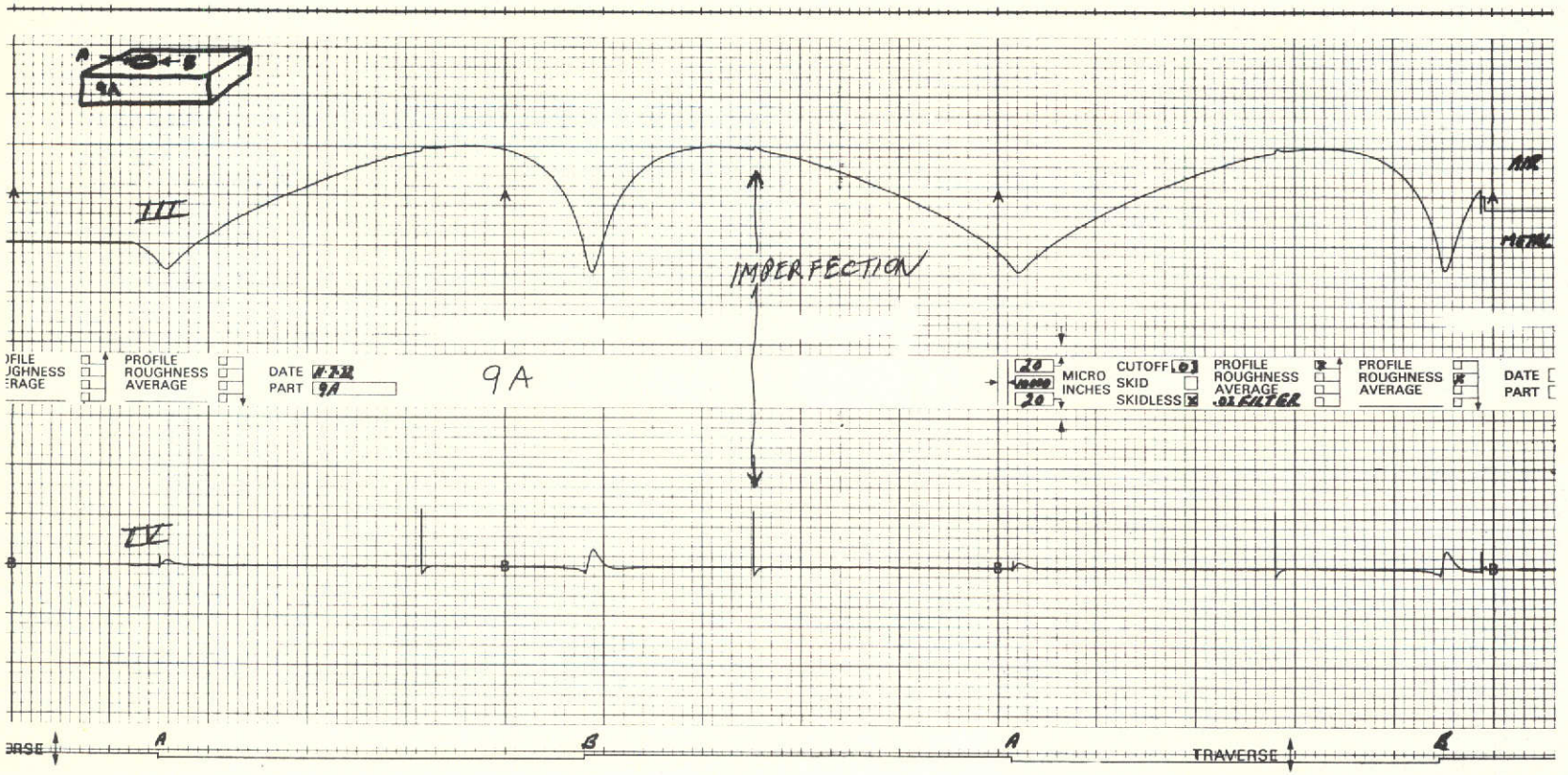

Fig. 3 -- Profile (curve III) and roughness (curve IV) traces of seed 9-A.

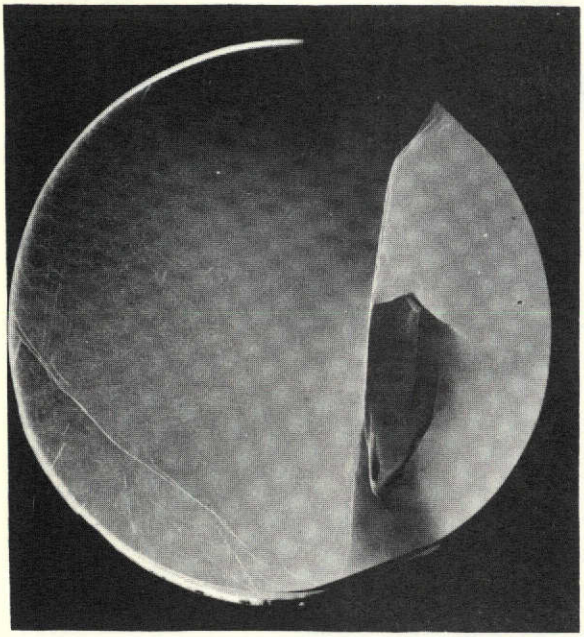

a

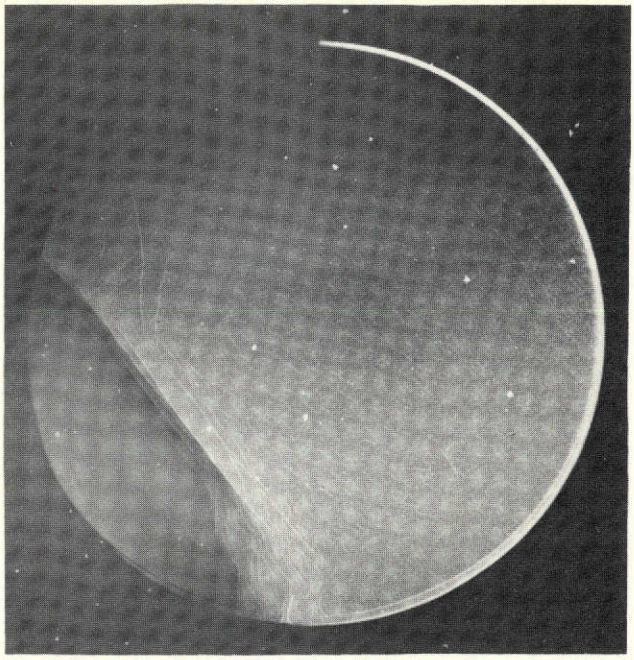

b

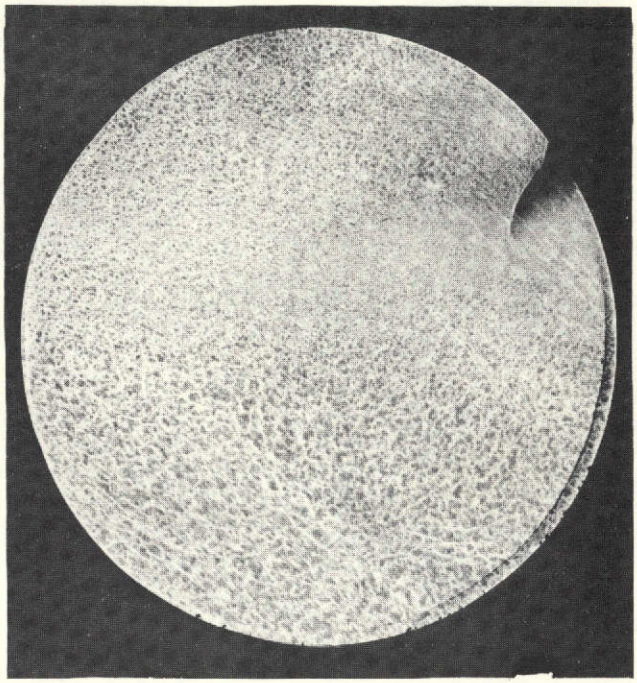

c

Fig. 4 -- Scanning back reflection topography, (a) substrate 2C, reflection (422); (b) substrate 4C, reflection (440); (c) substrate 1D, reflection (620).

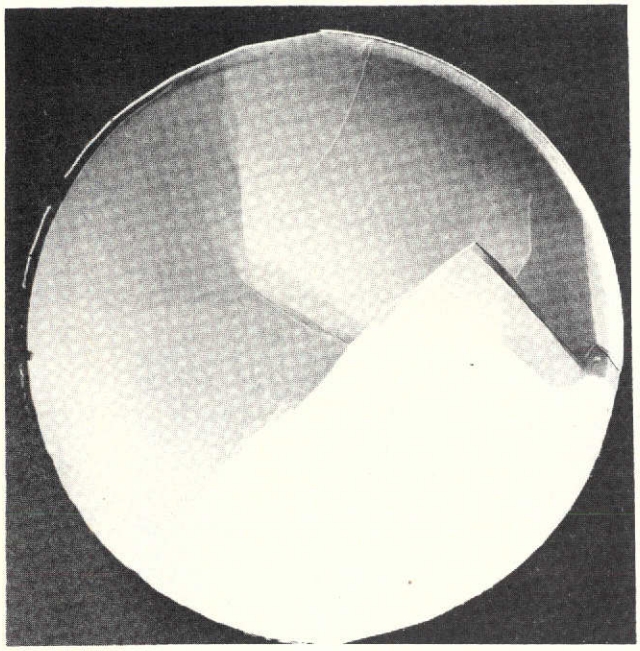

a

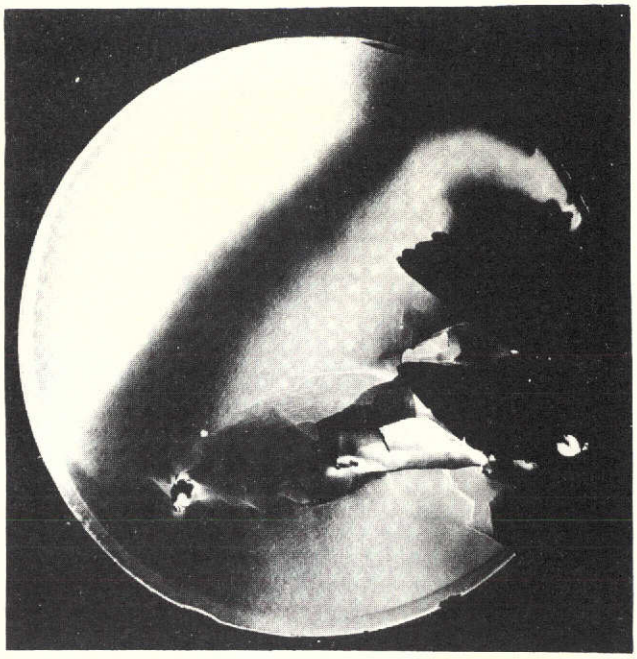

b

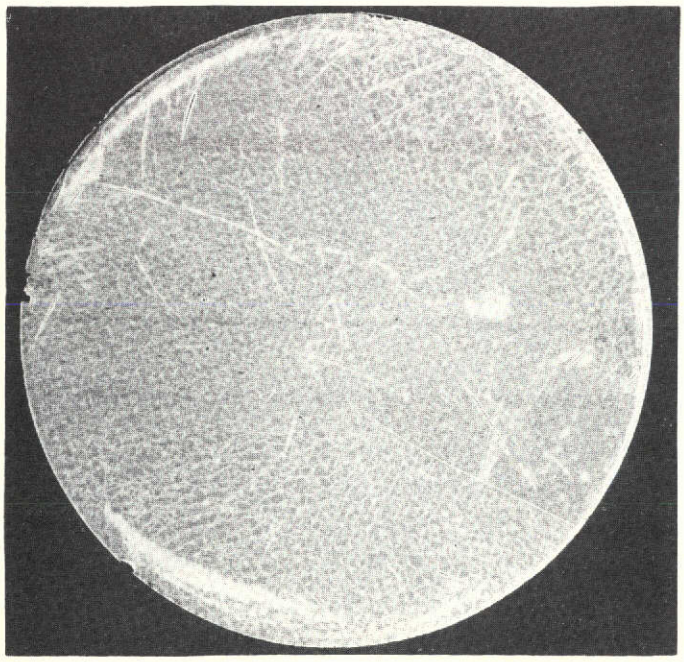

c

Fig. 5 -- SBRT, (a) substrate 3C, reflection (422); (b) substrate 3B, reflection (422); (c) substrate 13-8, reflection (531).

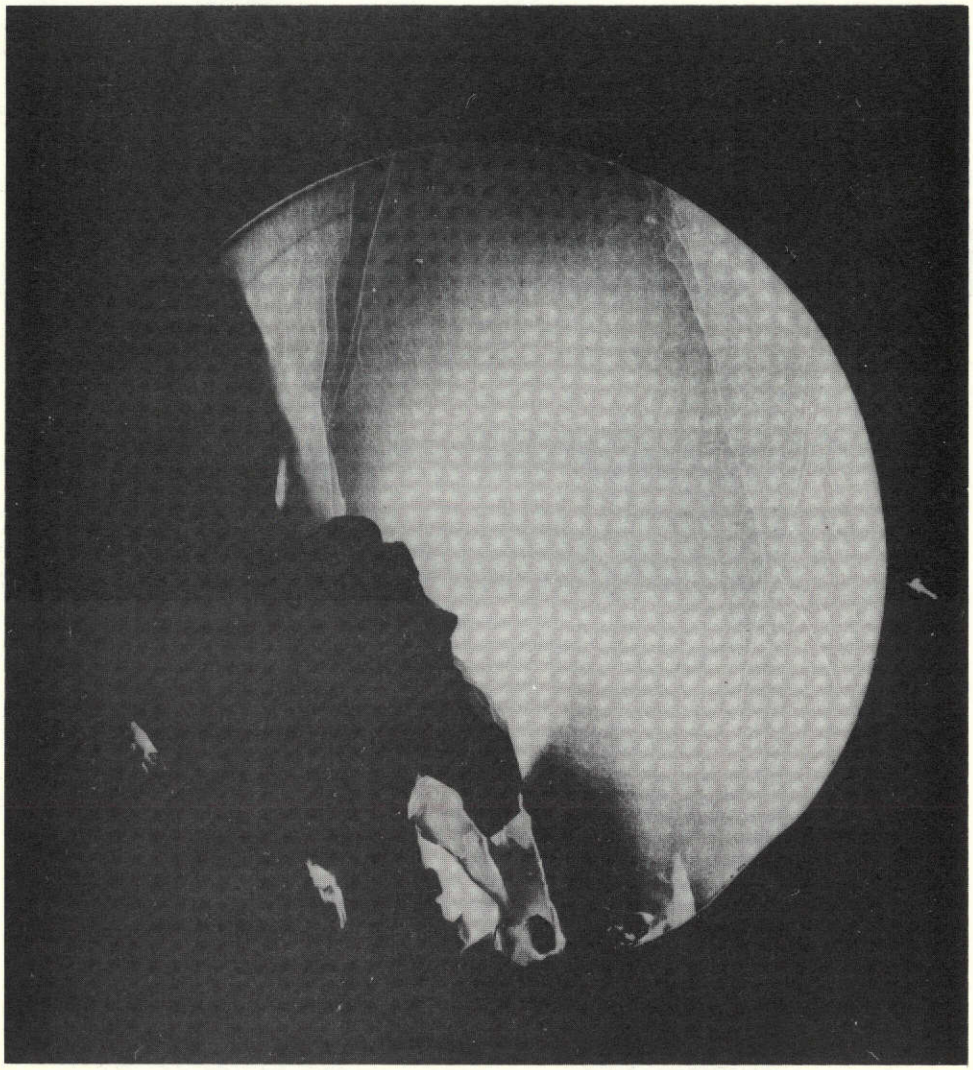

Fig. 6 -- SBRT photograph of rejected seed 1 C.

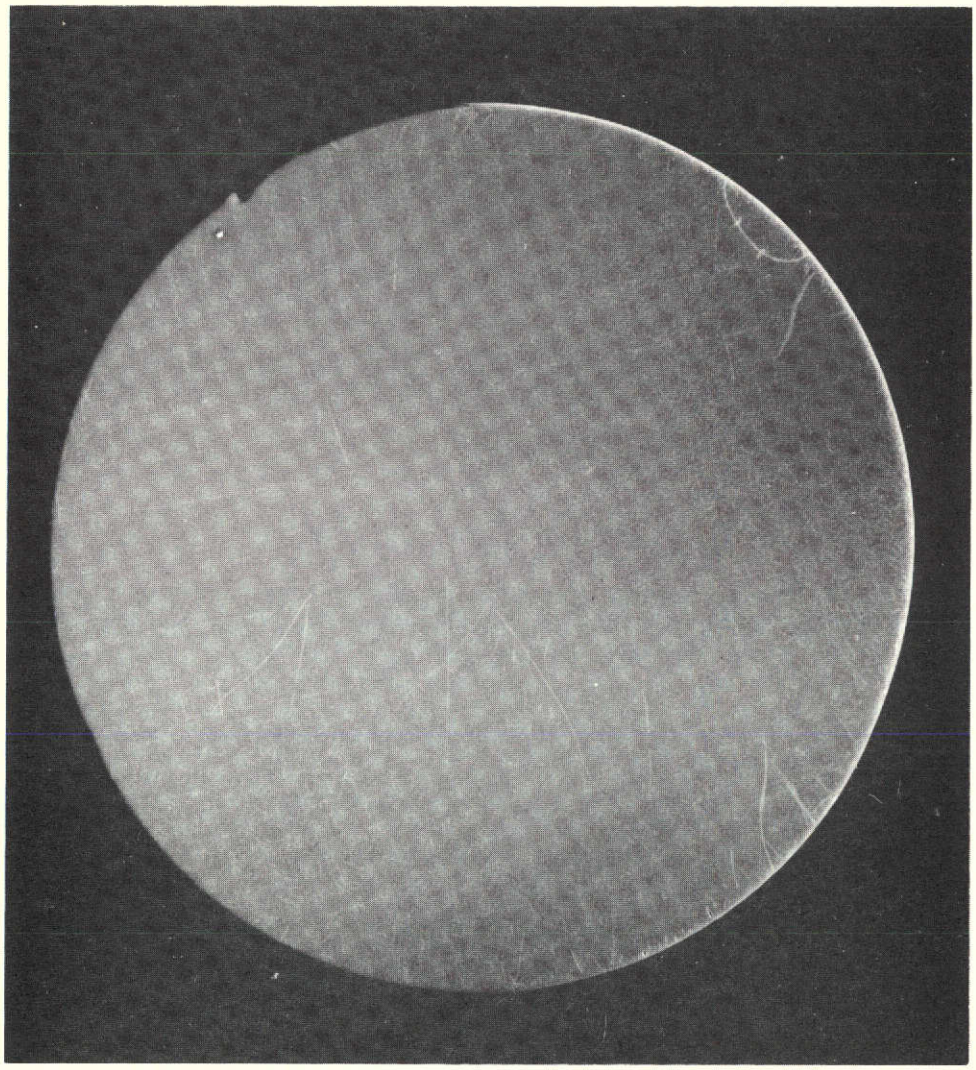

Fig. 7 -- SBRT photograph of flight seed 95-1 used in flight package ampoule 93-7.

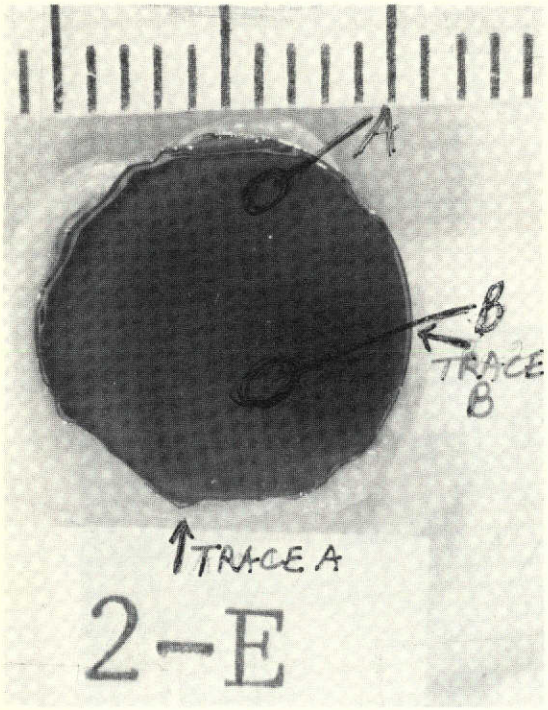

(a)

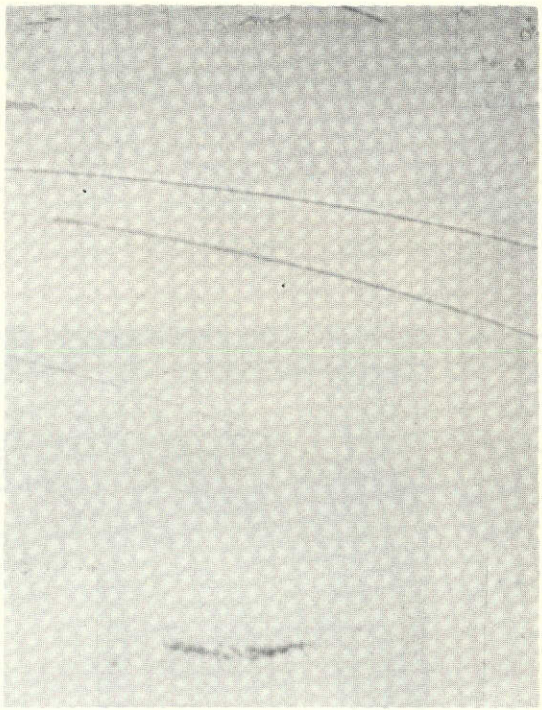

(b)

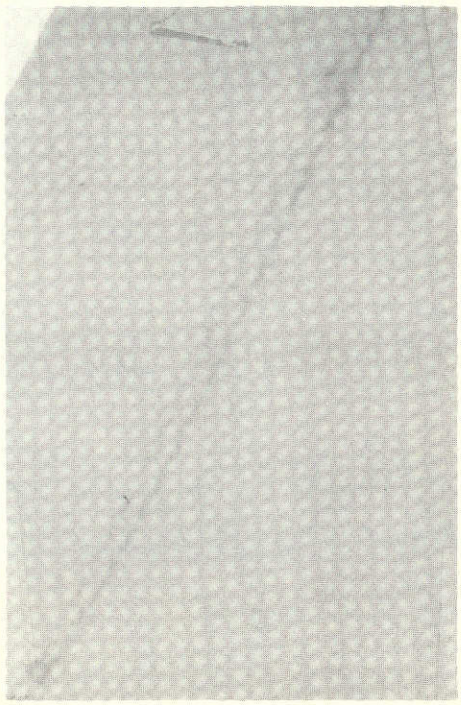

(c)

Fig. 8 -- Sample E-2. (a) Macrophotograph, positions A and B for microphotographic, arrows for traces A and B are for profile and roughness directions of traces; (b) 100X at point A (scratches); (c) 1000X at point B.

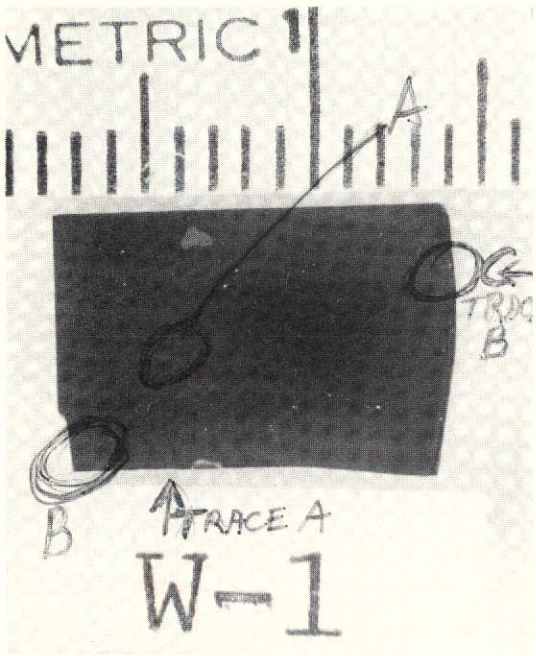

(a)

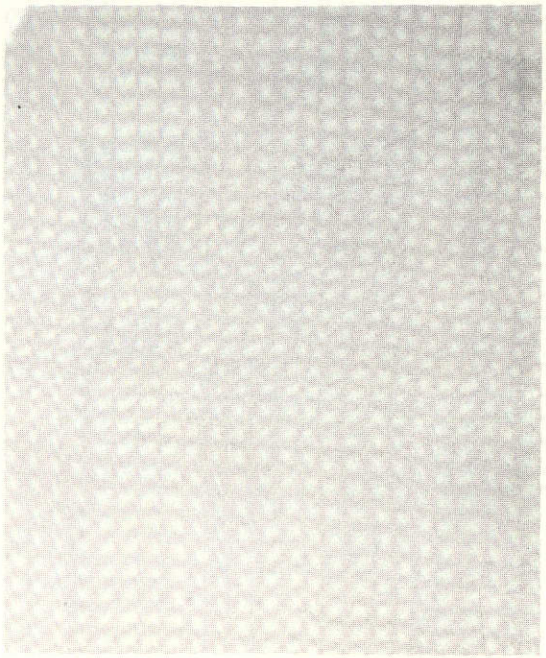

(b)

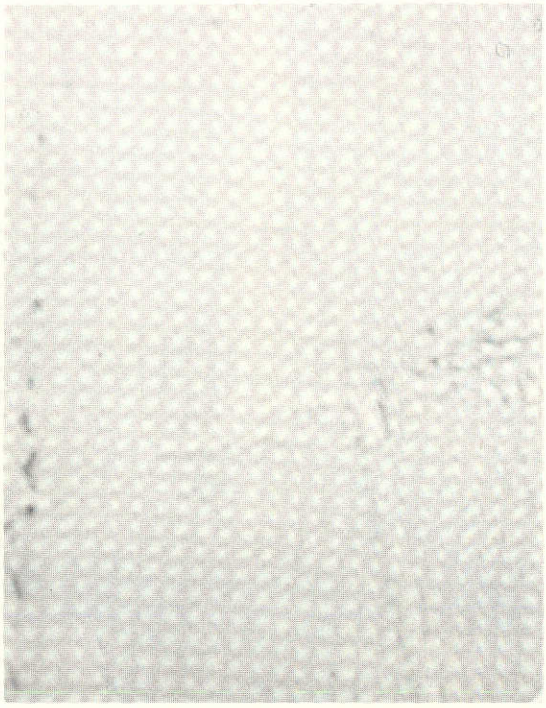

(c)

Fig. 9 -- Sample W-1. (a) Macrophotograph, positions B and C are areas for microphotographs, arrows for traces A and B are for profile and roughness directions of traces; (b) 100X at position B; (c) 100X at position C.

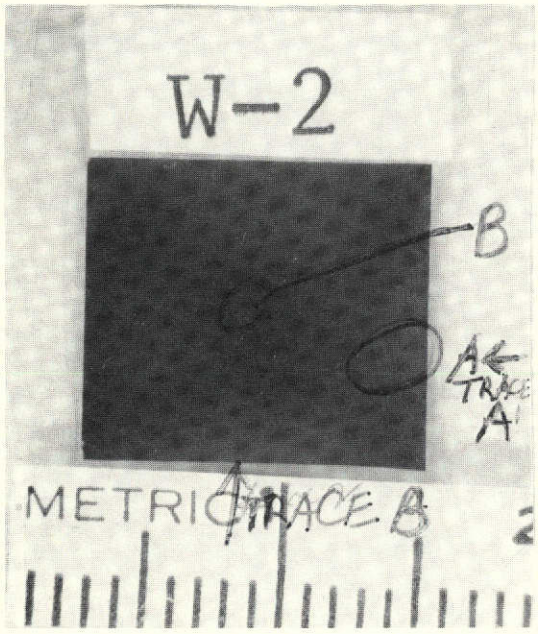

(a)

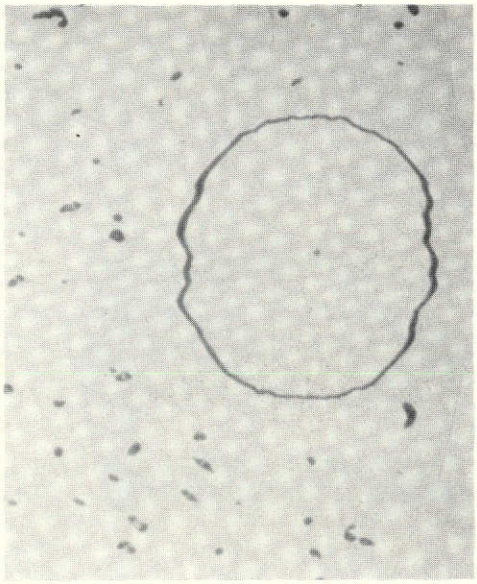

(b)

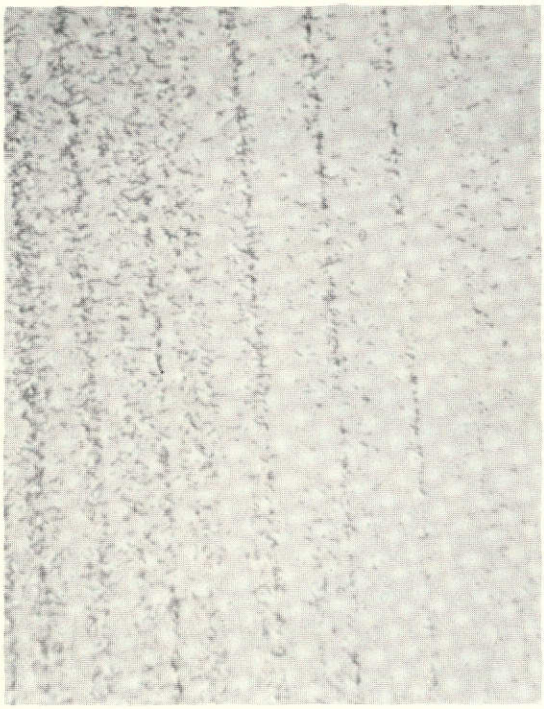

(c)

(d)

Fig. 10 -- Sample W-2. (a) Macrophotograph, positions A and B are areas for microphotographs, arrows for traces A and B are for profile and roughness directions of traces; (b) 300X at position B; (c) 100X at position A; (d) 800X at position A.

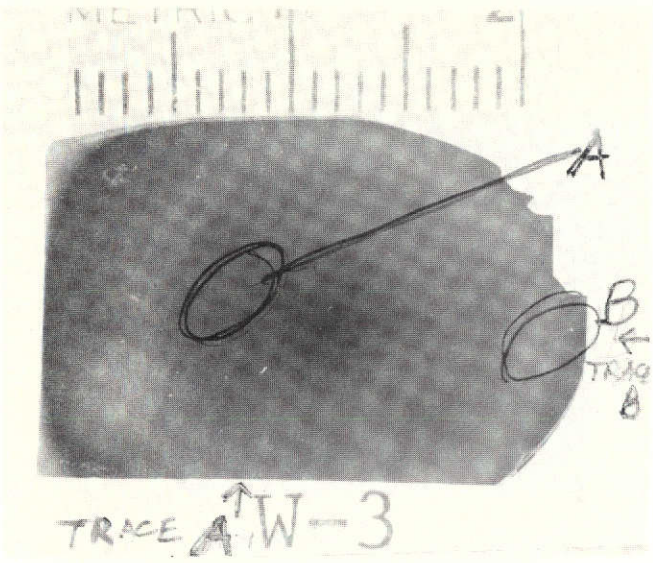

(a)

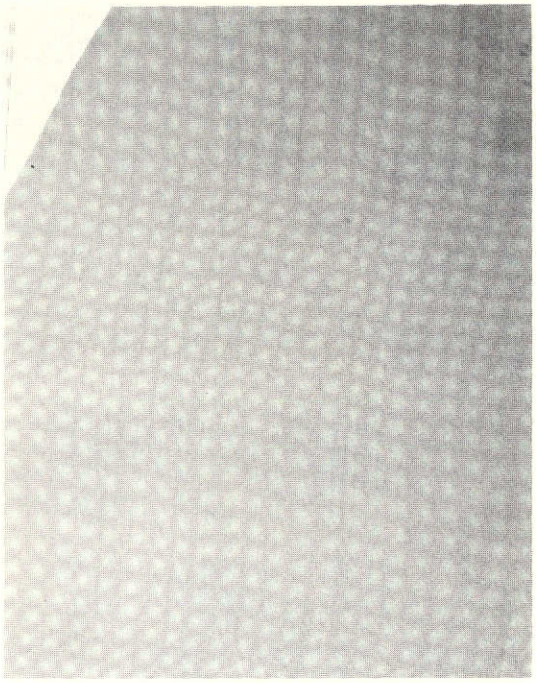

(b)

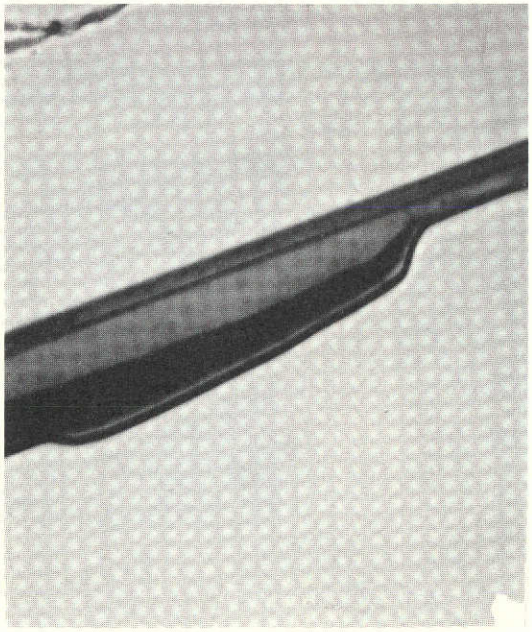

(c)

Fig. 11 -- Sample W-3. (a) Macrophotograph, positions A and B are areas for microphotographs, arrows for traces A and B are for profile and roughness directions of traces; (b) 100X at position A; (c) 100X at position B.

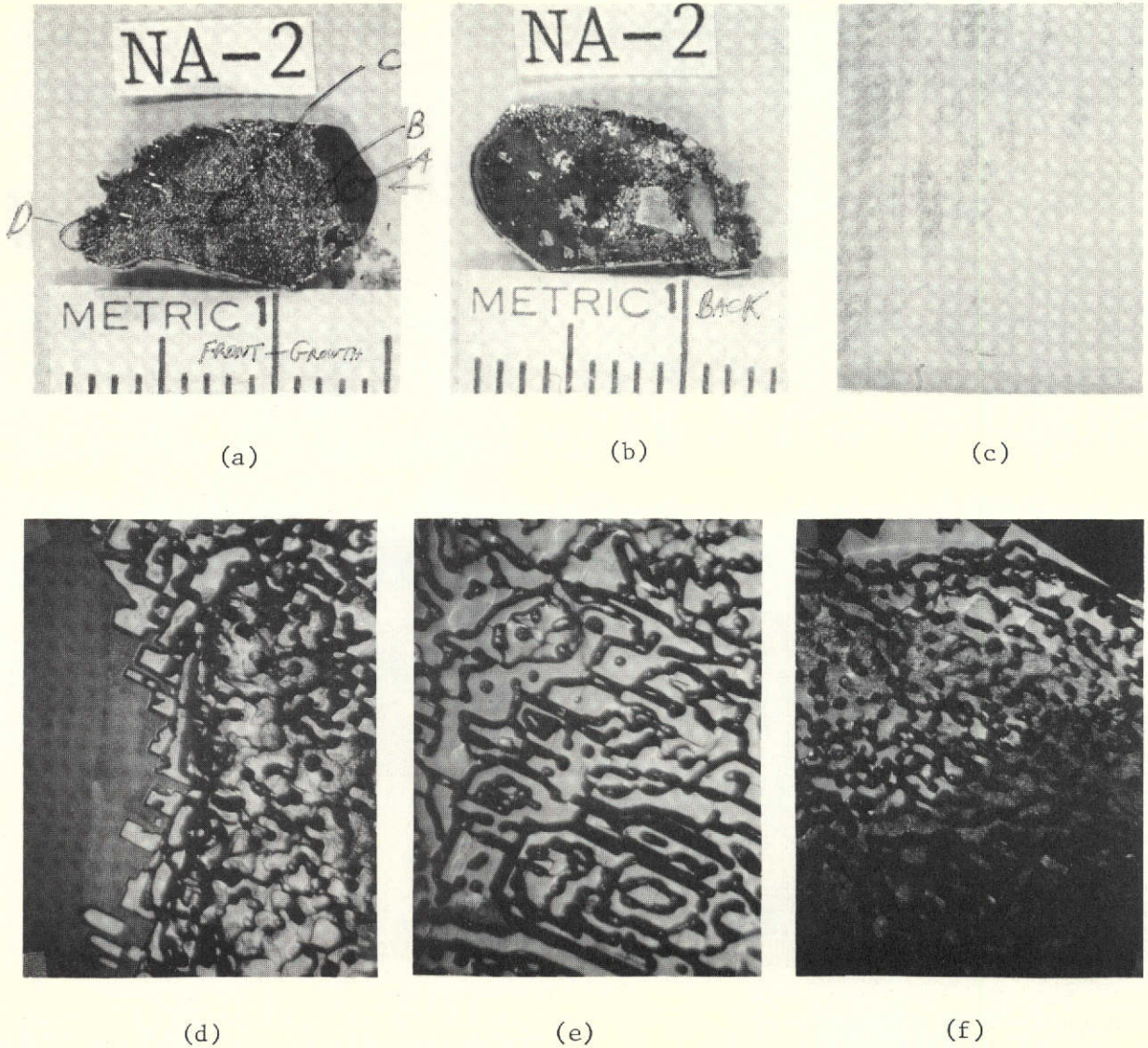

Fig. 12 -- Sample NASA-2. (a) Macrophotograph, growth surface positions A, B. D. C are areas for microphotographs; (b) macrophotograph, back, non-growth surface; (c) 300X at position A; (d) 100X at position B; (e) 100X at position C; (f) 100X at position D.

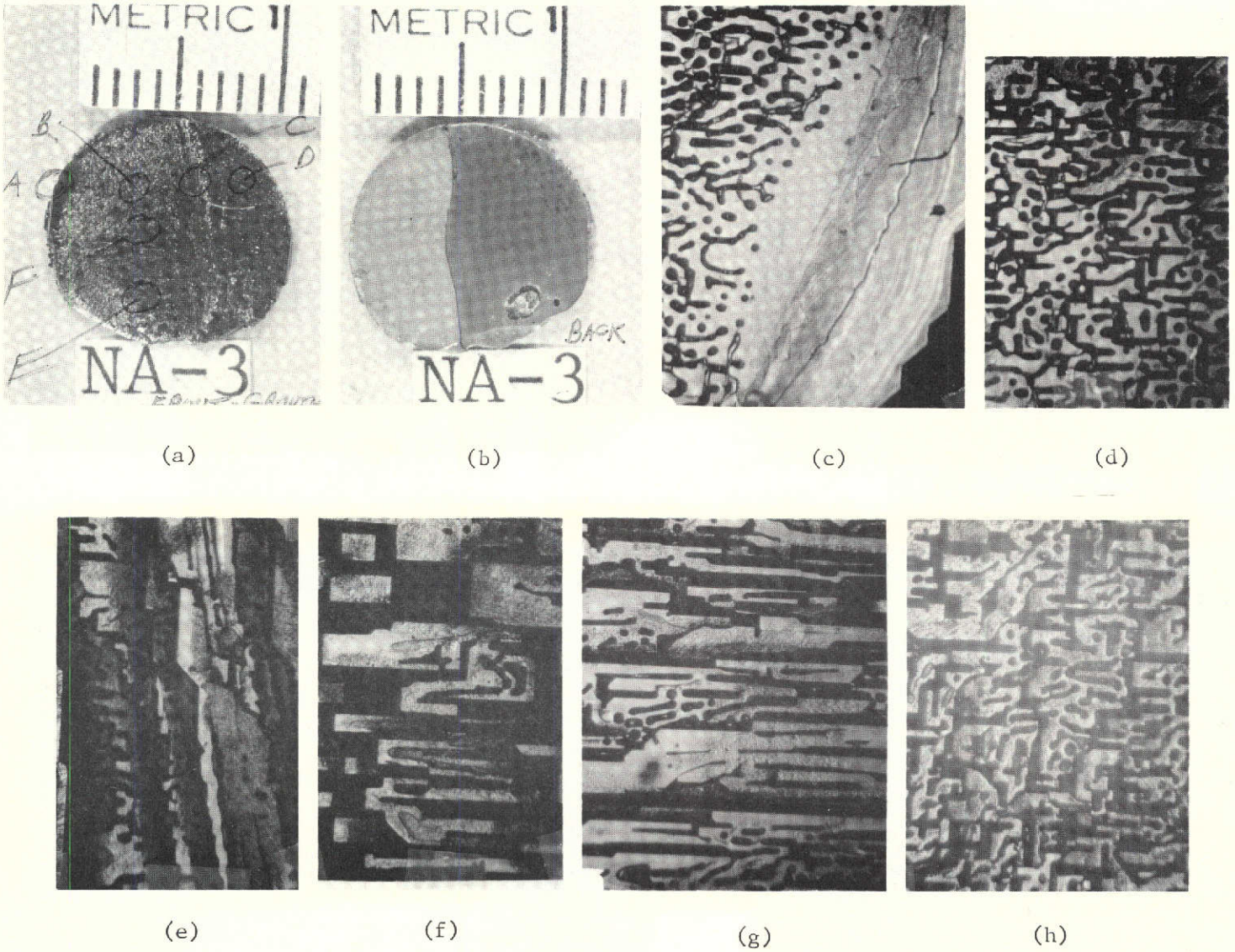

Fig. 13 -- Sample NASA-3. (a) Macrophotograph, growth surface, positions A, B, C, D, E, F are areas for microphotographs; (b) macrophotograph, back, non-growth surface; (c) 100X at position A; (d) 100X at position B; (e) 100X at position C; (f) 100X at position D; (g) 100X at position E; (h) 100X at position F.

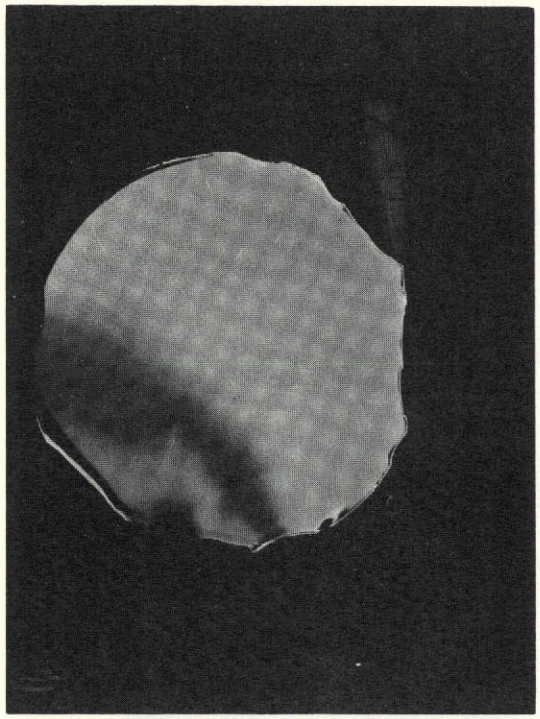

(a)

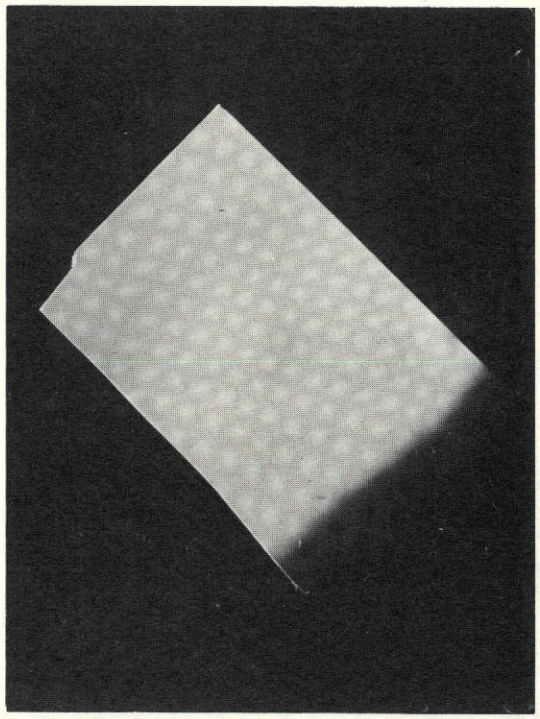

(b)

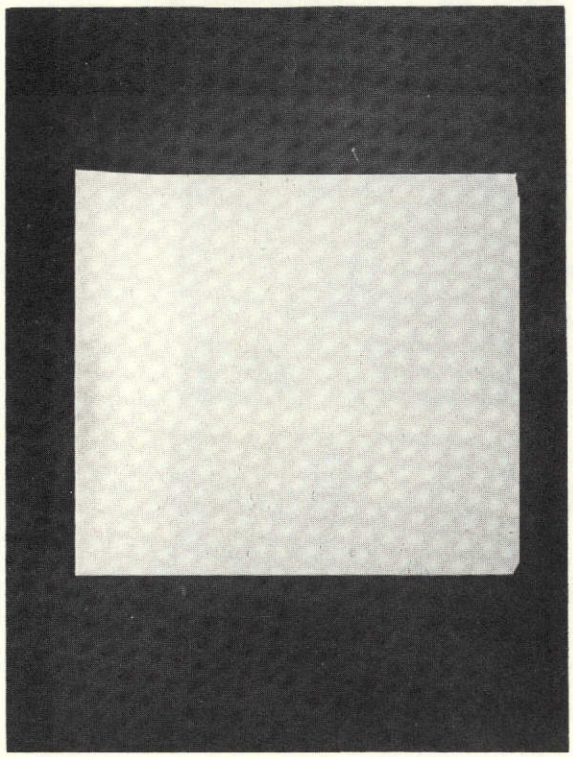

(c)

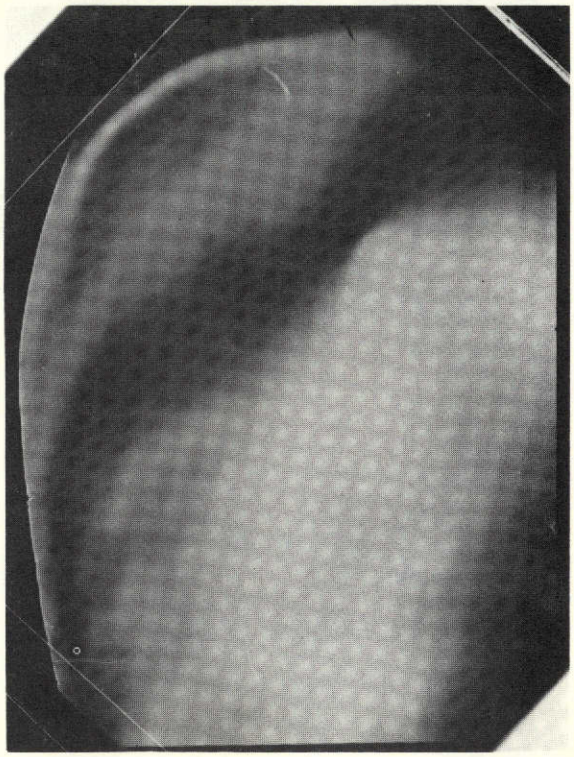

(d)

Fig. 14 -- SBRT, (a) E-2, reflection (422); (b) W-1, reflection (440); (c) W-2, reflection (422); (d), W-3, reflection (440).

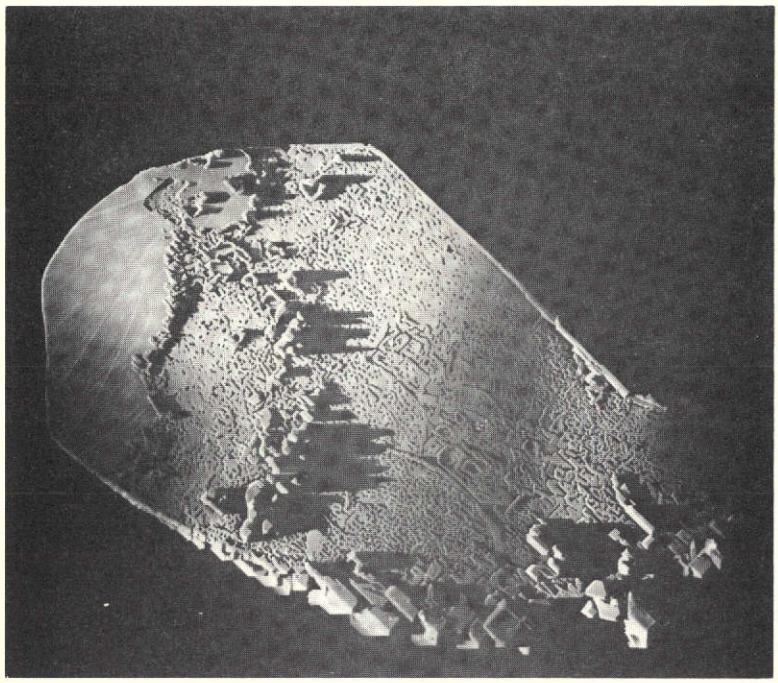

(a)

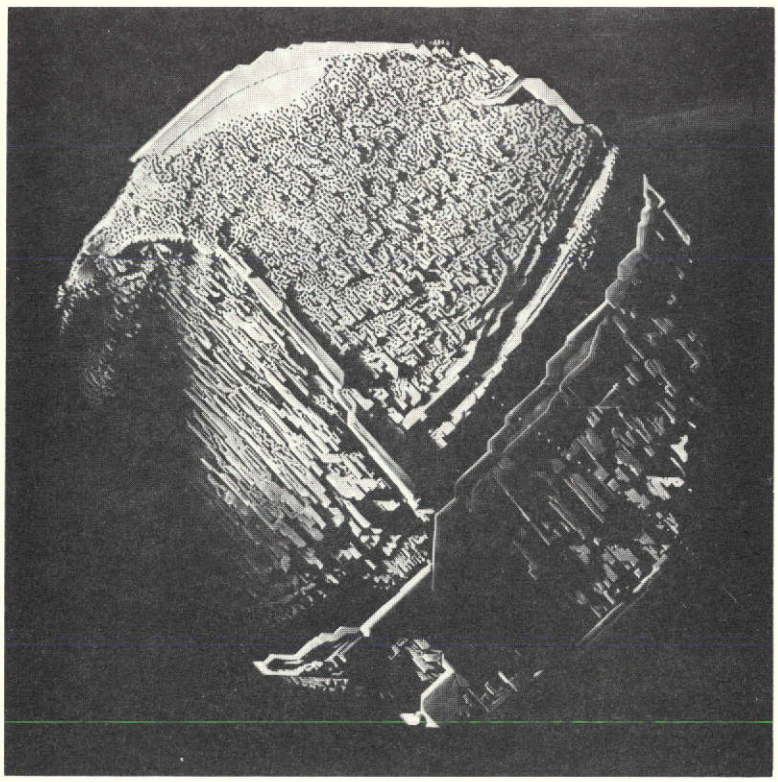

(b)

Fig. 15 -- SBRT, (a) NASA-2, reflection (440), (b) NASA-3, reflection (440).

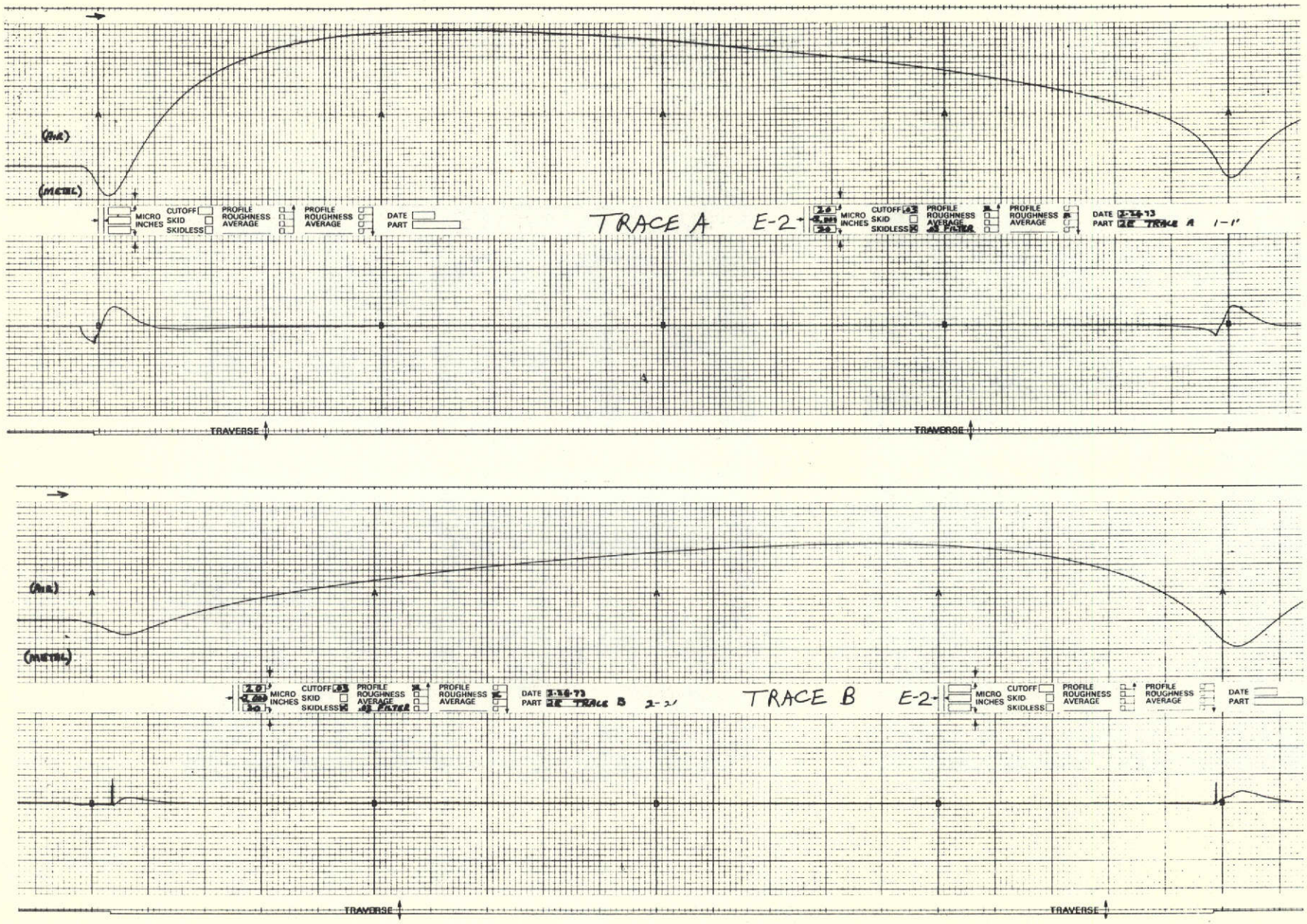

Fig. 16 -- Profile and roughness traces of E-2. Vertical scale -- 20 microinches per division, horizontal scale -- 2,000 microinches per division.

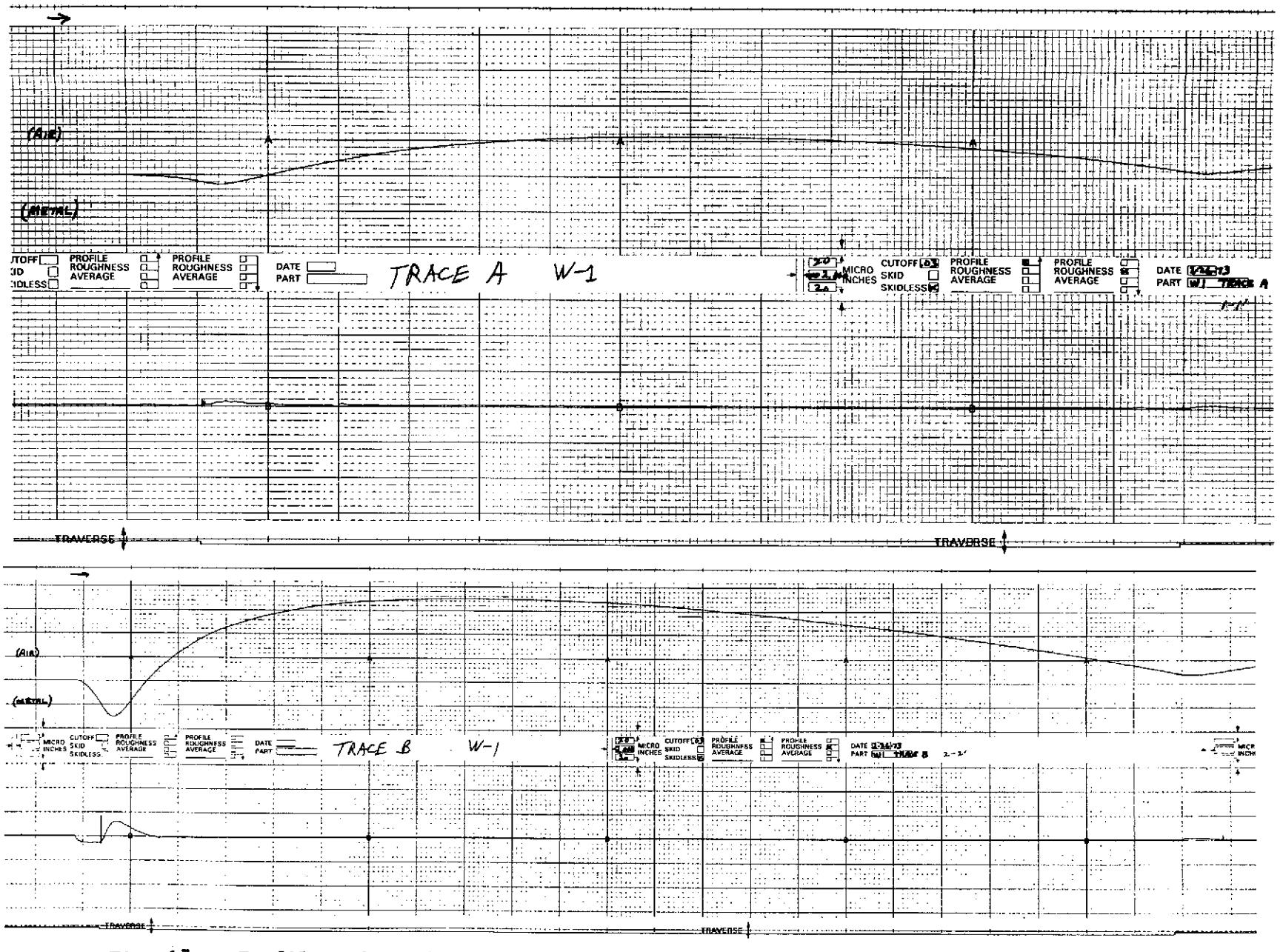

Fig. 17 -- Profile and roughness traces of W-1. Vertical scale -- 20 microinches per division, horizontal scale -- 2,000 microinches per division.

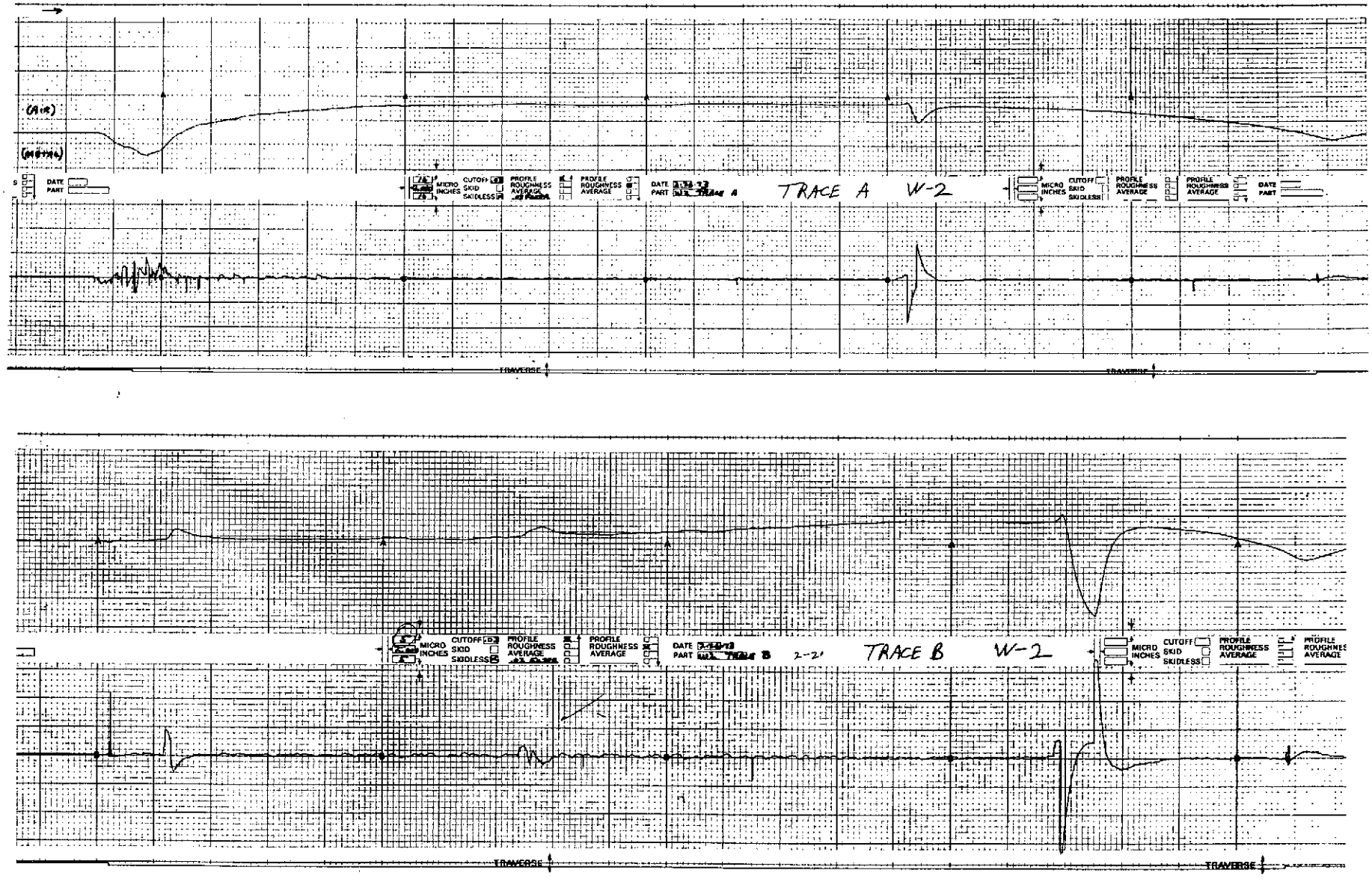

Fig. 18 -- Profile and roughness traces of W-2. Vertical scale -- trace A, 10 microinches, trace B, 5 microinches per division, horizontal scale -- 2,000 microinches per division.

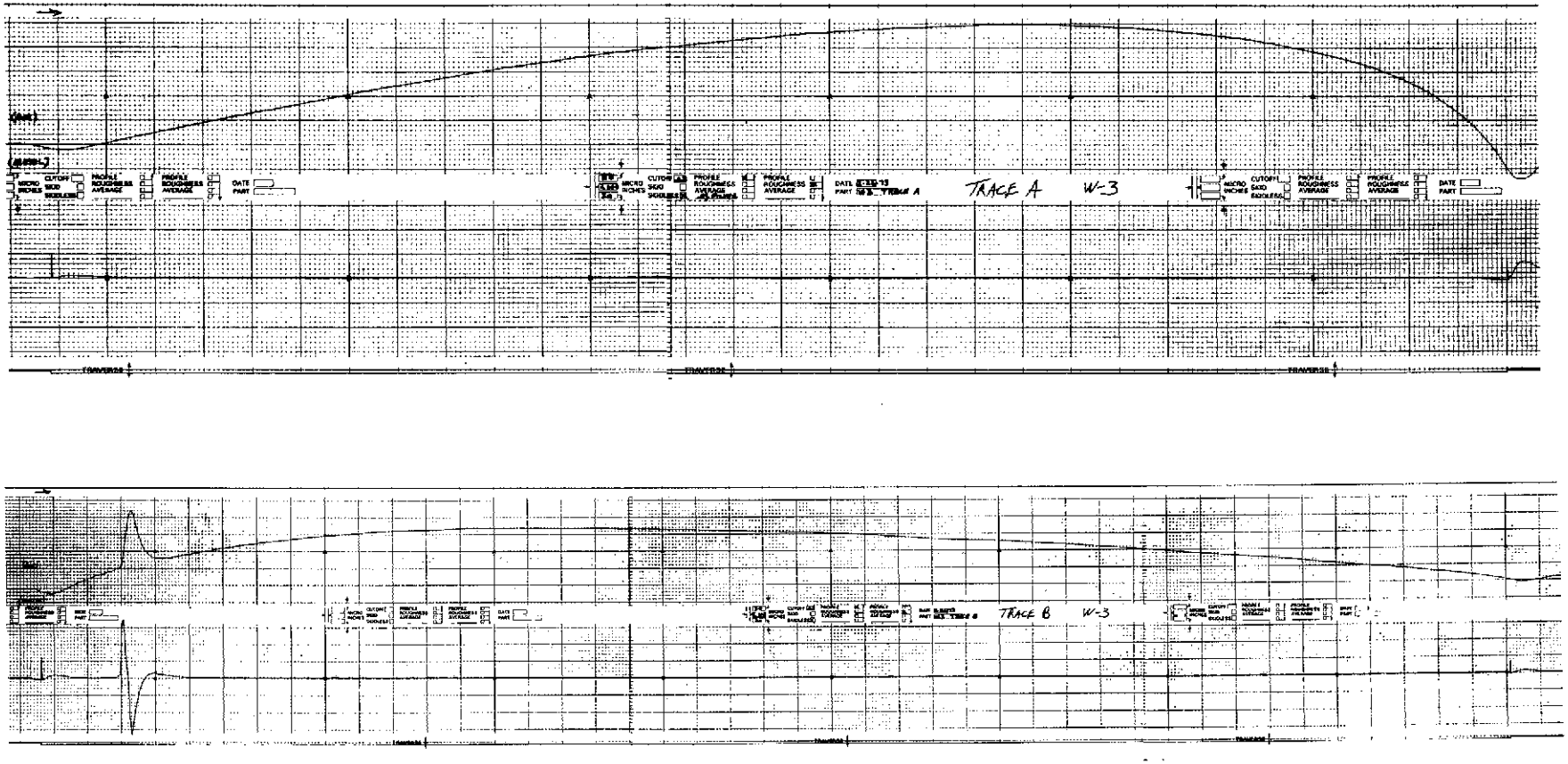

Fig. 19 -- Profile and roughness traces of W-3. Vertical scale -- 20 microinches per division, horizontal scale -- 2,000 microinches per division.

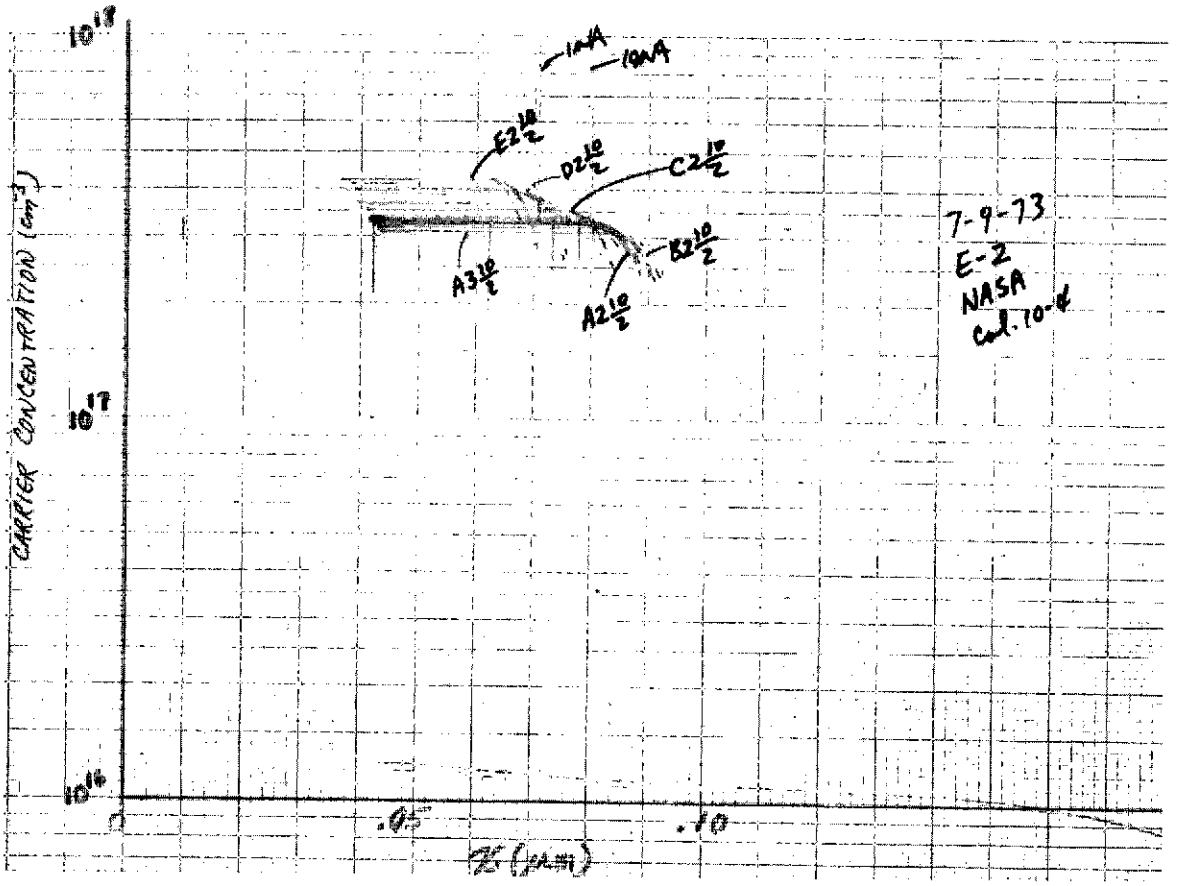

Fig. 20 -- Copeland profiles measured at the gold Schottky barrier dots on the sample E-2 (.010" dots used)

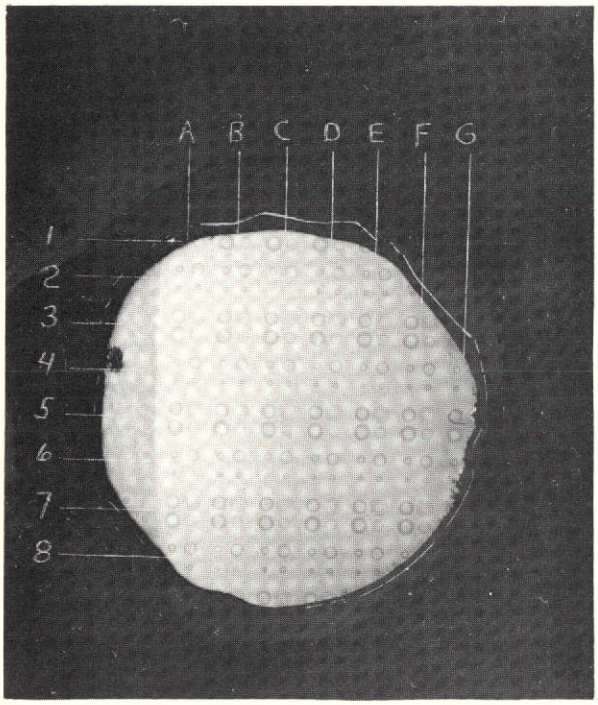

(a)

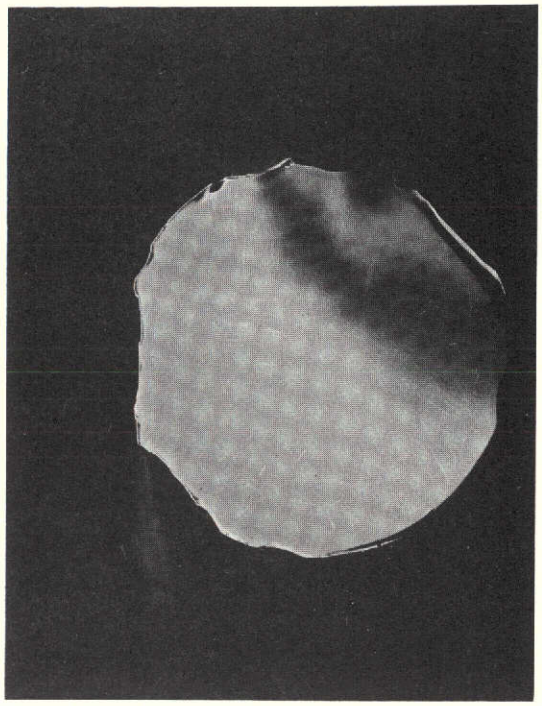

(b)

$(n \times 10^{-17})$

	A	B	C	D	E	F	G
1							
2	3.3	3.3	3.5	4.0	4.25		
3	3.1	3.35	3.3	3.8	3.9	4.3	
4	3.2	3.3	3.3	3.5	3.9	4.25	
5	3.1	3.2	3.25	3.4	3.6	4.1	
6	3.05	3.15	3.3	3.3	3.55	4.0	
7	3.05	3.25	3.3	3.25	3.35	3.7	
8	2.95	3.1	3.2	3.25	3.3		

(c)

Fig. 21 -- Concentration mapping on the surface and scanning back reflection x-ray topography. (a) Mapping of the Schottky barrier dots, (b) SBRT, and (c) mapping of the concentration on E-2.

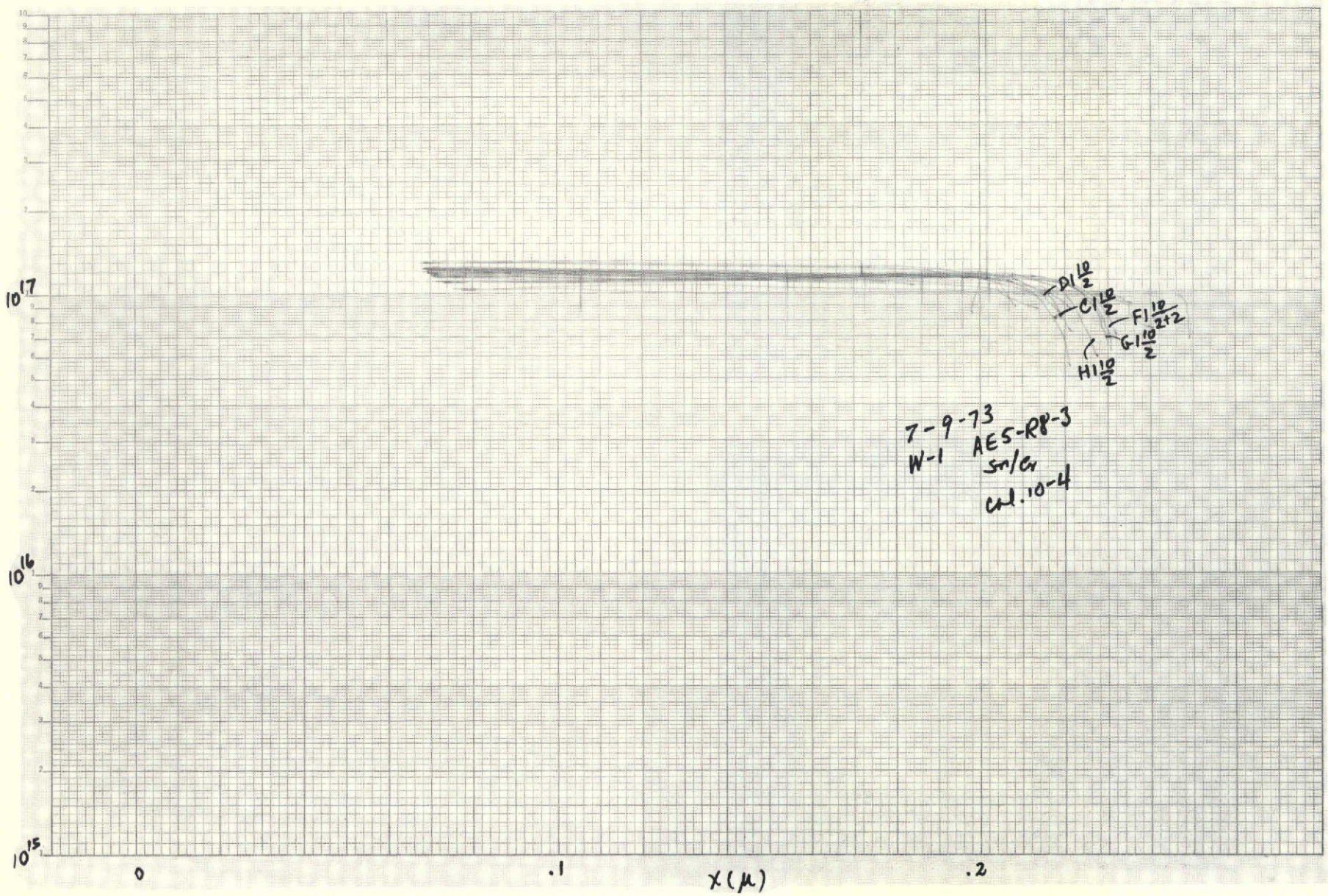

Fig. 22 -- Copeland profiles measured at the gold Schottky barrier dots on the sample W-1 (.010" dots used).

W-1 AE5-R8-3 Sn/Cr

$t \simeq 4.0\ \mu$

A B C D E F G H I

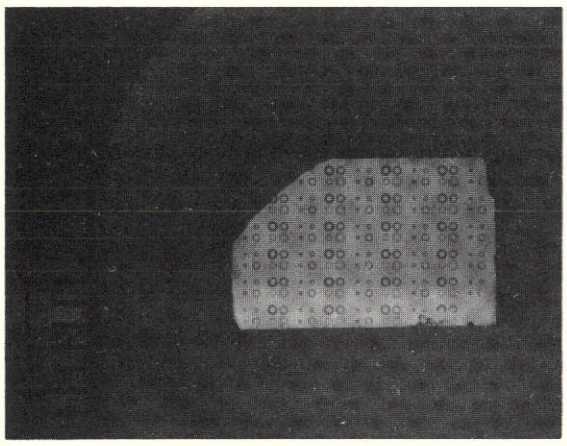

(a)

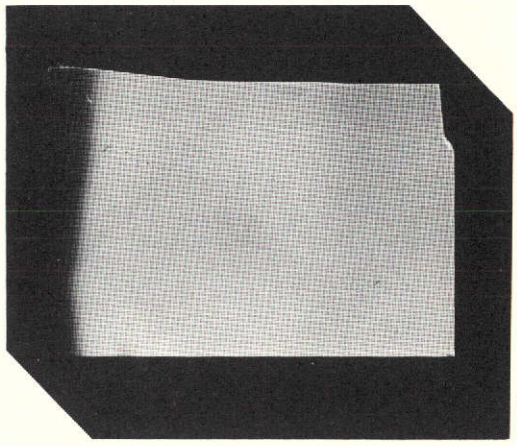

(b)

$(n \times 10^{-17})$

	A	B	C	D	E	F	G	H	I
1			1.2	1.2	--	1.15	1.2	1.2	
2			1.2	1.2	1.2	1.2	1.2	1.2	
3	1.25	1.25	1.2	1.2	1.2	1.15	1.15	--	
4	1.25	1.25	1.2	1.2	--	1.15	--	1.15	
5	1.25	1.2	1.15	1.1	1.1	1.1	1.1	1.1	
6				1.05	/	1.0			

(c)

Fig. 23 -- Concentration mapping on the surface and SBRT. (a) Mapping of the Schottky barrier dots, (b) SBRT, and (c) mapping of the concentration on W-1.

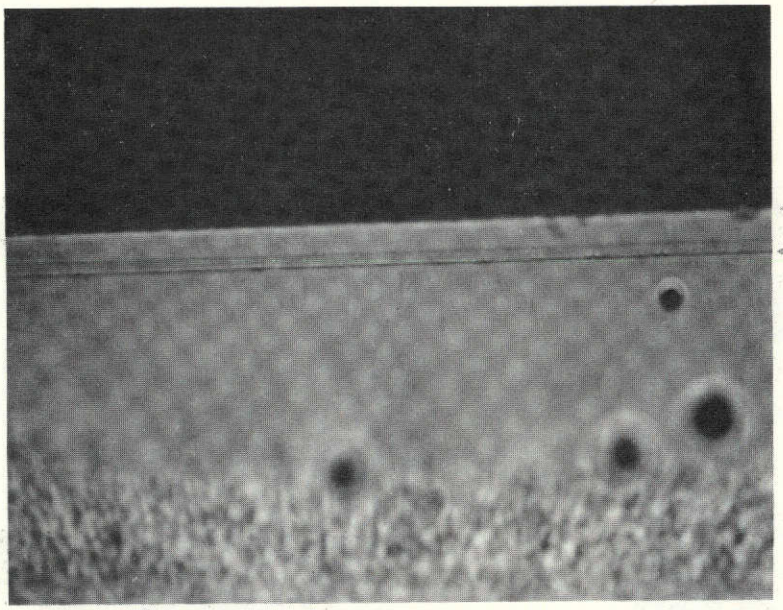

Fig. 24 -- Photomicrograph of the cleave-delineated cross-section in {110} of sample (A) W-1, (B) W-2.

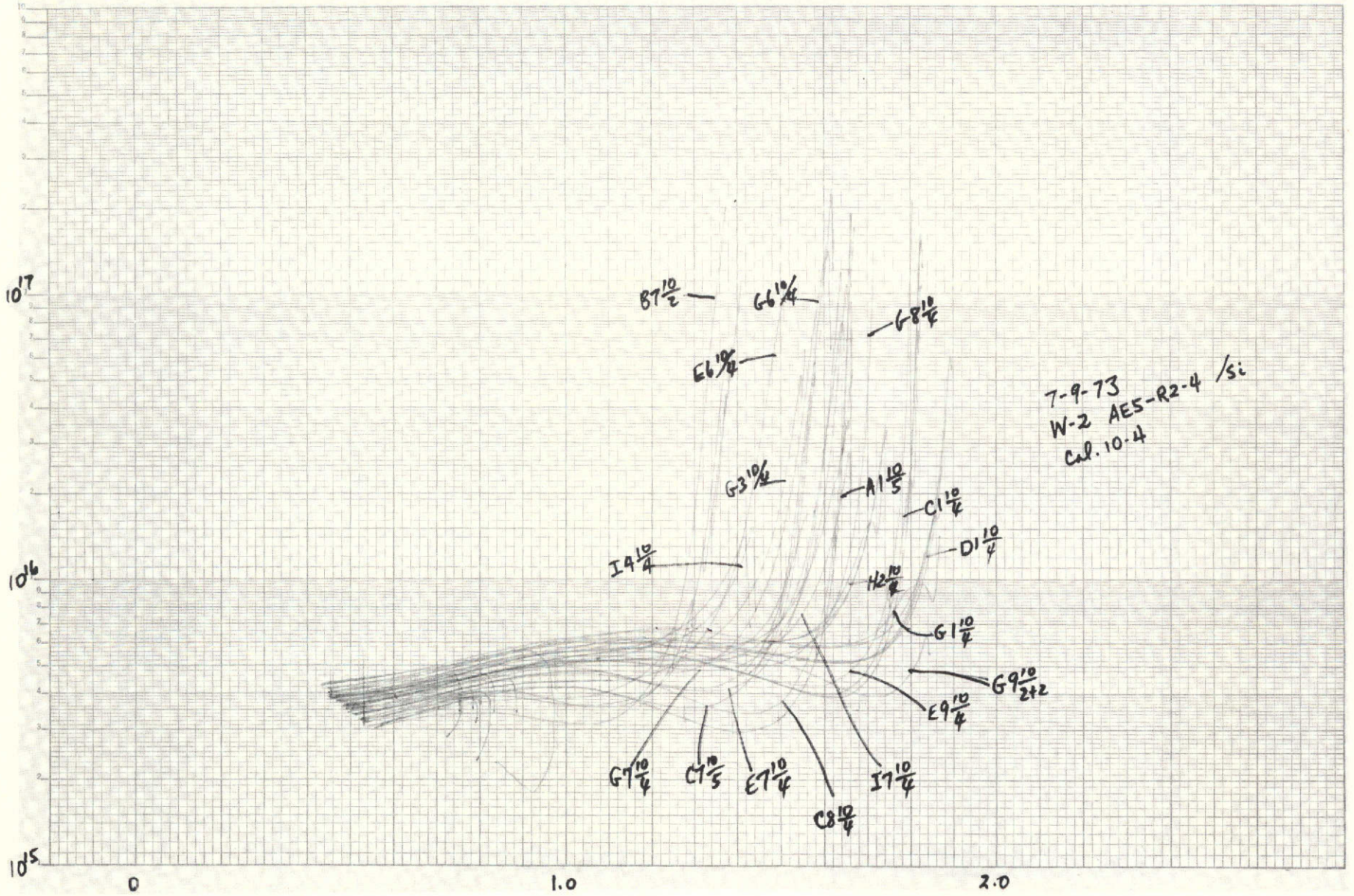

Fig. 25 -- Copeland profiles measured at the gold Schottky barrier dots on the sample W-2 (.010" dots used).

W-2 AE5-R2-4 /Si

t = 2.3 μ

A B C D E F G H I J

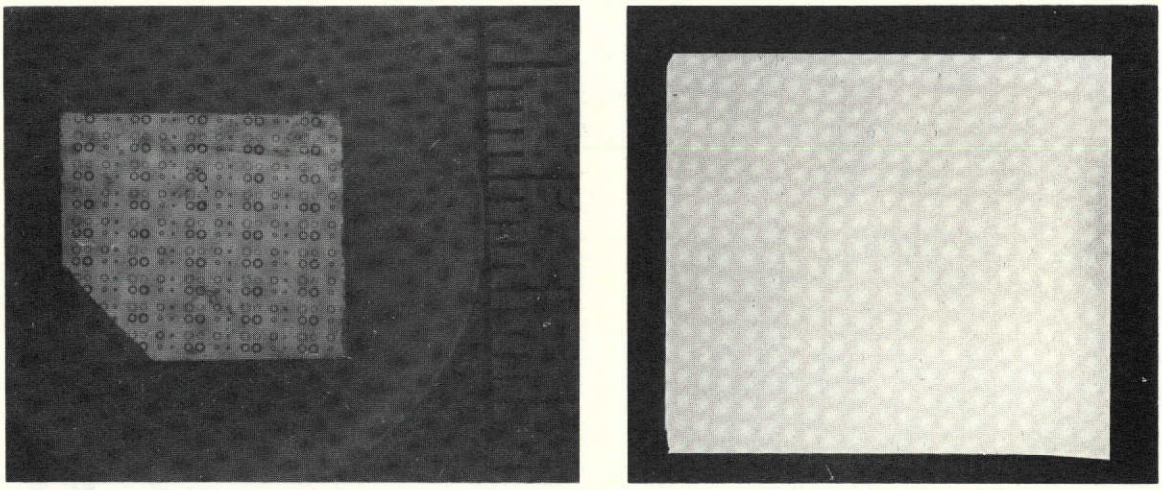

(a) (b)

$(n \times 10^{-15})$

	A	B	C	D	E	F	G	H	I
1	3-4		3.8-5.8	--	4-6.2	--	4.3-6.8	--	
2			3.6-5	--	3.8-5.4	--	4-6	4.3-6.7	stained
3		3.3-4	/	/	/	4-6	4-5.2	--	/
4			/	--	/	--	3.6-5	--	4-6
5			3.1-3.8	--	/	--	/	--	/
6			/	--	3.4-4.4	--	3.5-4.8	--	/
7		3-3.4	3.2-4.4	--	3.5-4.7	--	3.8-5.2	--	3.7-5.3
8			3.4-4.8	--	/	--	4.2-5.2	--	4.2-6.3
9					3.9-5.6	--	3.9-5.6	--	

(c)

Fig. 26 -- Copeland profiles measured at the gold Schottky barrier dots in the sample W-2 (.010" dots used).

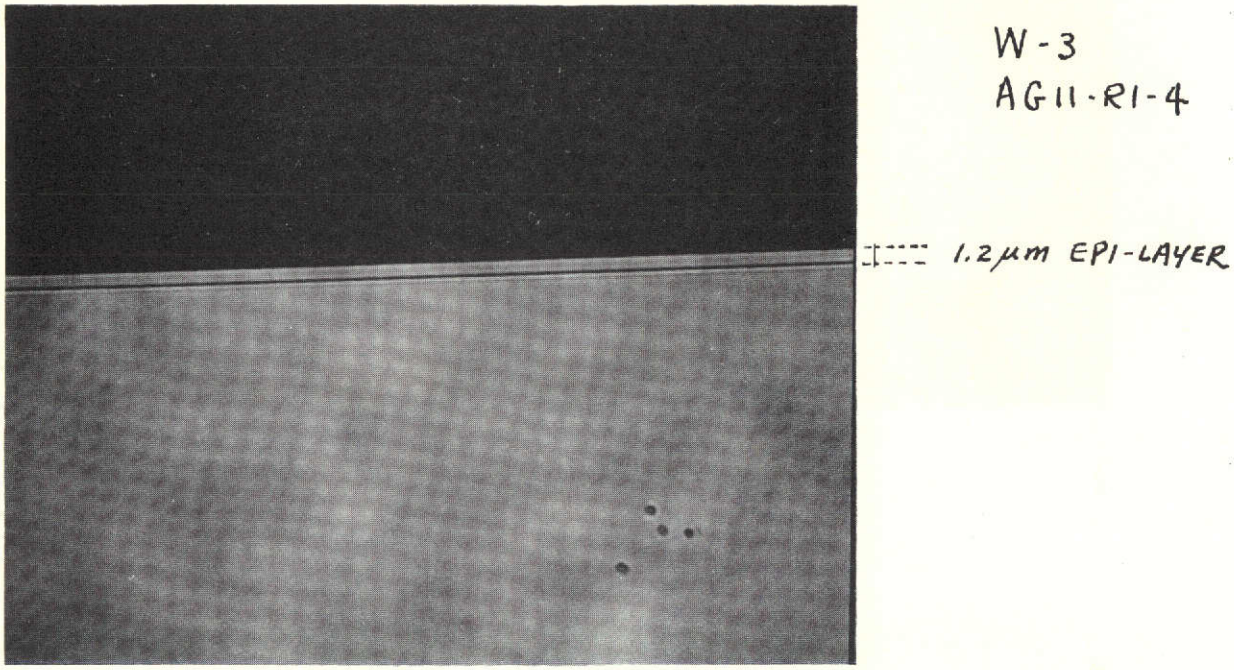

Fig. 27 -- Photomicrograph of the cleave-delineated cross-section in {110} of sample W-3.

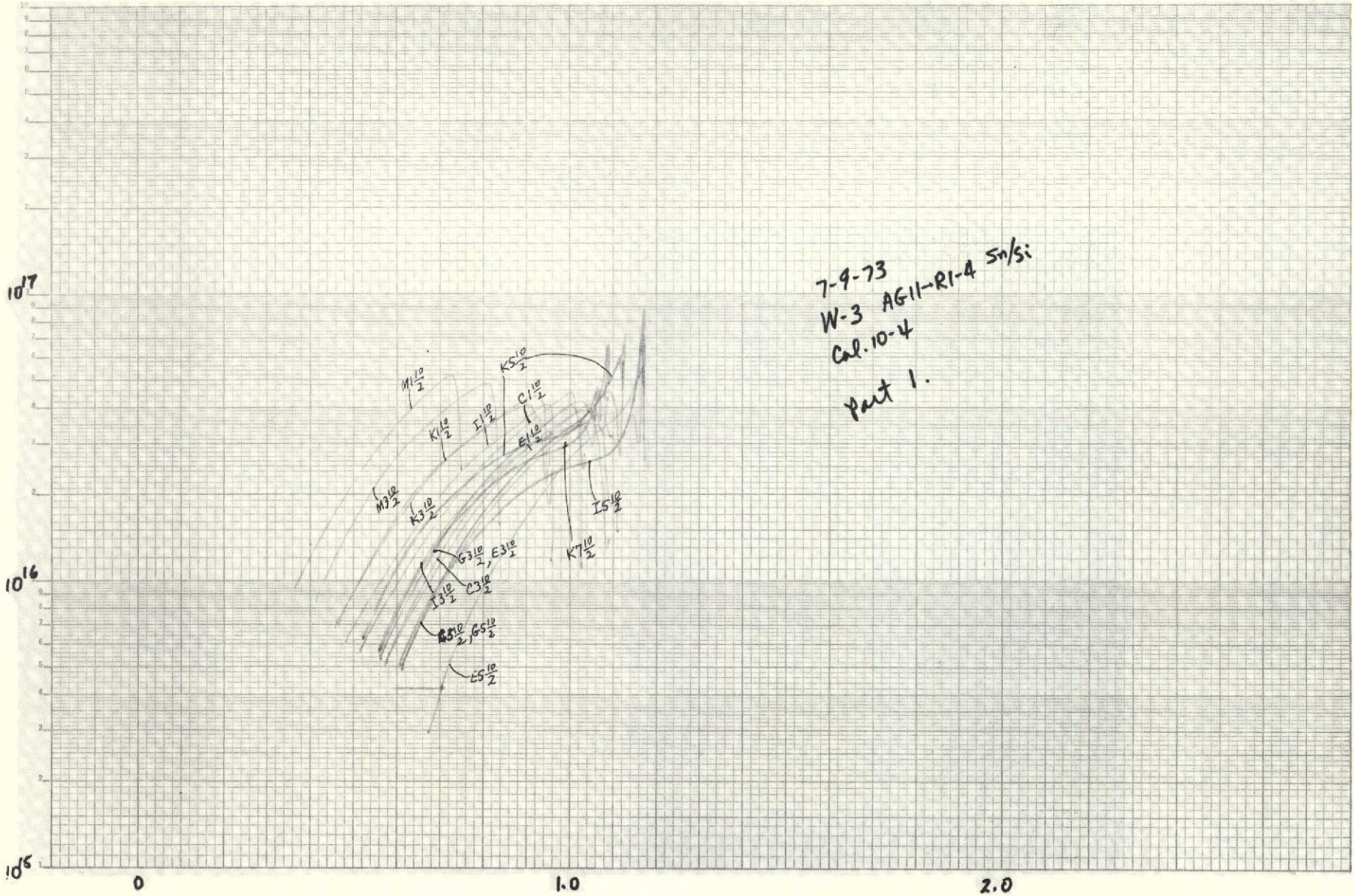

Fig. 28 -- Copeland profiles measured at the gold Schottky barrier dots on the sample W-3 (.010" dots used).

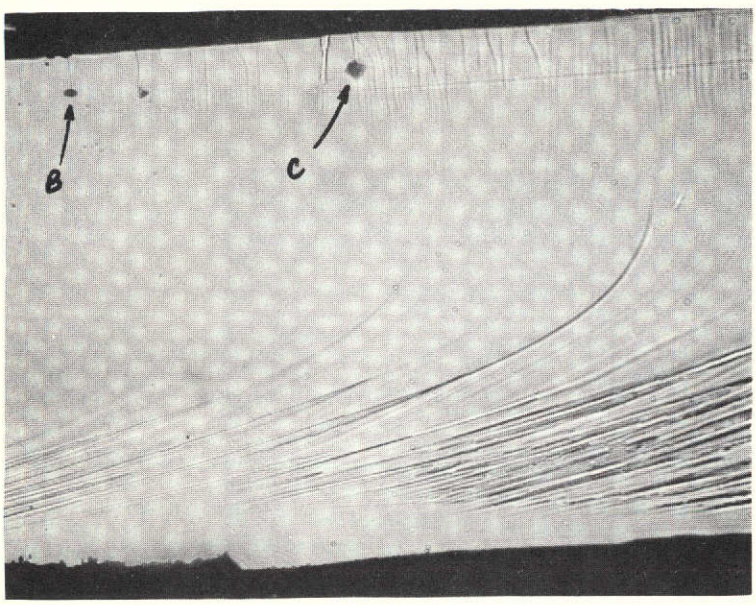

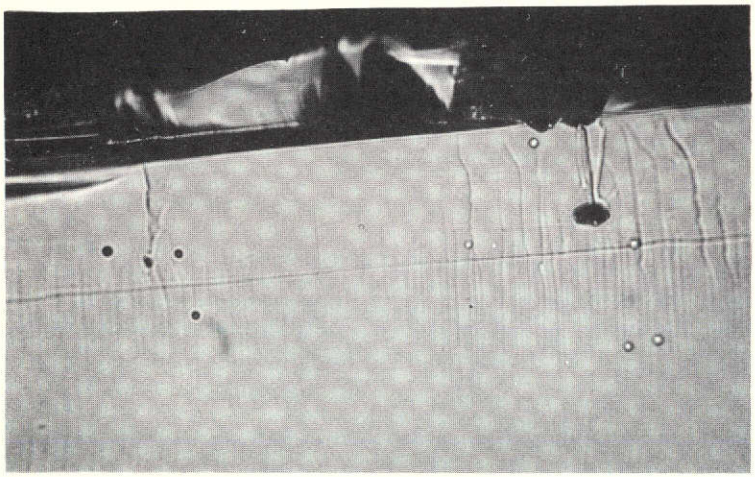

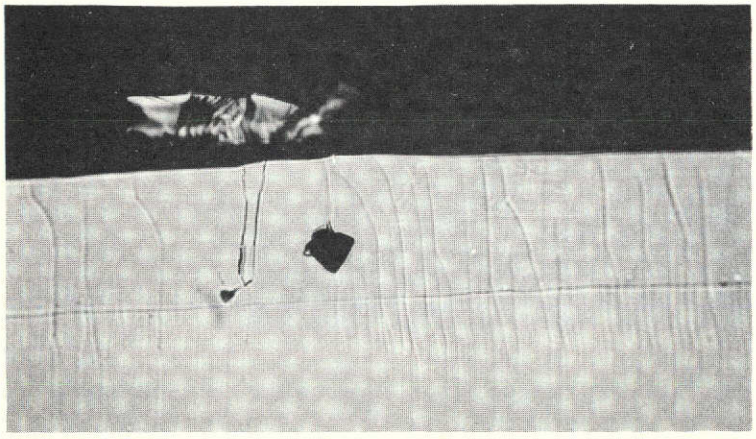

Fig. 29 -- Photomicrographs of the cleave-delineated cross-section in {110} of sample NASA-2.

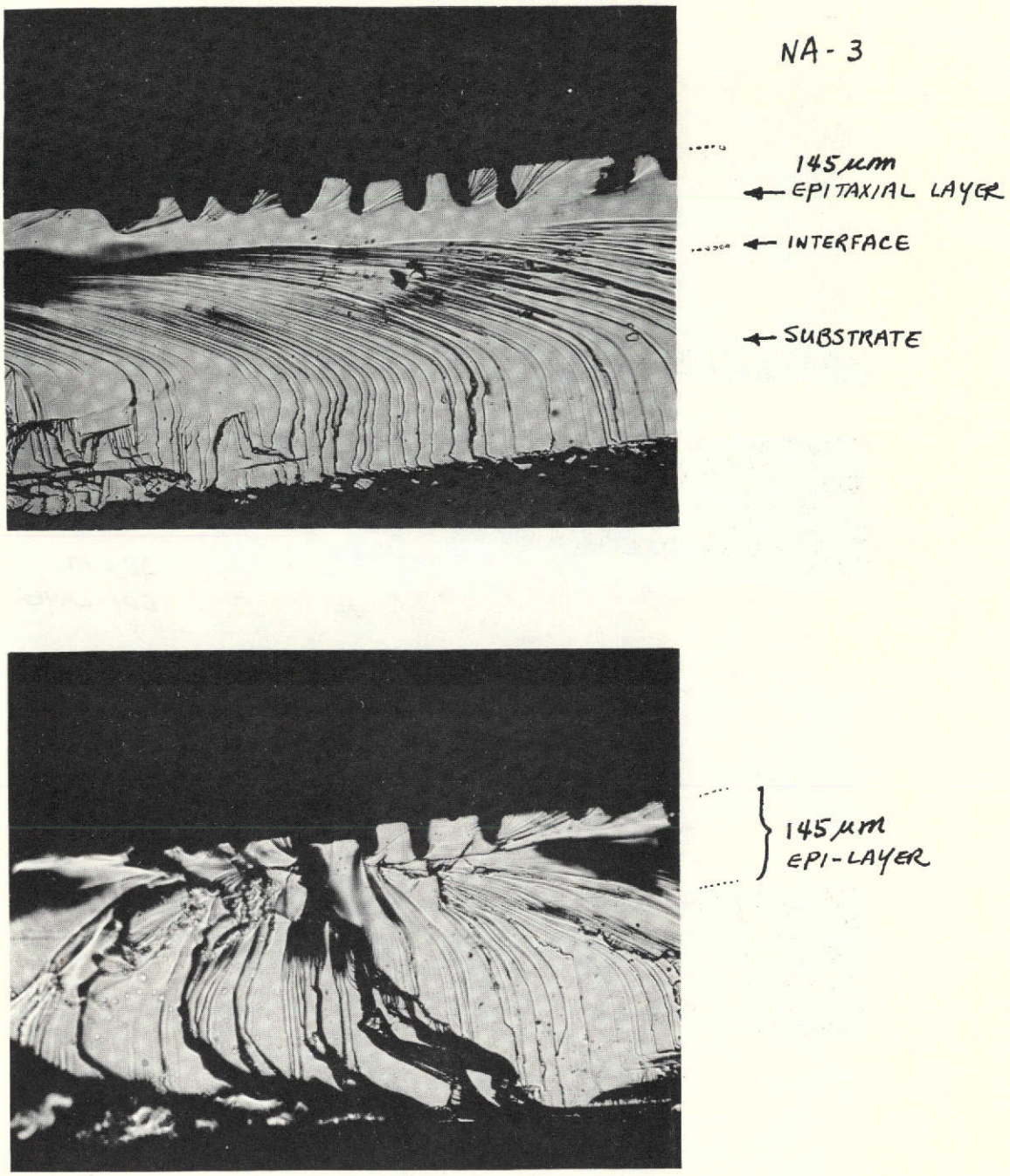

Fig. 30 -- Photomicrographs of the cleave-delineated cross-section in {110} of sample NASA-3.

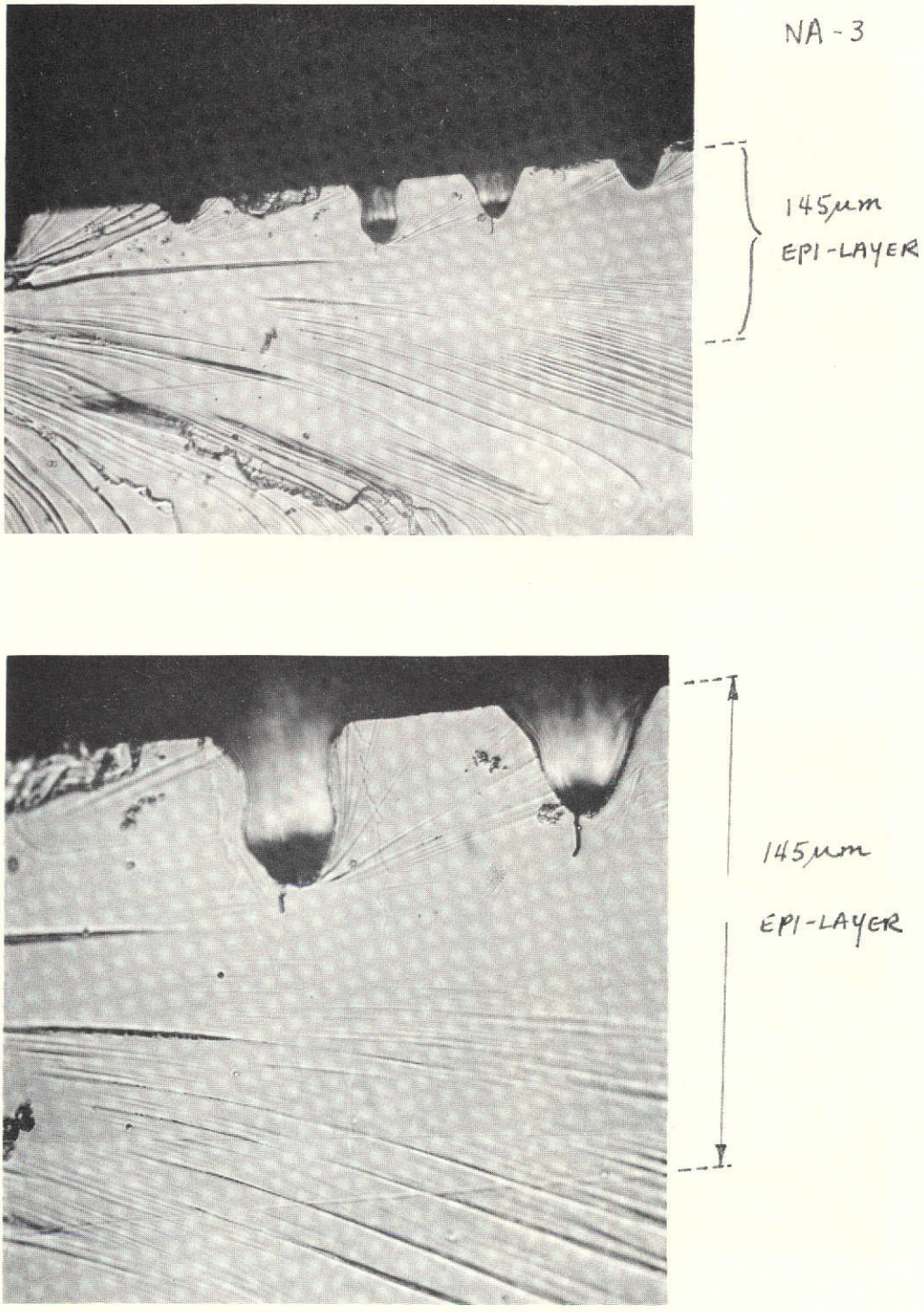

Fig. 31 -- Photomicrographs of the cleave-delineated cross-section in {110} of sample NASA-3.

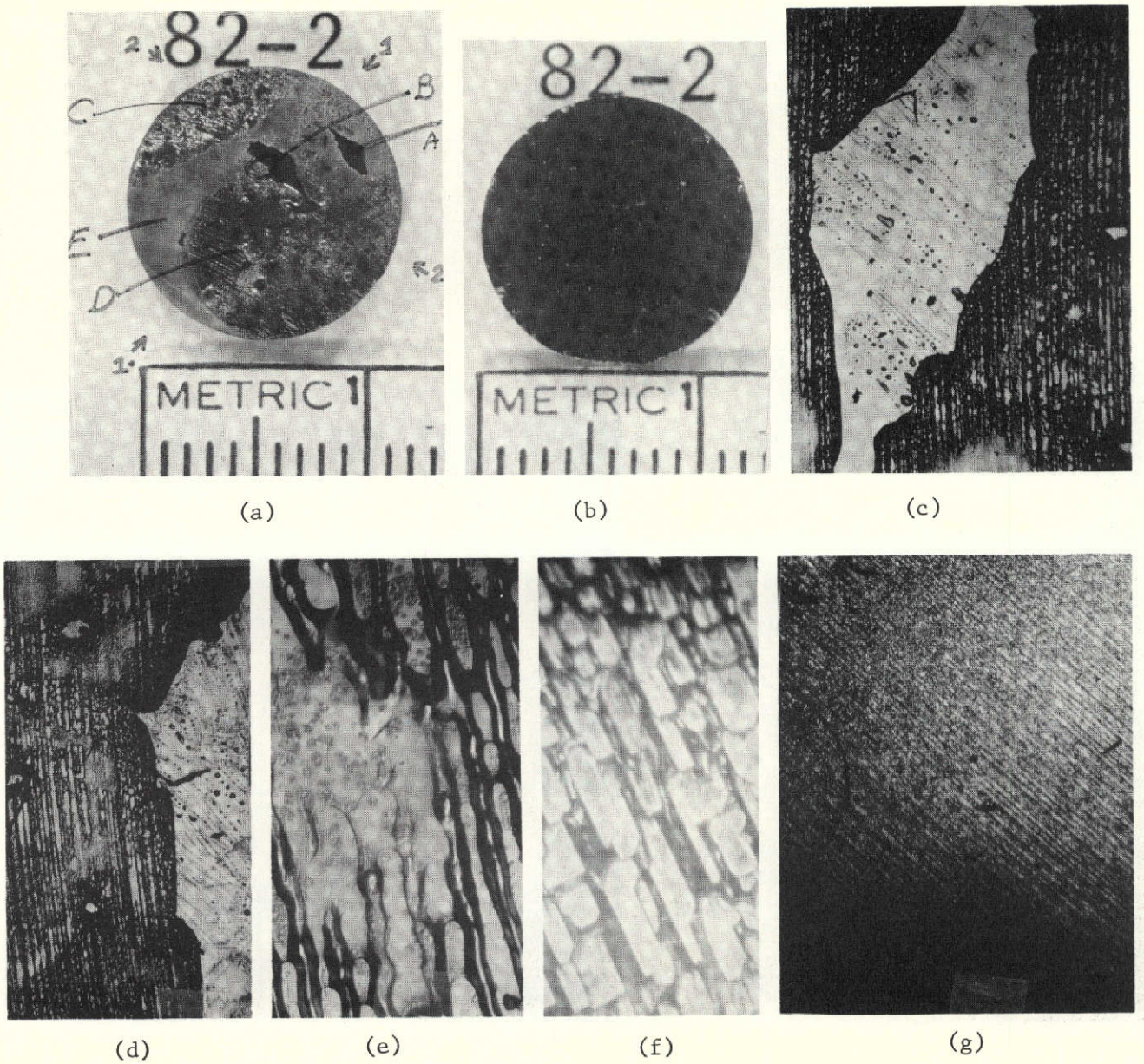

Fig. 32 -- Sample 82-2. (a) Macrophotograph, positions A, B, C, D, E for microphotographs, arrows for traces 1 and 2 are for profile and roughness directions of traces; (b) back surface of seed; (c) position A, 50X; (d) position B, 50X; (e) position C, 200X; (f) position D, 200X; (g) position E, 50X.

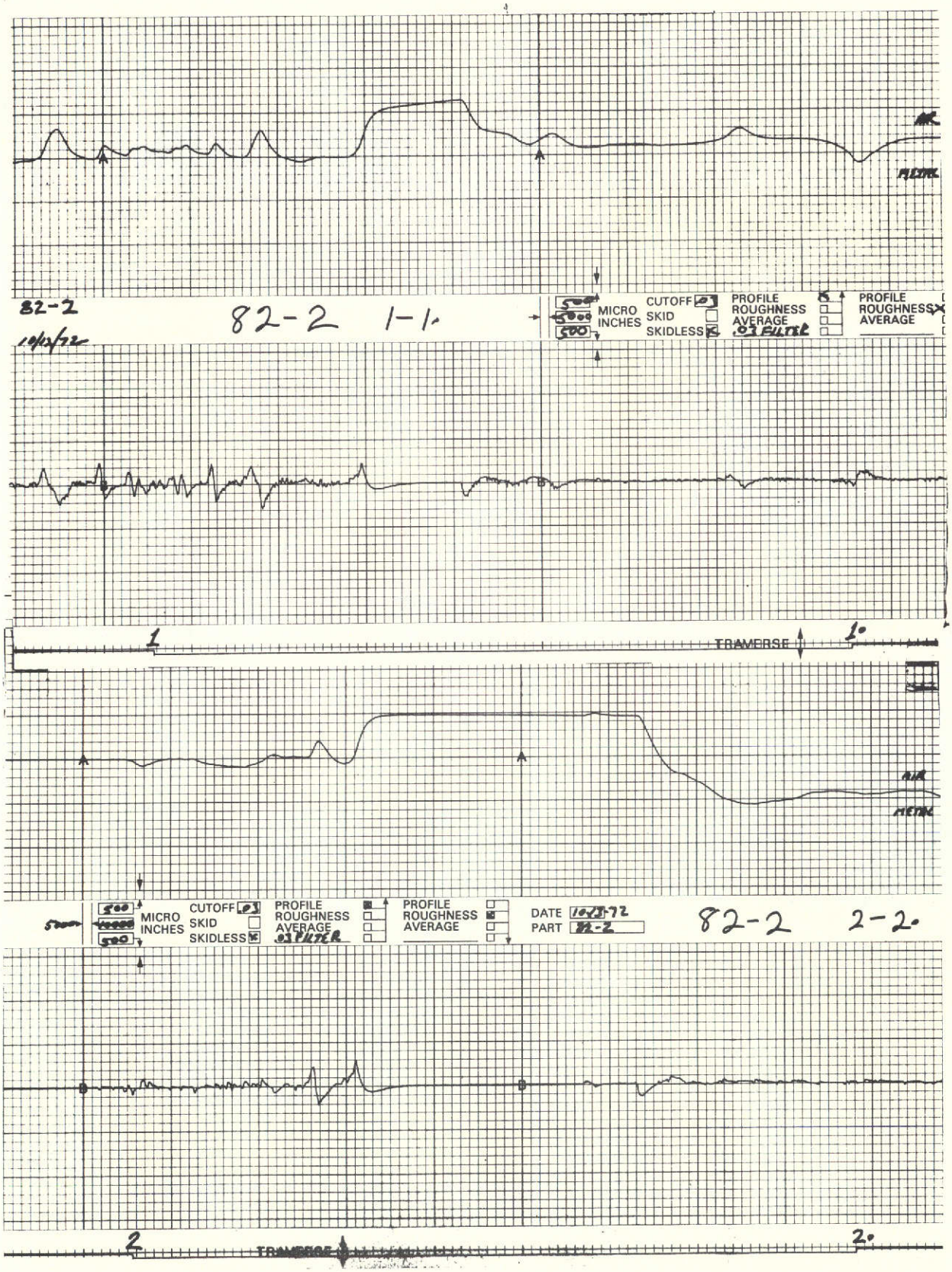

Fig. 33 -- Profile and roughness traces of substrate from 82-2.

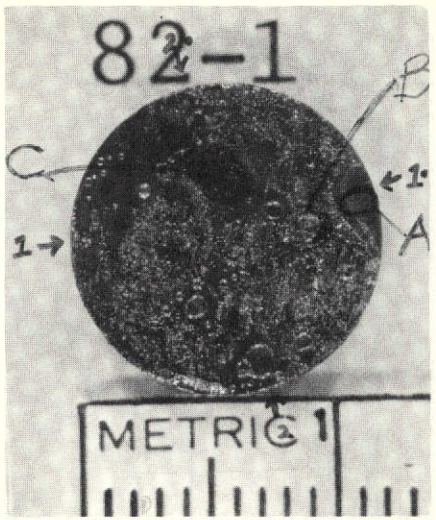

(a)

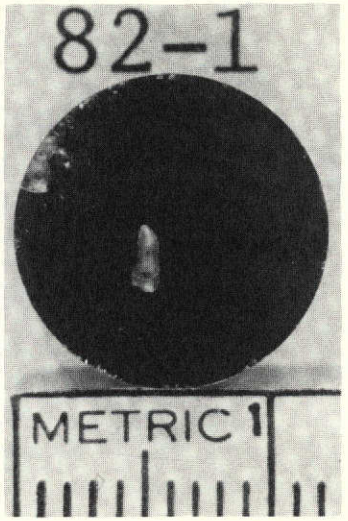

(b)

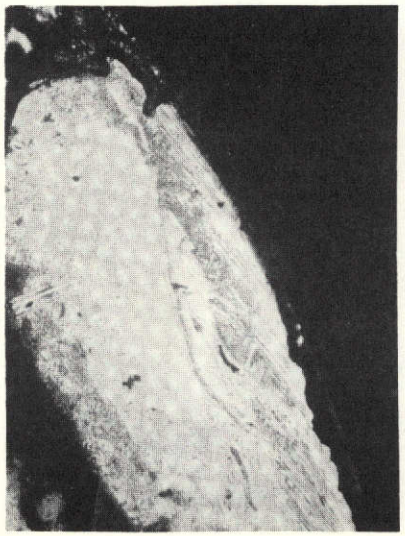

(c)

(d)

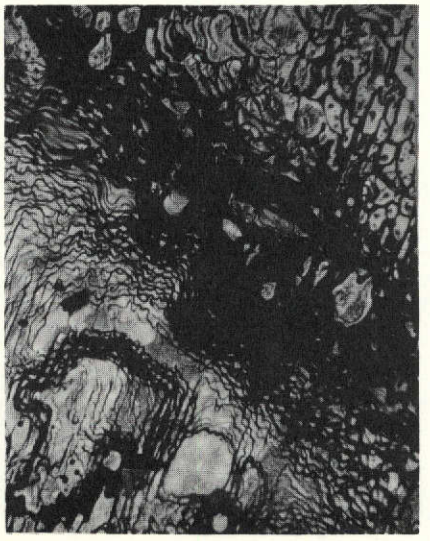

(e)

Fig. 34 -- Sample 82-1. (a) Macrophotograph, positions A, B, C for microphotographs, arrows 1 and 2 are for profile and roughness directions of traces; (b) back of substrate; (c) position A, 50X; (d) position B, 50X; (e) position C, 50X.

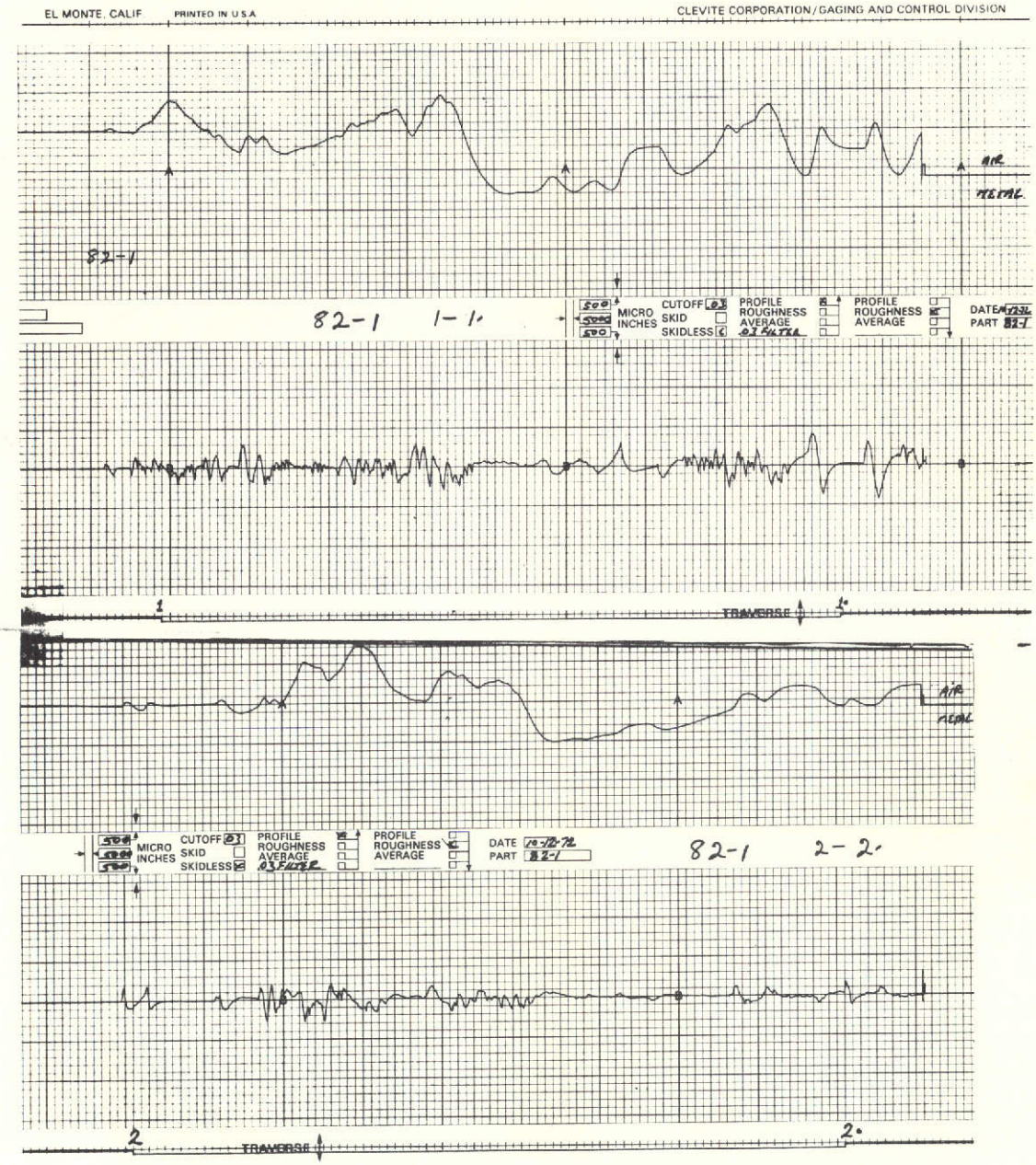

Fig. 35 -- Profile and roughness traces of substrate from 82-1.

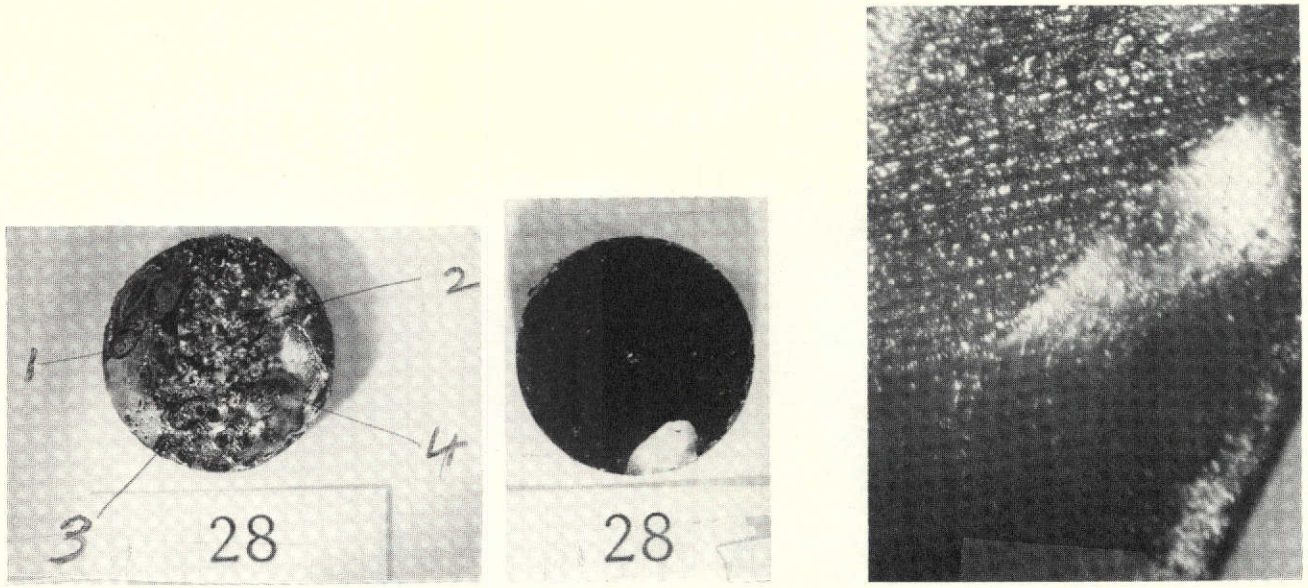

(a) (b) (c)

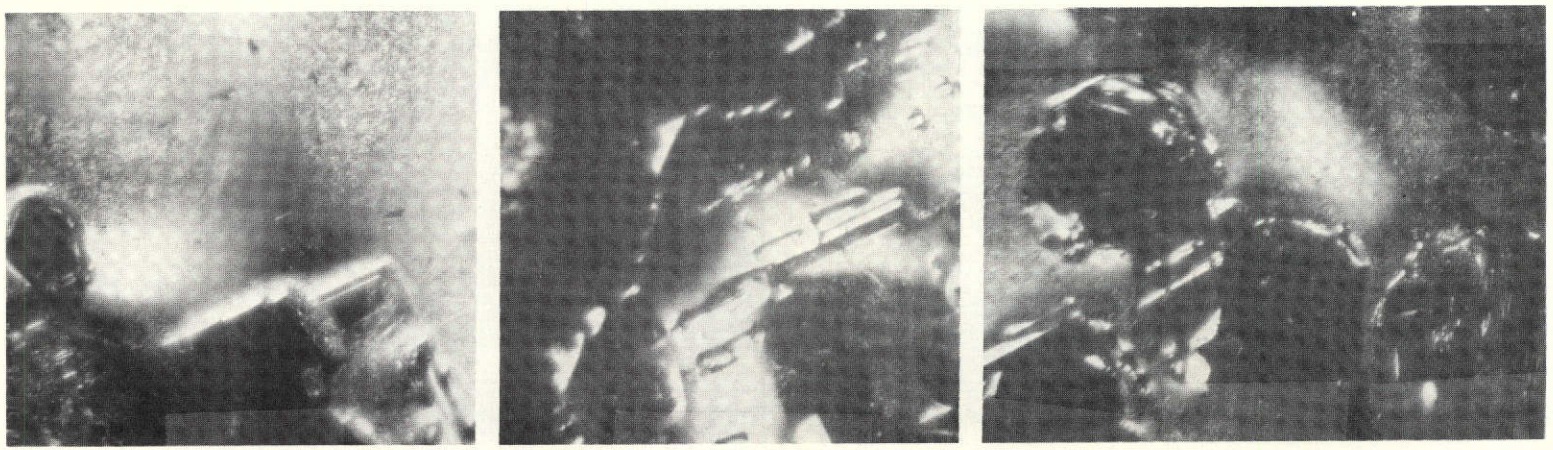

(d) (e) (f)

Fig. 36 -- Sample 28. (a) Macrophotograph with positions for microphotographs 1, 2, 3, 4; (b) back of substrate, (c) position 1, 100X; (d) position 2, 150X; (e) position 3, 100X; (f) position 4, 100X.

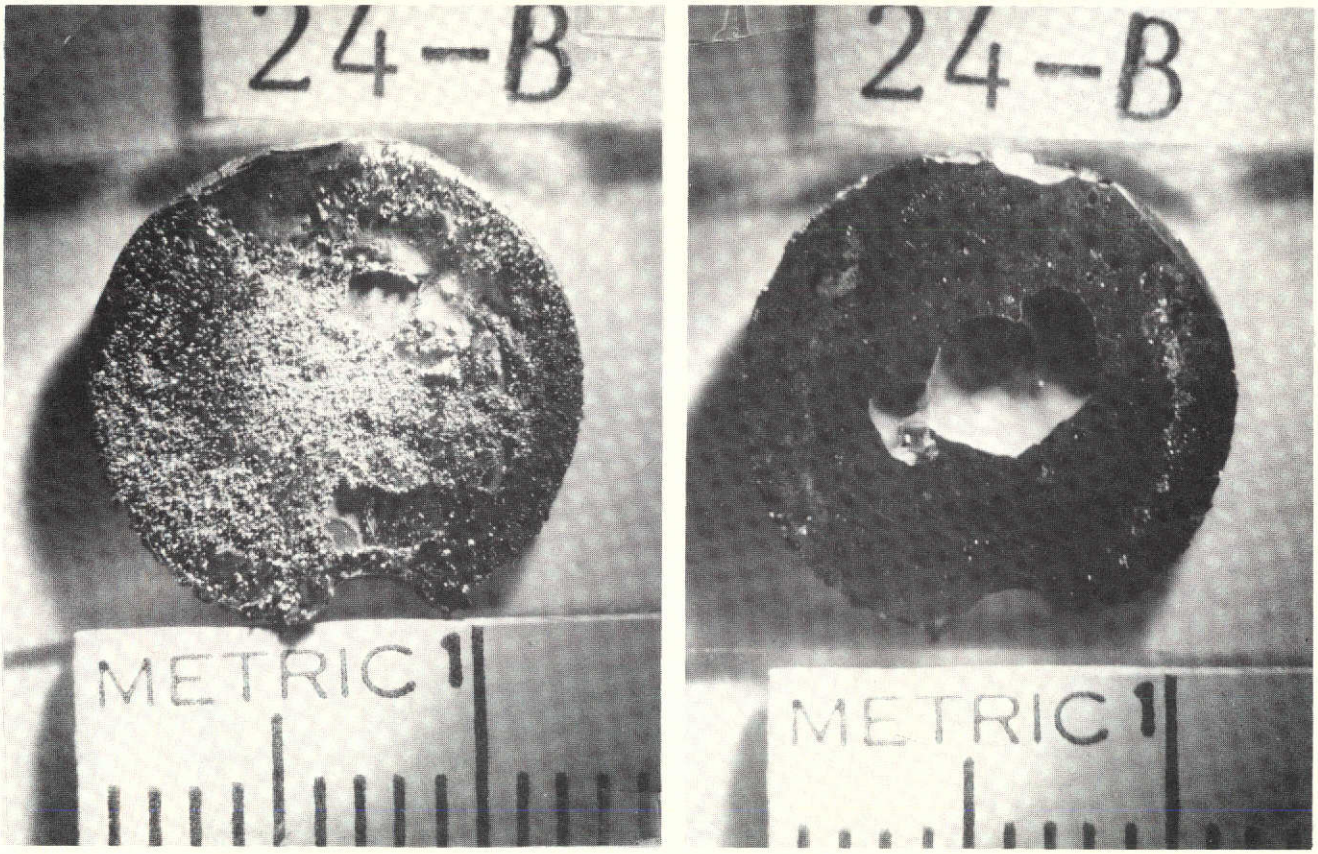

(a) (b)

Fig. 37 -- Seed from experiment 24. (a) Growth surface of substrate; (b) back on non-growth surface.

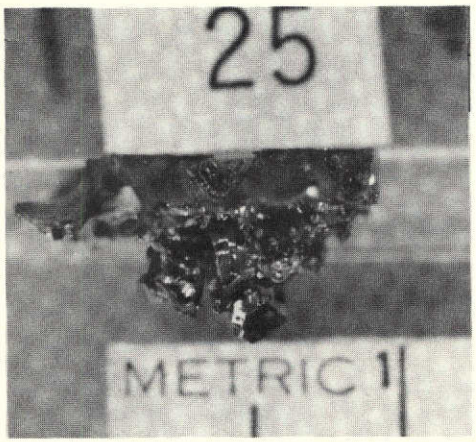

(a)

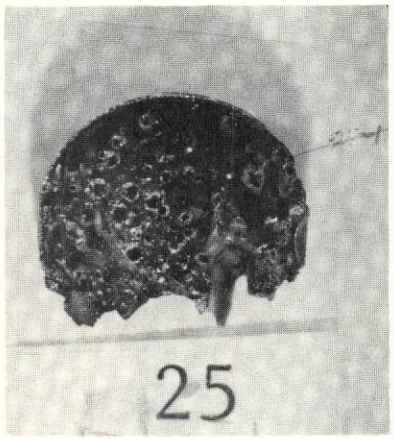

(b)

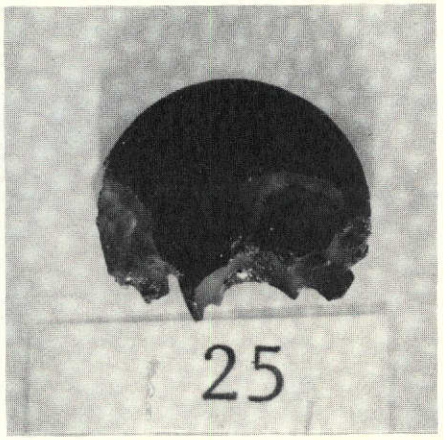

(c)

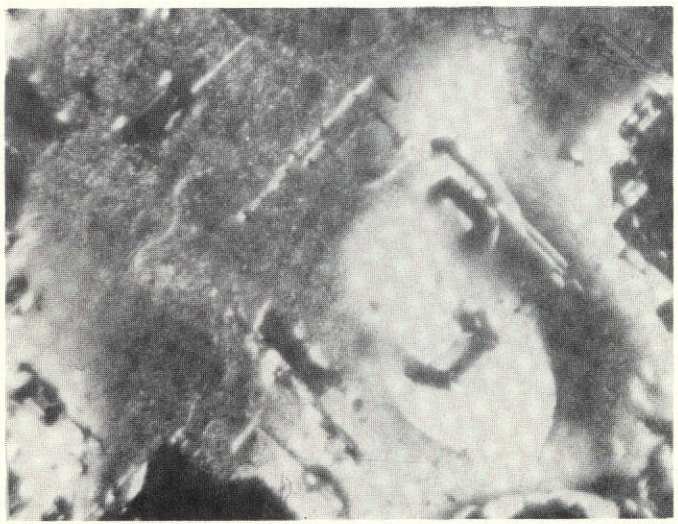

(d)

Fig. 38 -- Substrate from experiment 25. (a) Side view before secondary growth was removed; (b) and (c) macrophotographs after removal of secondary growth and back view respectively; (d) microphotographs as indicated in (b), 100X.

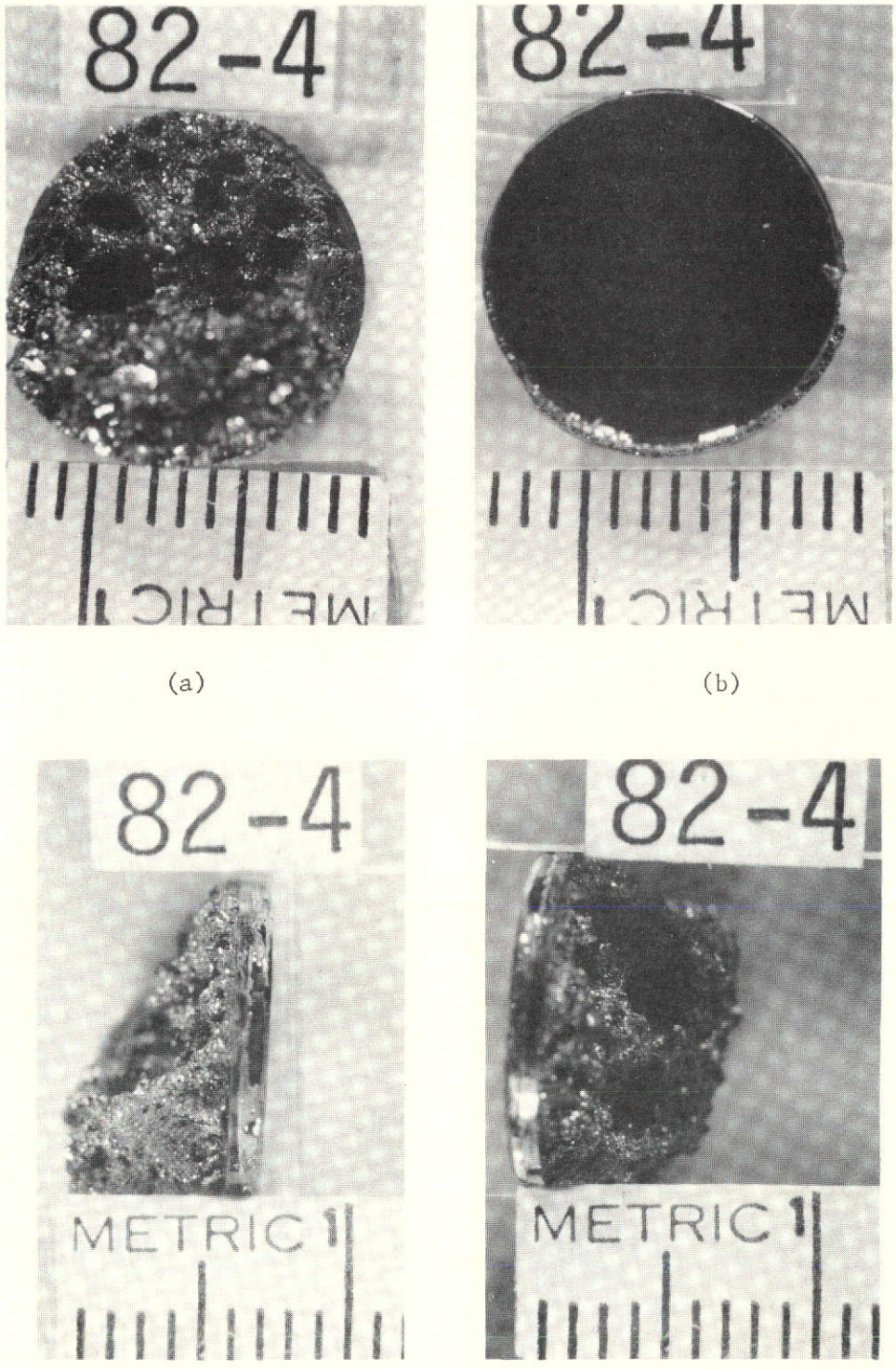

(a) (b)

(c) (d)

Fig. 39 -- Macrophotographs of 82-4, (a) growth side of seed; (b) back or non-growth side of seed; (c) and (d) side views of seed and growth.

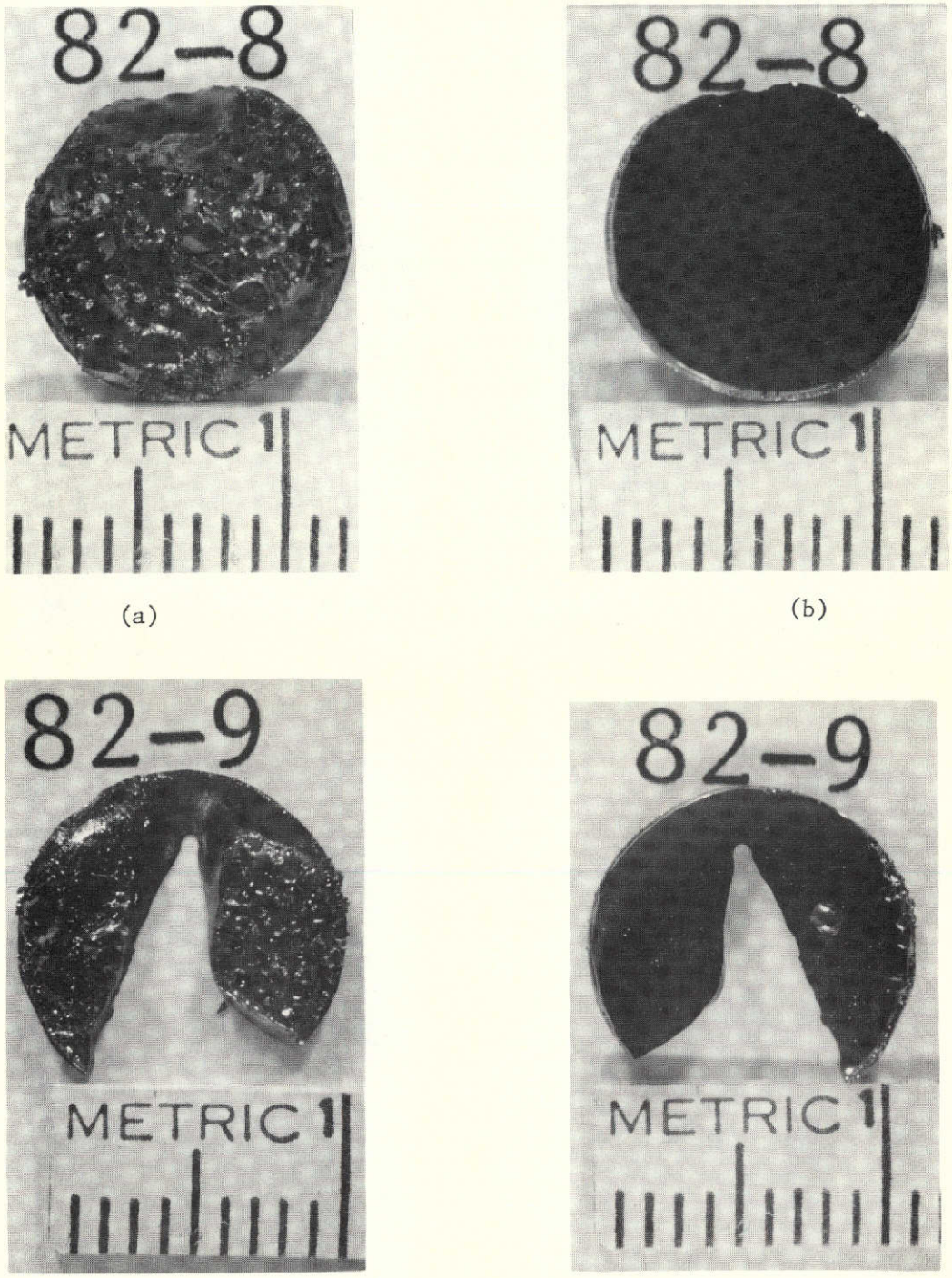

(a) (b)

(c) (d)

Fig. 40 -- Macrophotographs of runs 82-8 and 82-9. (a) and (c) growth surface; (b) and (d) non-growth surfaces.

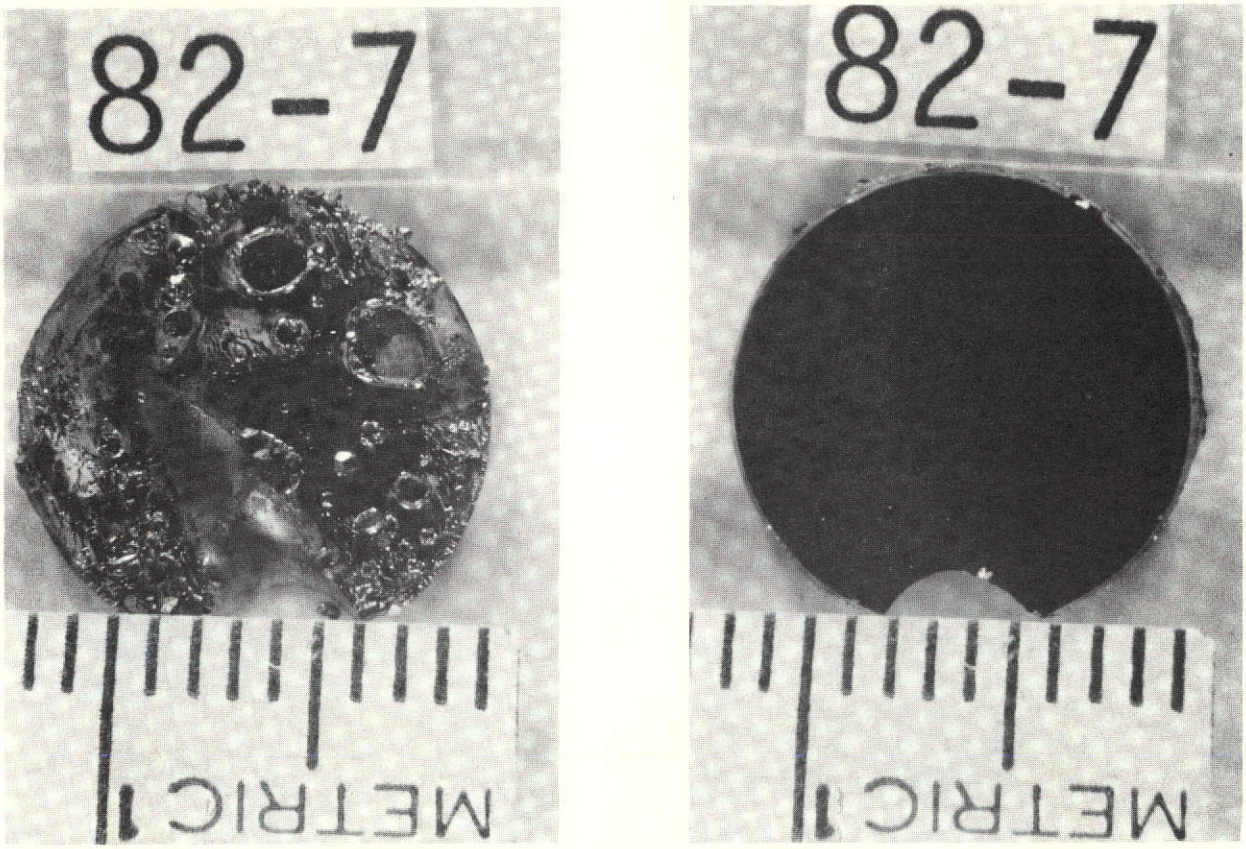

(a) (b)

Fig. 41 -- Macrophotographs of 82-7. (a) Growth surface; (b) non-growth surface.

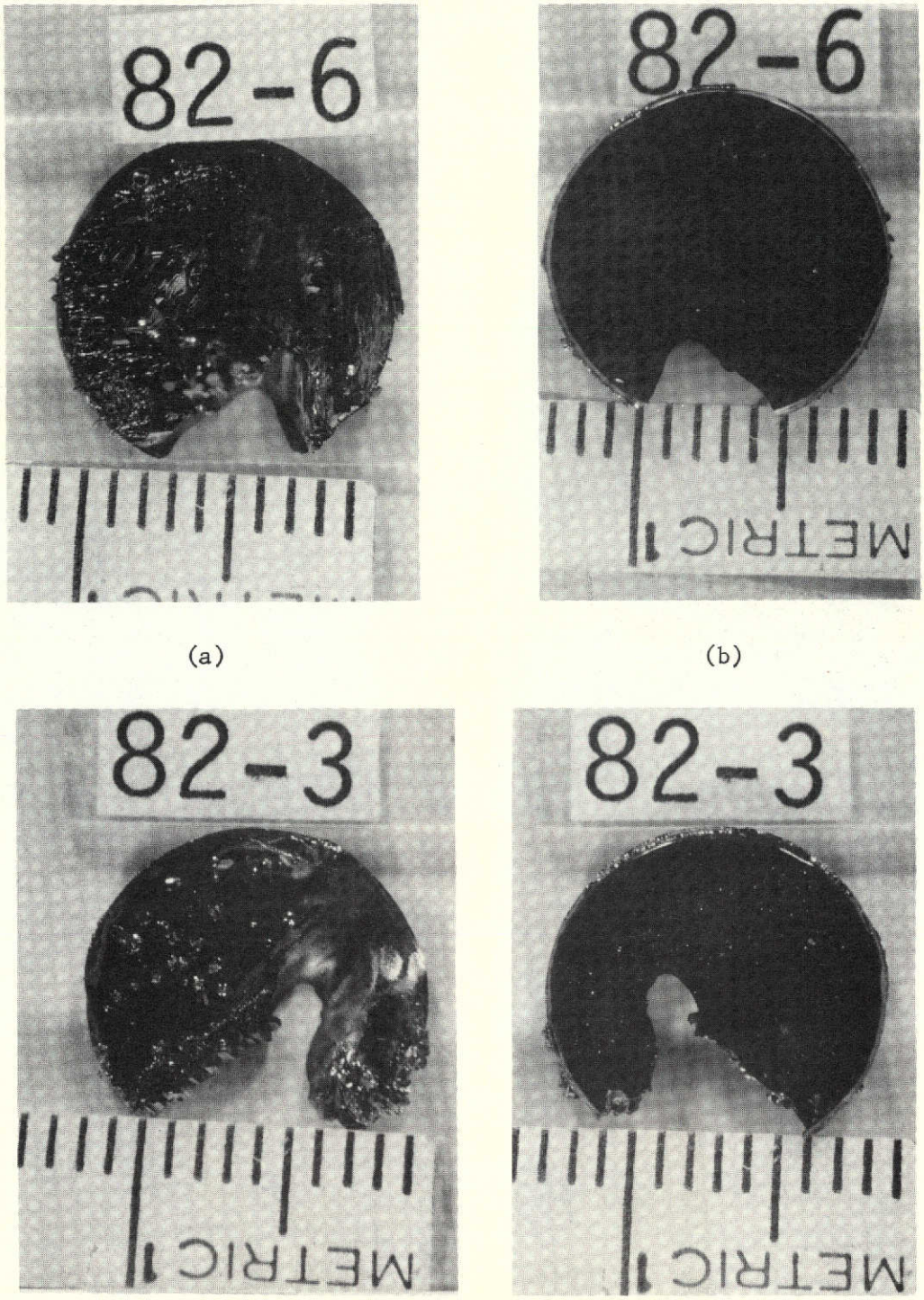

Fig. 42 -- Macrophotographs of substrates from runs 82-3 and 82-6. (a) and (c) growth surfaces; (b) and (d) non-growth surfaces.

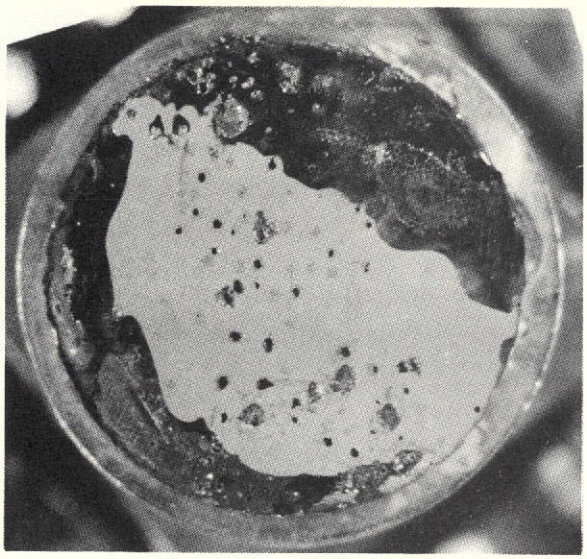

(a)

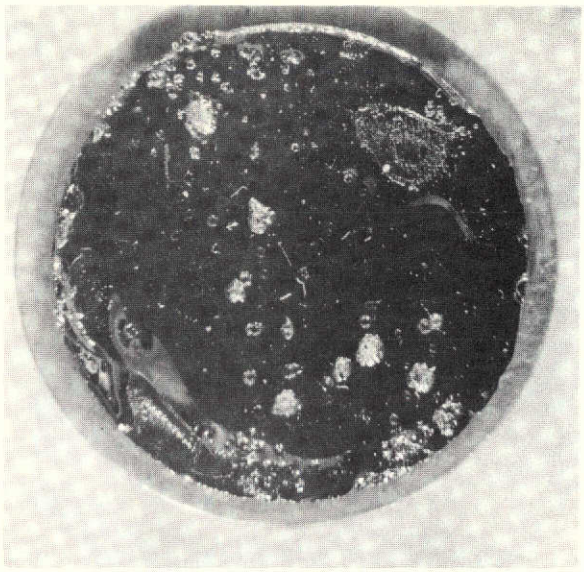

(b)

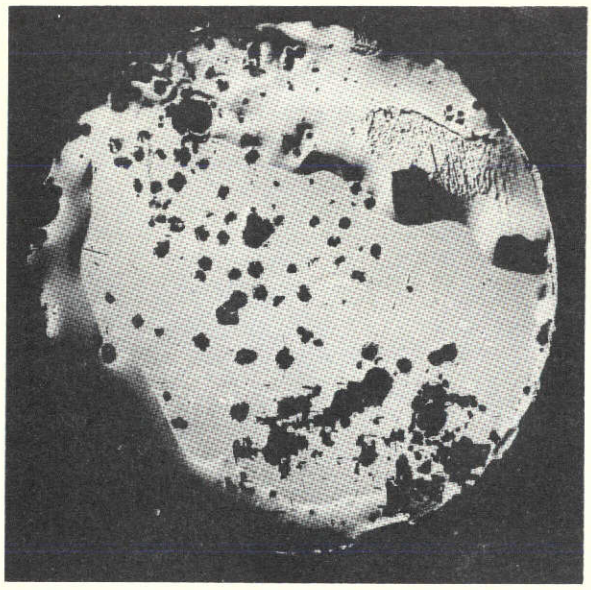

(c)

Fig. 43 -- Photographs of Seed with epitaxial GaAs from run 28. (a) lapped surface, (b) chemical polish etched surface, (c) SBRT photograph, (440) orientation.

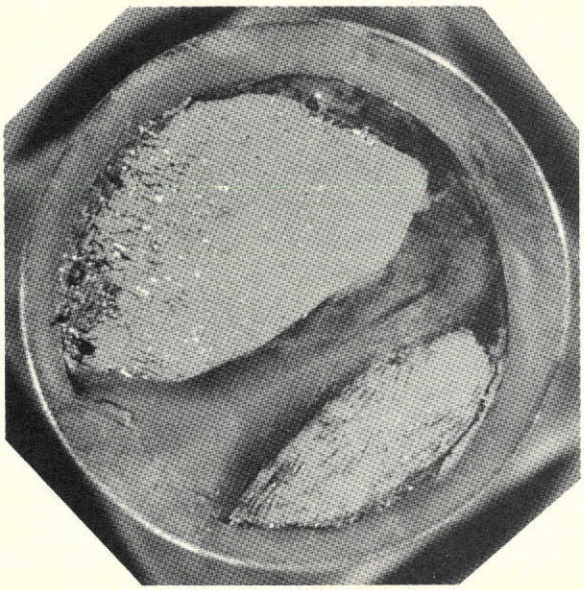

(a)

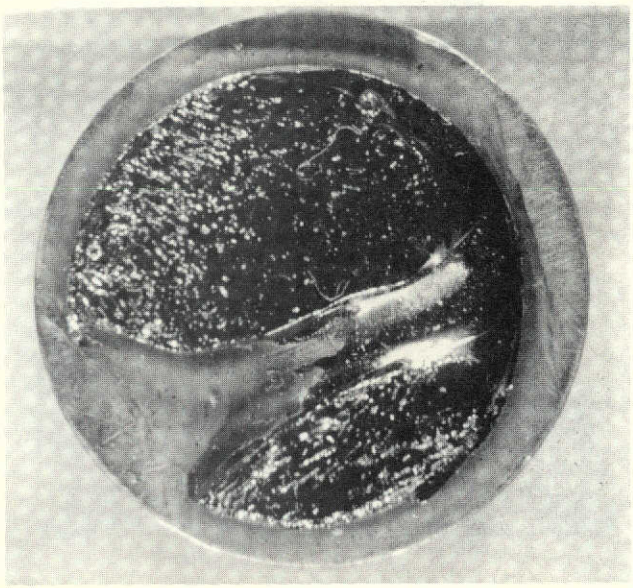

(b)

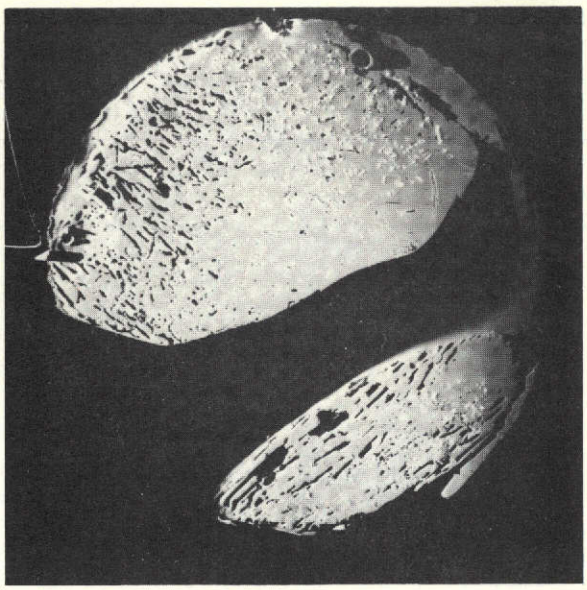

(c)

Fig. 44 -- Photographs of seed with epitaxial GaAs from run 82-6. (a) lapped surface, (b) chemical polish etched surface, (c) SBRT photograph, (440) orientation.

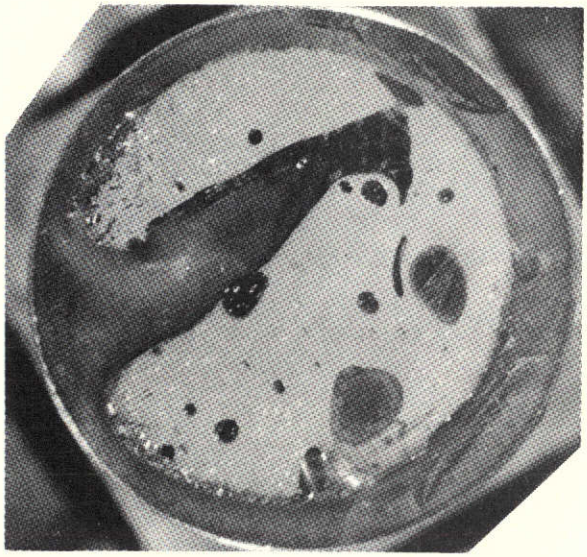

(a)

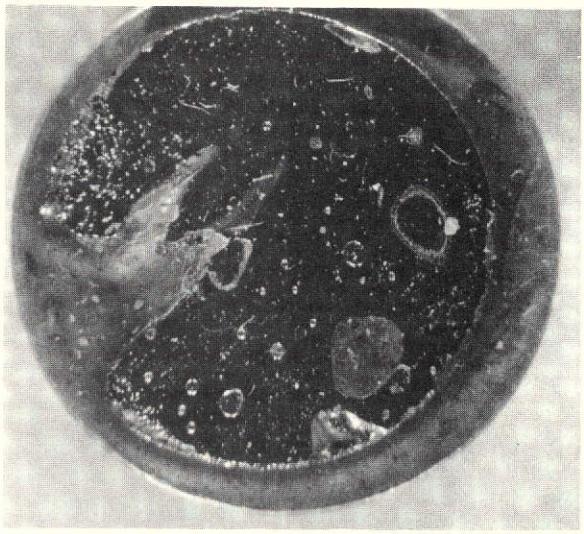

(b)

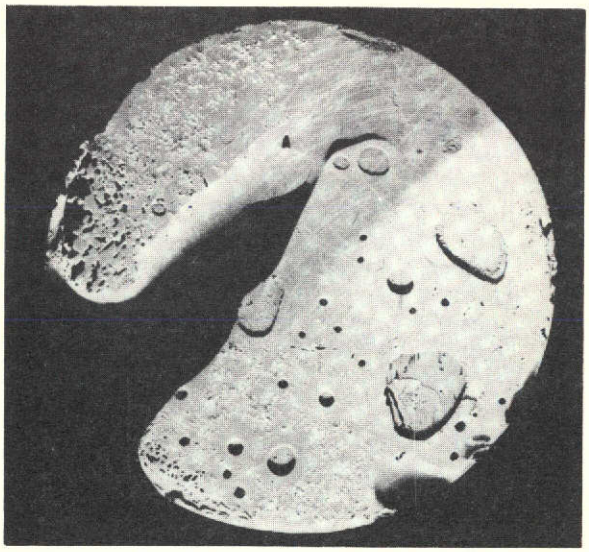

(c)

Fig. 45 -- Photographs of seed with epitaxial GaAs from run 82-7. (a) lapped surface, (b) chemical polish etched surface, (c) SBRT photograph, (440) orientation.

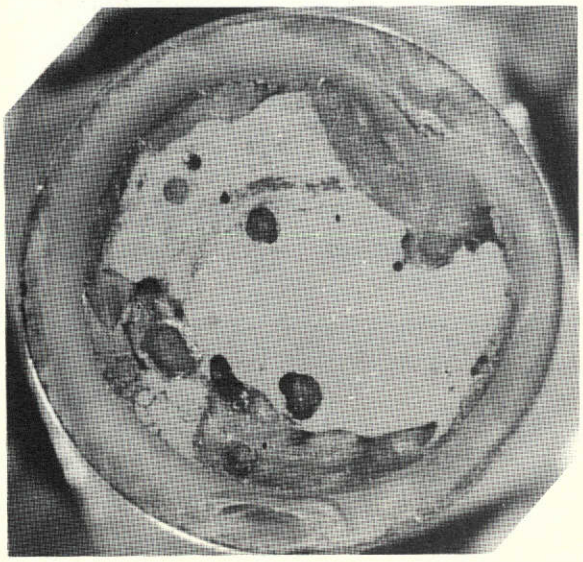

(a)

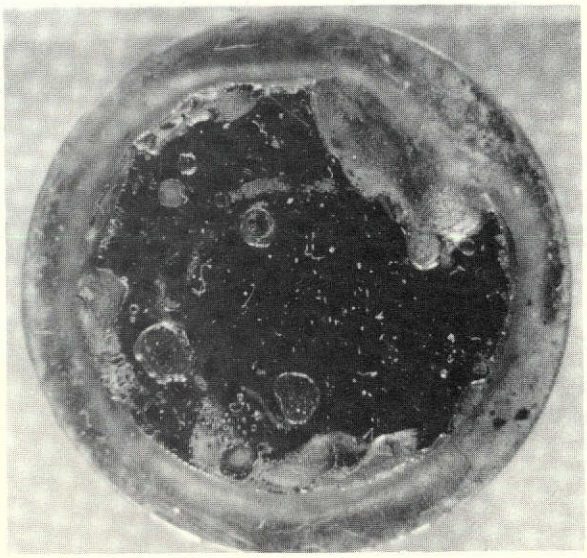

(b)

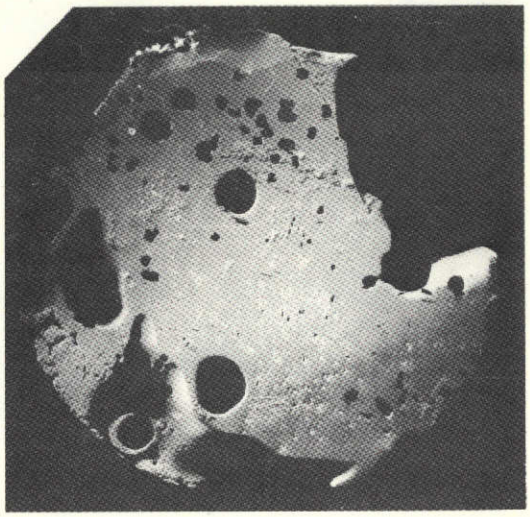

(c)

Fig. 46 -- Photographs of seed with epitaxial GaAs from run 82-8. (a) lapped surface, (b) chemical polish etched surface, (c) SBRT photograph, (442) orientation.

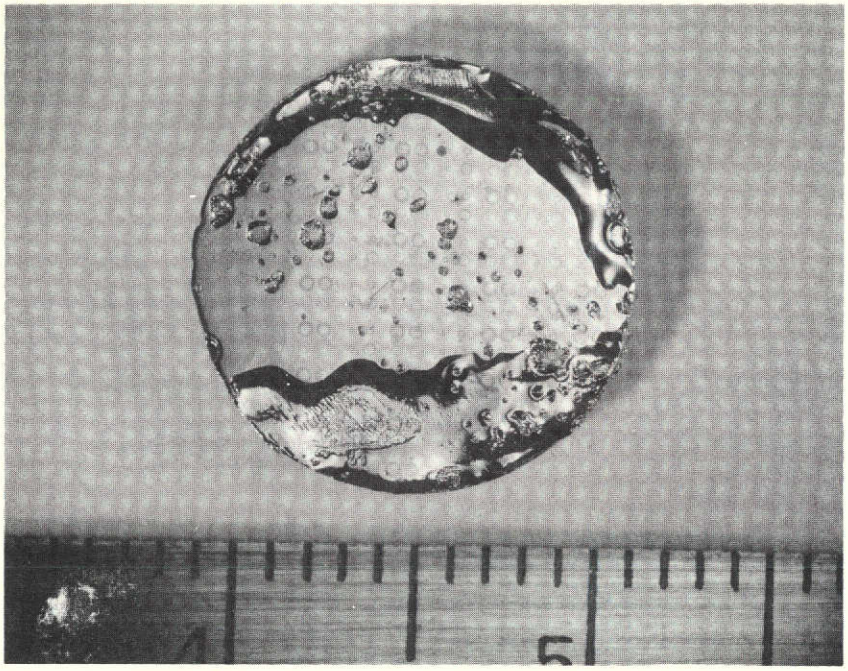

Fig. 47 -- Photographs of seed with epitaxial GaAs from run 28. Surface has been lapped, polished, and plated with gold.

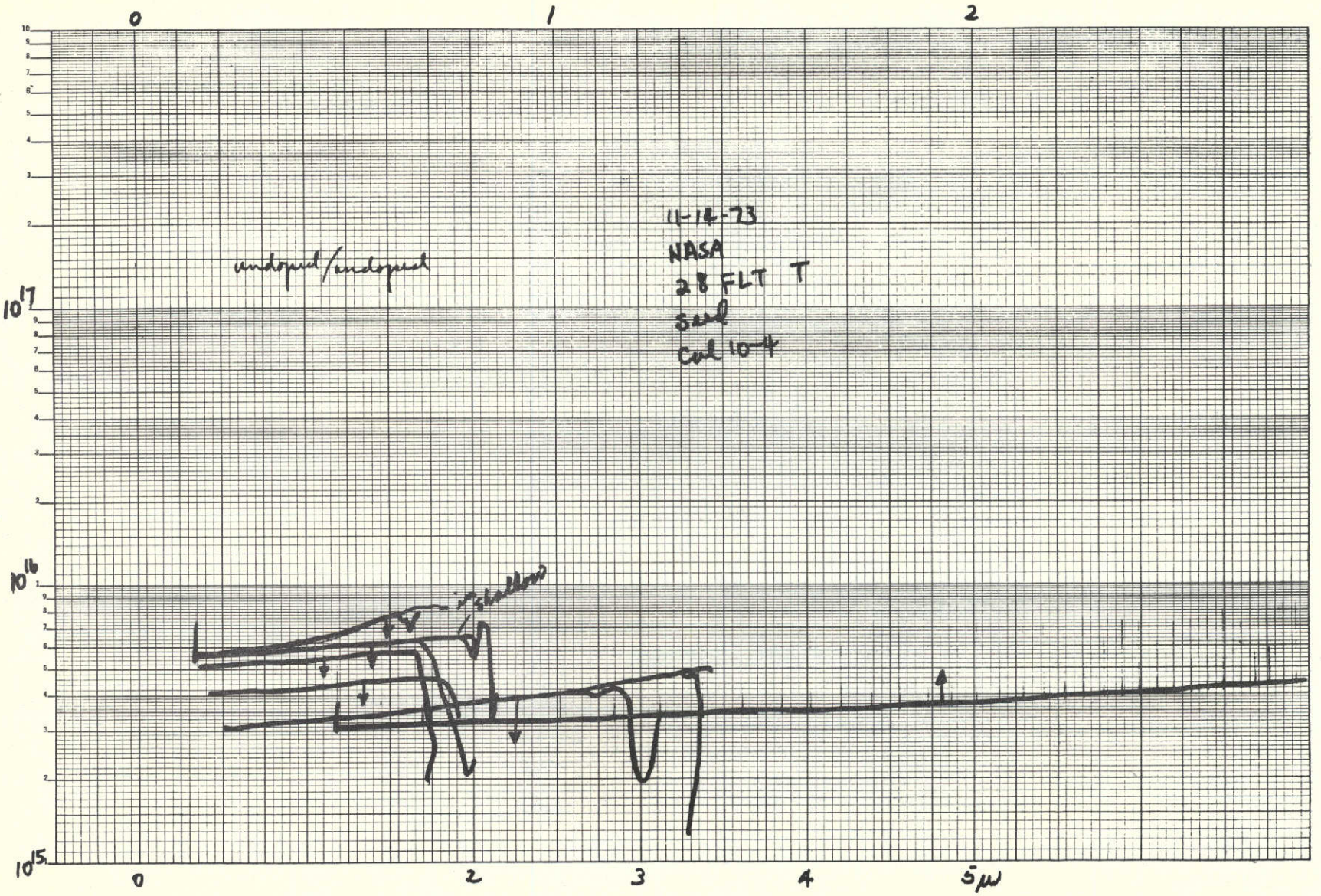

Fig. 48 -- Copeland profile measured at the gold Schottky barrier dots on the sample 28.

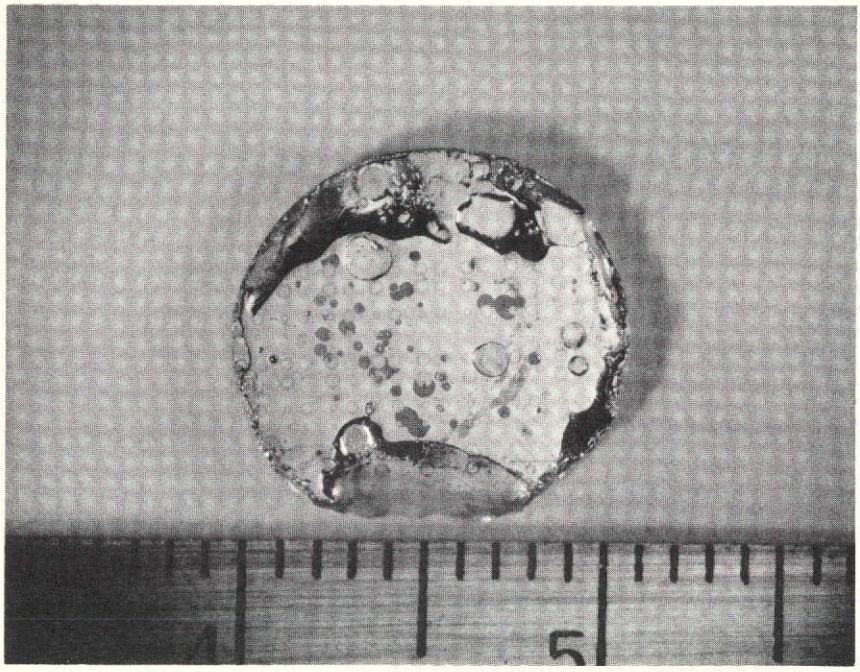

Fig. 49 -- Photograph of seed with epitaxial GaAs from run 82/8. Surface has been lapped, polished, and plated with gold.

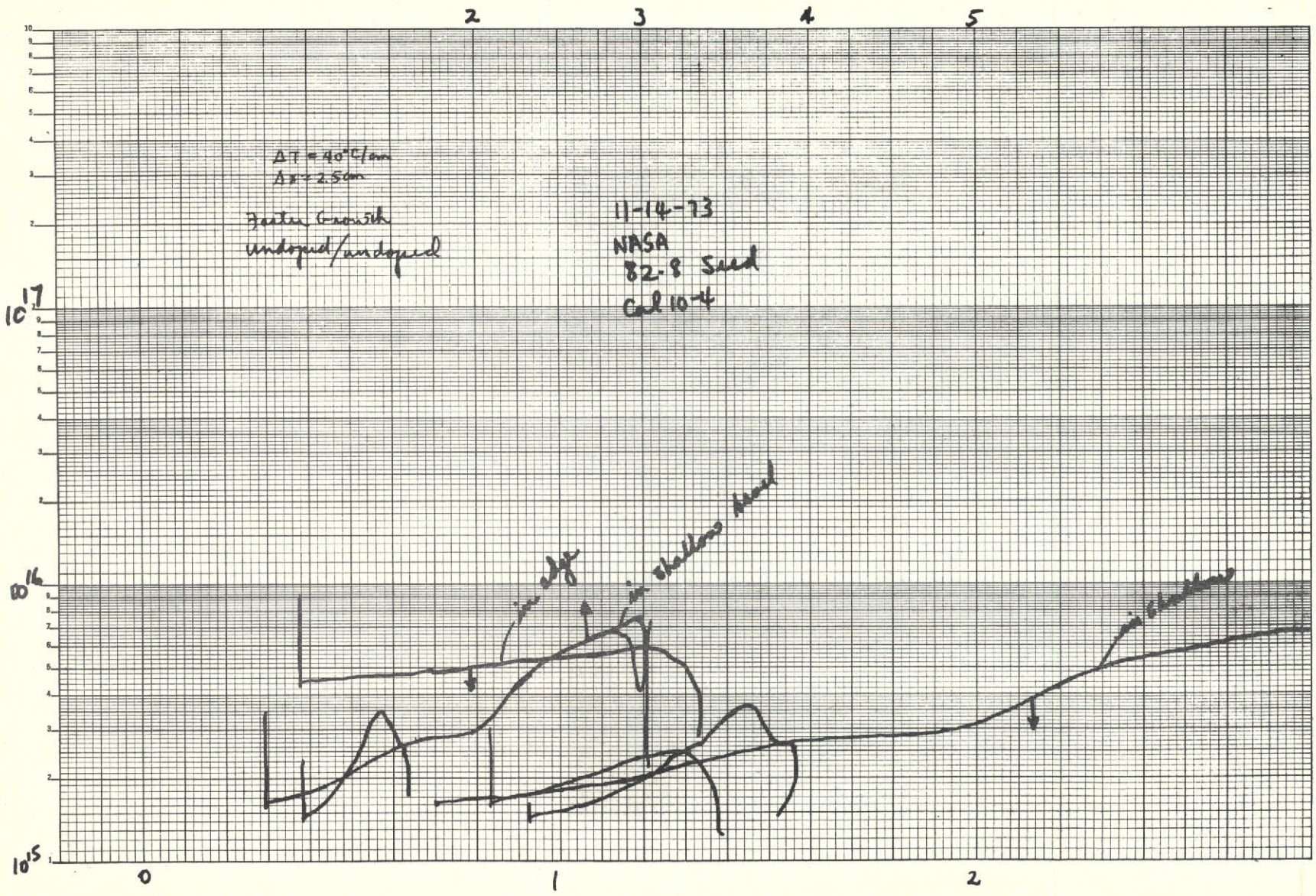

Fig. 50 -- Copeland profile measured at the gold Schottky barrier dots on the sample 82-8.

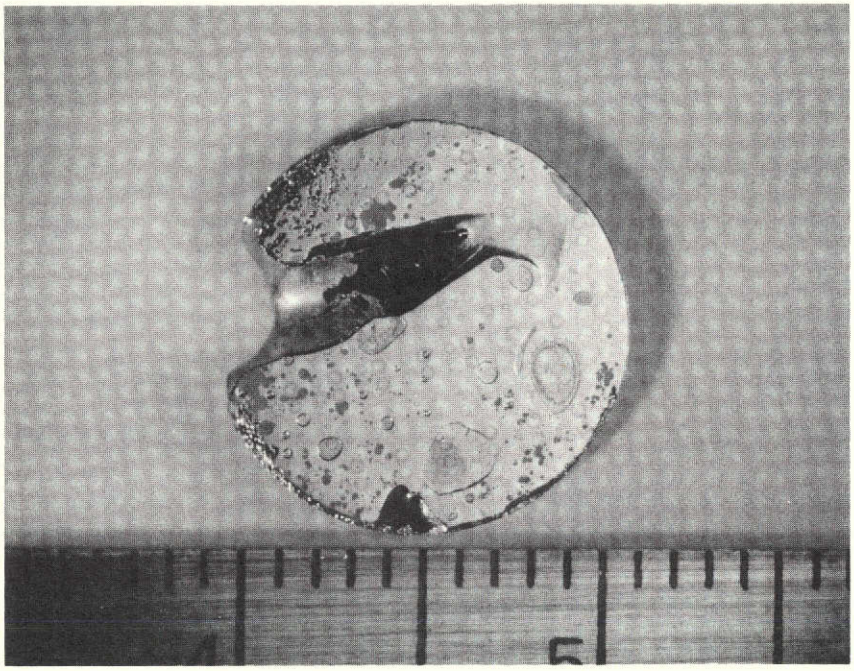

Fig. 51 -- Photograph of seed with epitaxial GaAs from run 82-7. Surface has been lapped, polished, and plated with gold.

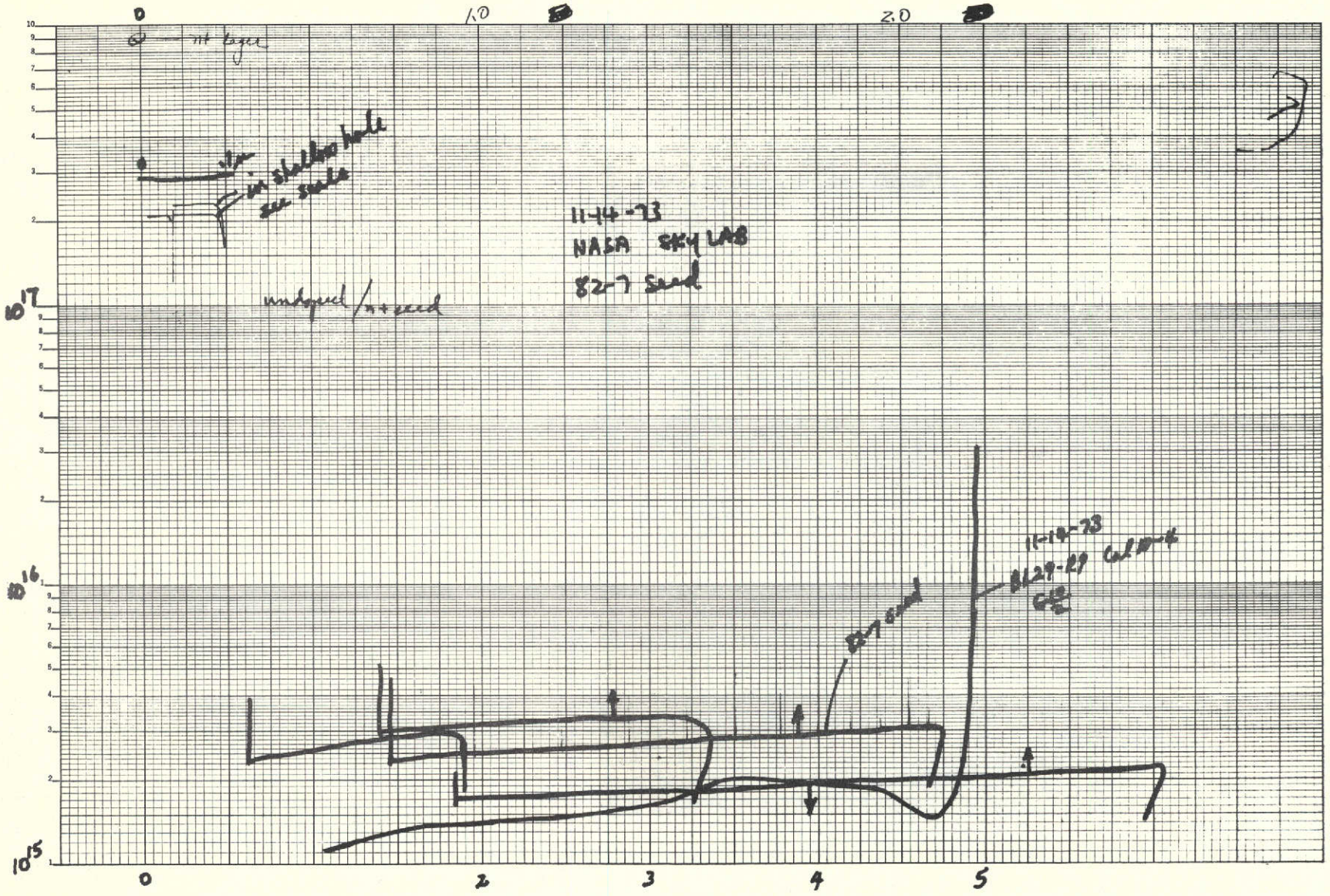

Fig. 52 -- Copeland profile measured at the gold Schottky barrier dots on the sample 82-7.

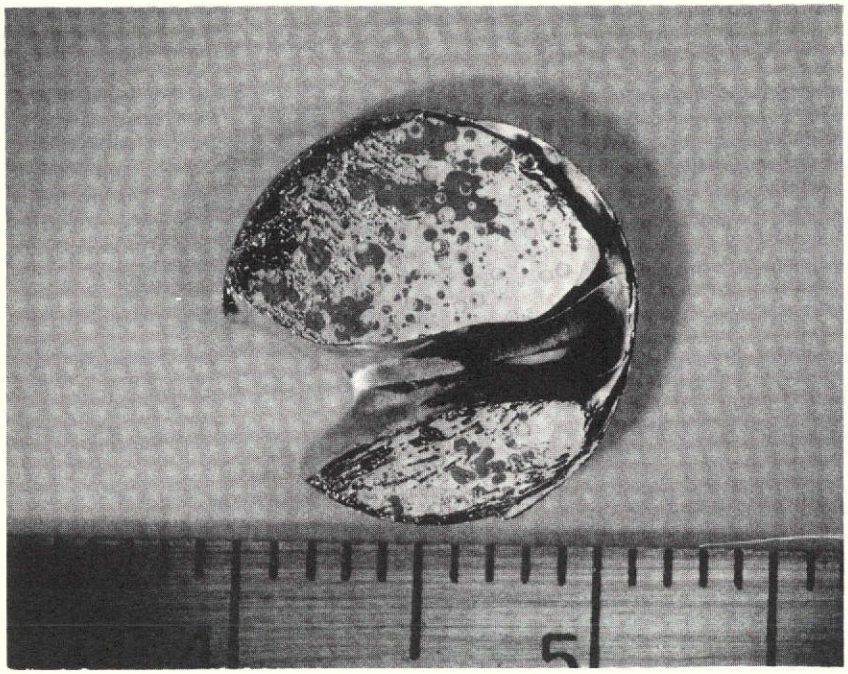

Fig. 53 -- Photograph of seed with epitaxial GaAs from run 82-6. Surface has been lapped, polished, and plated with gold.

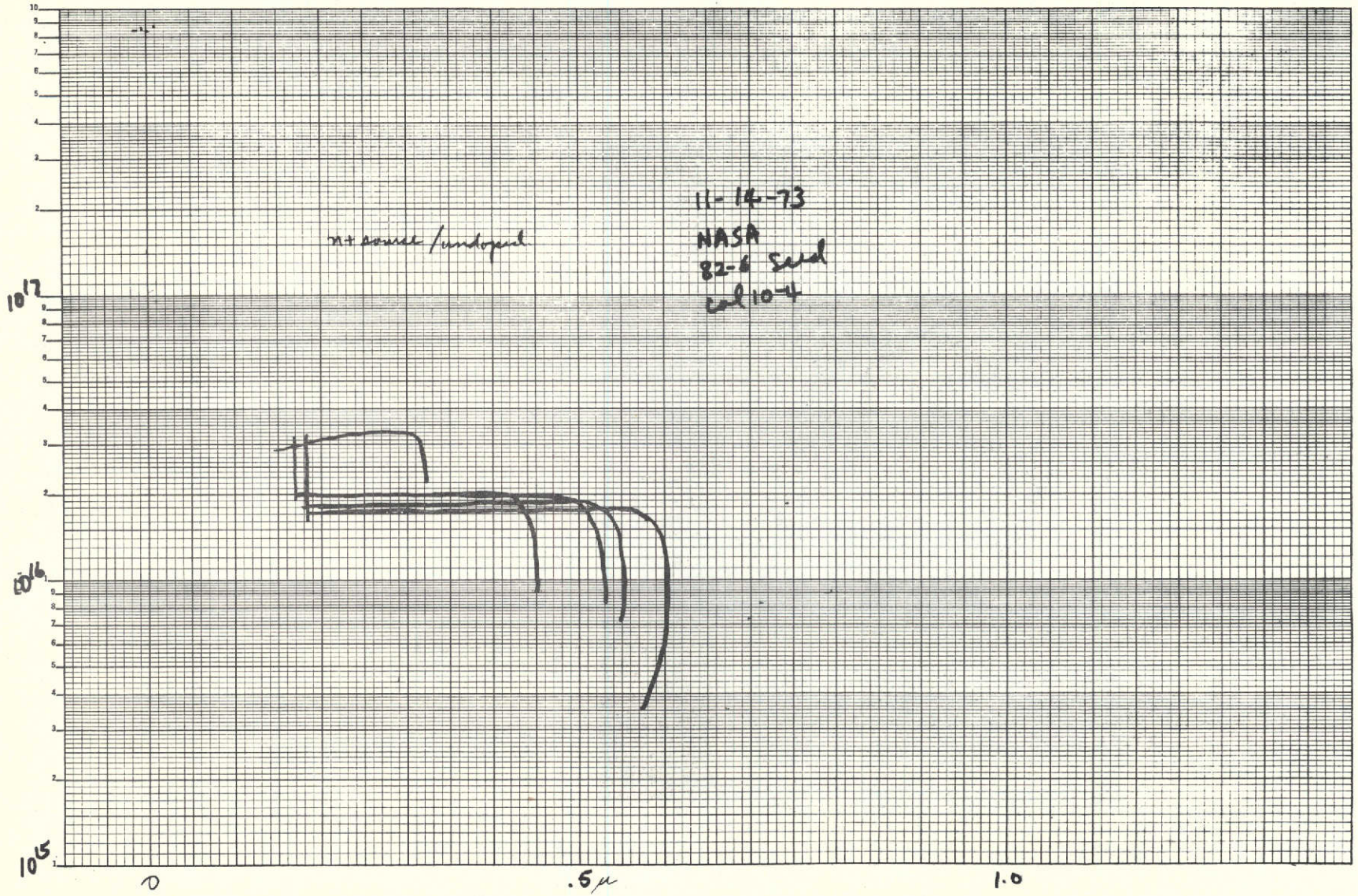

Fig. 54 -- Copeland profile measured at the gold Schottky barrier dots on the sample 82-6.

PUBLICATIONS

Paper presented at the Second International Conference on Vapor Growth and Epitaxy, Jerusalem, Israel, 21-25 May 1972. "A Solution Growth Experiment for Low Gravity Environment" by C.S. Duncan, R. Mazelsky, M. Rubenstein, and R.G. Seidensticker.

Paper published in J. Appl. Phys. 43, 584 (1972). "Thermal Conductivity of Liquid InSb and Liquid Ga" by R.G. Seidensticker and M. Rubenstein.

PROGRAM PLANNING CHART

WESTINGHOUSE ELECTRIC CORPORATION
RESEARCH LABORATORIES
PITTSBURGH, PENNA. 15235

AGENCY: NASA-MSFC-HUNTSVILLE
PROGRAM: RESEARCH STUDY ON MATERIALS PROCESSING IN SPACE EXPERIMENT #M512

CONTRACT NUMBER NAS8-28727
CONTRACT VALUE $107,100*
PERIOD OF THIS REPORT November 1 - November 30, 1973

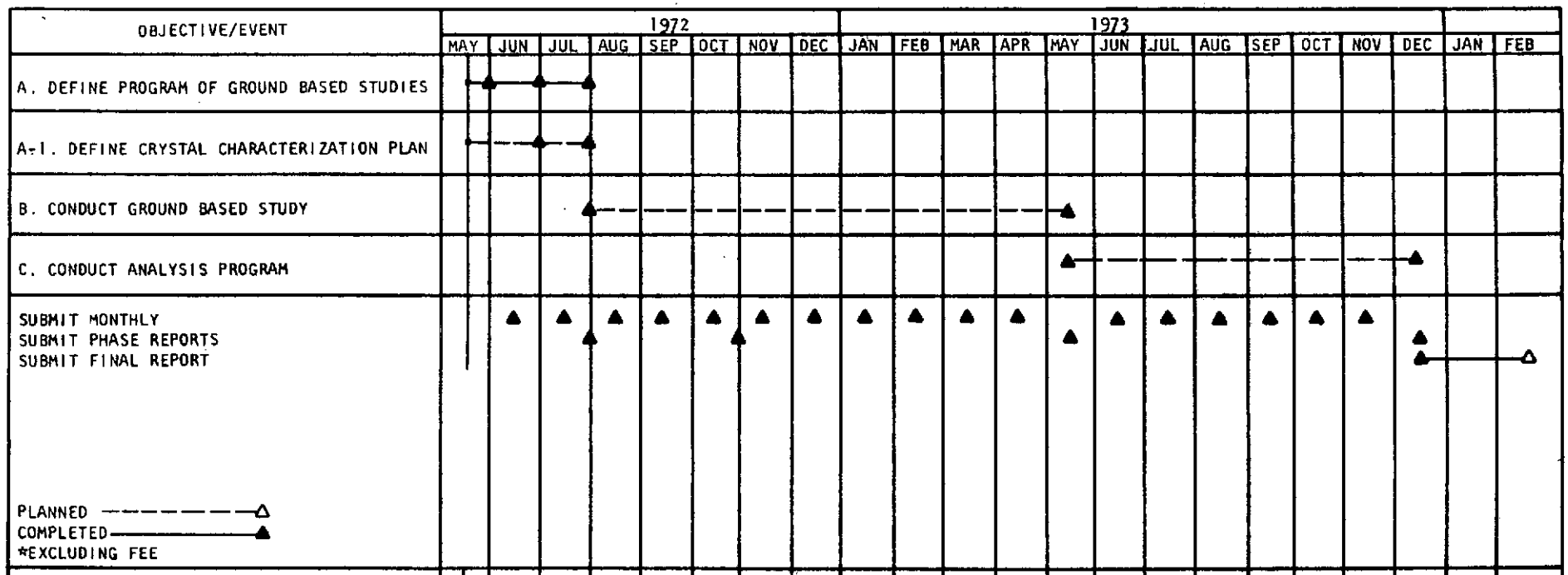

		JUN	JUL	AUG	SEP	OCT	NOV	DEC	JAN	FEB	MAR	APR	MAY	JUN	JUL	AUG	SEP	OCT	NOV	DEC	JAN	FEB
EXPENDITURES THIS MONTH*	$ X 1000	3.1	6.5	5.3	7.6	9.3	9.5	5.9	5.8	6.6	7.5	4.5	3.9	4.3	5.8	4.4	2.9	2.6	5.7			
EXPENDITURES TO DATE*	$ X 1000	3.1	9.6	14.9	22.5	31.8	41.3	47.2	53.0	59.6	67.1	71.6	75.5	79.8	85.6	90.0	92.9	95.5	101.1			
ESTIMATED FUNDS TO COMPLETION	$ X 1000	88.1	81.6	76.2	68.6	59.4	49.9	44.0	47.5	40.9	33.4	28.9	25.0	20.7	14.9	10.5	14.2	11.6	6.0			
ANTICIPATED OVER/UNDER RUN*	$ X 1000	0																				

* REFLECTS AMENDMENT (PHASE D)